A METHOD FOR DYNAMIC BALANCE

A Thesis

Submitted to the College of Graduate Studies and Research

in Partial Fulfillment of the Requirements

for the Degree of

Master of Science

in the

Department of Electrical Engineering

University of Saskatchewan

by

Shree Ram Nath Regmi

Saskatoon, Saskatchewan

May 1993

dedicated to

my beloved parents

COPYRIGHT

ACKNOWLEDGMENTS

The author would like to express his gratitude and appreciation to Dr. H. C. Wood for his guidance and consistent encouragement throughout the course of his work. His timely advice during execution of the project and assistance in the preparation of this thesis is thankfully acknowledged. The author takes this opportunity to thank Ian J. Macphedran for his advice in the use and operation of computer system throughout the work.

The author would like to thank his friends, namely, Thelma Howard, Greg Broten, Dandina Hulikantha Rao for their help during this work.

Special thanks are extended to his wife, Bhawana, for her encouragement during the study. The author takes this opportunity to acknowledge the encouragement and moral support provided by his parents and other family members.

Financial assistance provided by the Canadian International Development Agency (CIDA) in the form of Graduate Fellowship to develop Engineering Education in Nepal is thankfully acknowledged.

UNIVERSITY OF SASKATCHEWAN
Electrical Engineering Abstract 93A376

A METHOD FOR DYNAMIC BALANCE

Student: S. R. N. Regmi **Supervisor**: Dr. H. C. Wood

M. Sc. Thesis Presented to the
College of Graduate Studies and Research
May 1993

ABSTRACT

Dynamic balance is a very important function of the human biological control system. Humans have learned to walk on uneven terrain, keeping the body posture in the vertical position by sensing the direction of gravity. The adaptation of this skill to operations of a truly unstable autonomous mobile robot would be useful in dealing with an unstructured environment.

This thesis describes the dynamic balance of a single link inverted pendulum in flat and changing terrains. A gravity sensing technique has been developed and tested in simulation to measure the imbalance of the inverted pendulum from the vertical position regardless of the terrain conditions. A task oriented motion planning algorithm has been developed and tested. The planned motion allows the inverted pendulum system to perform the desired motion with an unbalance-balance cyclic motion in flat and changing terrains, similar to the way humans plan their motions.

The simulation results on the developed techniques, gravity sensing and motion planning, have indicated that the proposed methods can be used to balance an unstable mobile system in motion and at rest in changing terrains. A self guided unstable autonomous mobile robot could be built by incorporating the techniques with a modest control system.

Table of Contents

List of Figures

List of Tables

List of Abbreviations

D C	Direct current
ASV	Automatic Suspension Vehicles
AMV	Autonomous Mobile Vehicles
g	Gravitational Constant
SAMV	Stable Autonomous Mobile Vehicles
UAMV	Unstable Autonomous Mobile Vehicles
IP	Inverted Pendulum
P	Pendulum
SHM	Simple Harmonic Motion
OSU	Ohio State University
USC	University of Southern California
ARTA	Advanced Robot Technology Research Association
CMU	Carnegie Mellon University
EMG	Electromyograph
CM	Center of Mass
CG	Center of Gravity
IAV	Intelligent Autonomous Vehicles
DOF	Degree of Freedom
CPU	Central Processing Unit
SUN	Stanford University Network

C++	Computer Language
UNIX	Operating System
KBS	Knowledge Base System
KV	Knowledge Vector
DV	Desired Vector
MRAC	Model Reference Adaptive Control
PID	Proportional plus Integral plus Derivative

1. INTRODUCTION

Dynamic balance is an important human skill that is yet to be satisfactorily duplicated by machines. Humans can balance themselves on different terrains, on slopes, and on surfaces of different consistency with or without an additional load. Humans can perform various motions, such as running, climbing, jumping, or walking on complicated surfaces according to changing task requirements and without falling on the ground.

An autonomous mobile robot would be useful in the areas of tele-operation in space and in other hazardous environments. In space, for example, the robot could be used to explore the surface of other planets where humans cannot be sent. The inspection and repair of aging nuclear reactors and site cleanup of radioactive waste materials are some future important applications of autonomous mobile robots.

Research into machines that walk safely in difficult terrain, where existing vehicles cannot go, has been directed toward the problems of static and dynamic balance. An automated mobile robot that can balance dynamically can also depart from the static balanced position. Unlike a statically balanced robot, which always operates in or near the vertical position, an actively balanced robot can be an unstable machine that can for short times be unbalanced but is able to recover to a stable position.

1.1 STABILITY

Static and dynamic stability distinguishes the two types of mobile machines that have become active areas of research in robotics. A statically stable system keeps its center of mass in such a position that it never gets in a situation where falling is possible whereas dynamically stable systems keep from falling down by balancing. Statically stable systems have at least tripod support while dynamically stable ones may have as few as only one leg. The main discriminator is the use of balance in the control of body attitude by dynamically stable systems. Insects, alligators and other many-legged creatures walk with statically stable gaits. Higher animals like horses, cats, and humans, walk with dynamically stable gaits.

Static Stability:

The main attraction of statically stable walking machines is that they are safe with the power or the control computer turned off. Regarding statically stable machines, it has been said that if something fails one has a piece of statuary, not a piece of wreckage [1]. In the modern era, early walking machines began with small machines that relied on static stability.

There are several walking machines, relying on static balance, like insects or arthropods, that have been developed over the course of the last twenty years. Sutherland [2] built a six-legged, semi-automated crawling machine. This machine was statically balanced on three legs while in motion on a smooth terrain. McGhee at University of South California (USC) built a four-legged machine in 1966 [3]. Another very popular machine, in this category, was the Ohio State University (OSU) Hexapod robot which first walked in Jan. 1977 [4]. This machine had three degrees of freedom and was actuated by electric motors. McGhee and Pai [5] studied the design of a statically stable quadruped. This work was the extension of the work in the same area reported by McGhee and Frank [6]. Many multi-legged walking robots have been developed [7][8] and are being used in industries. Such robots are balanced statically and require large amounts of energy to maintain their posture. Normally these types of robots are large

and have the capability to carry the required sources of energy to maintain their body attitude. A small sized insect like an ant can move around in difficult terrain, but large creatures like alligators cannot walk with such ease. There is an energy constraint in the use of such a model for a walking robot.

With improvements in the understanding of the mechanics of locomotion and ease in controller design, research on autonomous mobile vehicles based on static stability began. Kessis *et al.* [9] reported an architecture of a statically stable autonomous hexapod built at the University of Paris in 1980. This robot uses a tripod gait used by many six-legged arthropods. A research effort at OSU has resulted in the successful design, fabrication and testing of a six-legged fully computer controlled autonomous vehicle called Adaptive Suspension Vehicle (ASV) [10]. The ASV has over 100 sensors including an inertial sensor package consisting of a vertical gyroscope, rate gyroscope for the pitch, roll and yaw axes, and three linear accelerometers providing information to determine the body velocity and position. Pfeiffer *et al.* [7] investigated the gait dynamics of the walking stick insect (Carausius morosus) modeled by a six-legged multi-bodied mechanical system. Advanced Robot Technology Research Association (ARTA) developed an intelligent autonomous multi-leg walking robot [8] to replace humans in tasks that have to be carried out in a hostile environment.

Dynamic Stability:

A dynamically stable mobile system preserves its balance under circumstances in which the machine might otherwise fall down. Humans and higher animals are categorized in this class. A human keeps its center of mass right over the feet in the balance condition. The nature of these systems is to be unstable. The problem of controlling a dynamic system is much greater than that of controlling a static one for two reasons. First, the mechanical system must be capable of responding fast enough to control the balance, and second, the controller must be very accurate otherwise the machine might fall into a piece of wreckage. These problems have caused a lack of development of dynamically balanced robots.

Fewer dynamically stable robots have been developed than statically balanced ones. The first dynamically stable robot was the four-legged walking truck constructed at General Electric by Ralph Mosher's group during the 1960s [11]. This machine was human controlled. A human operator provided the necessary sensing and closed loop control that controlled the hydraulic system. Several other dynamic and pseudo-dynamic machines have been built in North America and abroad. Raibert's single legged hopping machine built at Carnegie Mellon University (CMU) [12] was perhaps the most prominent in this class. This machine consists of two main parts, a body and a springy leg. It was the first successful statically unstable but dynamically stable machine and it balanced dynamically on a single pneumatically driven leg.

Normally unstable machines, such as biped walking machines, need to utilize dynamic balance to maintain an upright position. Miura and Shimayama [13] built a biped that walks like a human. This machine moves forward with a motion that can be described as a Charlie Chaplin.

1.2 MOTIVATION OF WORK

The maintenance of a stable posture is important to all animals. For humans it is challenging because of our physical structure. Humans are able to learn to walk on uneven terrain, keeping the body posture upright with respect to the line of gravity that passes through the feet and the body center of mass. This skill allows them to walk on different shaped surfaces without falling. Humans balance their body attitude in the upright position dynamically even though the center of mass of the human body is located 2/3 of its height above the ground in the normal balance posture [14]. Like humans, some animals also maintain active balance that allows them to walk freely in difficult terrain.

Balancing, in the area of robotics, has many facets, many definitions, and many subsets. One subset begins by simply wanting to know "Where am I with respect to the direction of gravity?" and then expanding upon that simple statement with information required on how to get from "Where am

I?" to "Where do I want to be?" [15]. The first question is related to knowing the position of the center of gravity and the second question is related to the control of body attitude and position in space.

Dynamic balancing is based on the position of the body in an inertial frame, and the act of balancing requires detecting the direction of gravity. This requires a gravity sensor system that can determine the position of the center of mass in the inertial frame. A balance controller adjusts the body position on the basis of the information provided by the sensory system. In flat terrains, the direction of gravity remains constant with the terrain, however, in uneven terrains, the direction of gravity with respect to the terrain surface is changing. These changes depend upon the characteristics of the terrain.

To develop a mobile robot that can be operated in changing terrains with dynamic balancing, the body attitude requires a system that detects the direction of gravity. An important problem in the current research on autonomous mobile vehicles is their inability to perceive the shape and structure of the terrain on which they are operating. A logical starting point in the realization of such machines is research on a technique to determine the direction of gravity.

1.3 STATEMENT OF OBJECTIVES

The first objective of this project is to develop and test a simulation of a sensory system that can determine the direction of gravity in a changing terrain. The obtained results will be used to model the balance of an inverted pendulum machine moving in changing terrains.

The second objective of this project work is to develop and test an algorithm and a model for motion planning of an inverted pendulum system in unknown terrains. This work will involve a preliminary examination of a control system for motion and balance control.

These planning techniques could be employed in bipedal autonomous mobile robots.

1.4 OVERVIEW OF THE THESIS

A comprehensive survey of the available literature in the areas of human and machine balance, inverted pendulum systems, and autonomous mobile robot systems has been carried out. An overview of this survey is presented in Chapter 2.

The mechanics and dynamics of unstable mechanical systems are another area of this project. Lagrangian dynamics have been used to form the necessary differential equations of the physical model. The dynamics of the physical system and the corresponding mathematical models are discussed in Chapter 3.

Simulations of the mathematical model of the system, based on the theory of Chapter 3, have been developed in Chapter 4. The results of the simulations are also shown in this chapter.

Motion planning for the inverted pendulum system has been discussed in Chapter 5. This chapter also describes methods for the dynamic control of the inverted pendulum system in changing terrain. The results of simulations are also shown in the chapter.

Chapter 6 includes a brief summary and conclusions of the work reported in this thesis. The potential areas for further research have also been identified in this chapter.

Five appendixes are also included at the end of the thesis.

2. BALANCE IN HUMANS AND MACHINES

2.1 INTRODUCTION

There is a large class of robotics applications in which the robots have to operate in unstructured and uncertain domains. The uncertainties currently limit the operation of robots, however, with recent advances in robotics and allied sciences, more generalized mobile robots have become feasible and present very attractive prospects for several applications. Past researchers have realized the importance and use of autonomous mobile robots in hostile environments, for example, cleaning up radioactive waste in nuclear plants, where humans can not be sent to perform the desired task.

Generally two types of land-based autonomous lifeforms exist in nature: stable and unstable. For example, alligators are stable whereas humans are very unstable. The mobility of these lifeforms is limited by body structure. Alligators cannot make complicated motions whereas humans can without losing balance completely. It is the human biological control system that balances the body in the upright position.

Autonomous mobile robots are by definition free from external aid. The type and features of an autonomous mobile robot depend upon the required task that is to be performed by them. These robots could also be classified into two classes, stable and unstable.

Most autonomous mobile robots are constructed on the basis of stable creatures, like alligators or arthropods. These robots can be called Stable Autonomous Mobile Vehicles (SAMV). Normally, these robots exist with more than two supports (legs or wheels). The main feature of these robots is their stable posture. A simple control algorithm can be used to control their

motion. A serious disadvantage of this robot is its limited motion. These robots have limited motion where the terrain is unpredictable.

Building an unstable autonomous mobile robot that could be used more efficiently than existing stable robots in unstructured terrain, has become an active area in robotics research. This robot could be used to replace the existing SAMVs in terrains where the SAMV cannot be operated. The distinction between this proposed robot and the SAMV is balance.

For an autonomous robot to be like a human, it should have sensing mechanisms corresponding to a human's biological sensors. To clearly understand the human balancing techniques, the past work in posture and balance will be reviewed. An inverted pendulum is a classical problem of dynamic balance. The balancing of an inverted pendulum is basic to controlling the body attitude in humans. Similar ideas could be used to control the body position of an unstable autonomous mobile robot in motion or at rest in an inertial frame.

The next section reviews some research in human biological balance. The dynamic balance of an inverted pendulum in different situations will be reviewed together with a review of inertial systems.

2.2 REVIEW OF HUMAN BALANCE

The human biological system maintains the body in the upright position regardless of the shape of the terrain. Two types of balance descriptions are appropriate in humans, quasi-dynamic and dynamic. Quasi-dynamic balance maintains the body in the balanced position during standing, and dynamic balance is used during motion. Humans are very unstable even in near-static balance; the center of gravity tends to oscillate about an equilibrium position no matter how still the human stands. This unstable angular motion, about the vertical, indicates the posture is constantly swaying. Since the body posture has to be upright, a controller is required to produce an appropriate force or torque within a short time to keep the body in a balanced position. This inherently unstable posture is

used to assist in propelling the body forward during motion. This property of humans has allowed them to use a comfortable and very efficient mode of motion [16], keeping the body mass well above the ground. Three types of sensory systems are involved in the human postural balance: vestibular, proprioceptive, and vision [14].

The vestibular system has been recognized as one of the prime biological sensors involved in postural adjustment [17]. The vestibular sensory systems determine the angular orientation of the human head in the inertial frame. This helps to determine the balance and imbalance of the body. The proprioceptive system provides the body with kinematics information, such as the degree, direction, and rate of change of the body position in motion. Sensors for this system are located in the muscles, tendons and joints and are stimulated by the motions of the body. The visual system provides a point of reference. The eye predicts the environment, for example, the terrain gradient ahead that would be the next environment where the motion has to be carried out. These three sensory systems are integrated with the system to balance the body's center of mass in the unstable upright position.

The systems which maintain the dynamic balance includes the vestibular, visual, proprioceptive sensory systems, the central nervous system, and musculo-skeletal system [14]. Figure 2.1 shows a schematic diagram of the human postural adjustment system,

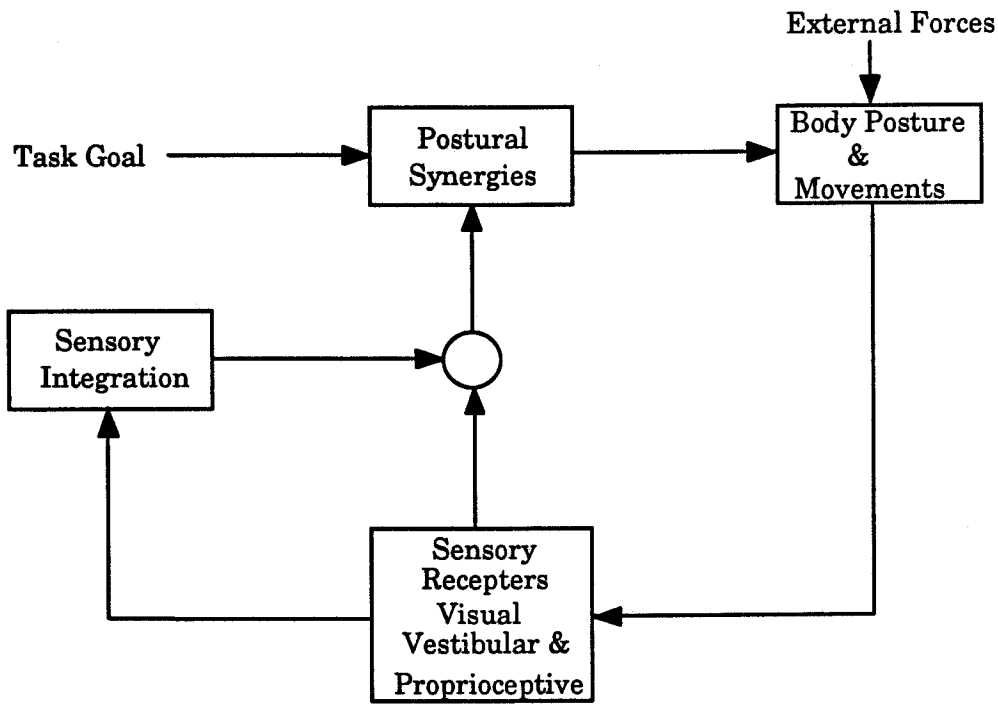

Figure 2.1: A conceptual schematic diagram of the postural control system [from [14], Fig. 1].

The central nervous system, and especially the cerebellum, integrates and evaluates the rich array of information coming from different sensory systems together with messages from the motor cortex of the brain. An appropriate action plan must be decided upon within a short time (a few milliseconds) before the body goes beyond control. This action plan is very critical in the balancing act. Researchers have tried to perceive these action plans by performing experiments on postural balance in a variety of destabilizing, imbalanced conditions [14][16].

The musculo-skeletal system has the responsibility to execute the action plan to regulate body posture to the vertical. Muscle activation produces the forces that correct the imbalance. The type and number of muscle activations are determined by the action plan that was made by the cerebellum. For example, the torques generated about the ankle axes of rotation are primarily responsible for restoring balance during the standing posture.

The objective of the regulation of body posture, near the unstable equilibrium, in the upright position, is that the center of gravity of the body remains inside the controllable region, i.e, the area of the feet. Perturbations of the center of gravity cause the destabilization of the body. In such a case the center of gravity deviates from the equilibrium position. Sometimes the perturbation of the center of gravity is so large that the center of gravity moves outside the foot area; in this condition the recovery of balance becomes very difficult. The corrective force is proportional to the magnitude of imbalance or deviation of the center of gravity from the upright position, thus, the magnitude of the deviation of the center of gravity, or sway, needs to be measured. Many researchers have employed different approaches to estimate the sway of the center of gravity [18][19][20].

There are a number of conditions that necessitate postural adjustment to maintain a reasonably balanced standing position. These include standing on either an up hill or down hill slope, standing on even and uneven terrain, and standing on a moving surface. In all of these cases, the normal human body can be relied upon to adjust automatically through the function of the sensory system and the feedback control mechanism. Humans exhibit typical behaviors in maintaining the body with it's geometrical mass right above the base of support so that the posture remains balanced. The human anatomical system is made of multiple link segments that do not have uniform densities. This contributes different degrees of inertial forces about the hip and ankle. Posture remains balanced when the sum of these moments about the ankle becomes zero. This sum can be made zero in different ways.

The mathematics of postural dynamics studied a decade ago was mainly based on the single link inverted pendulum to represent the human body [18]. The first investigation was done by McGhee and Kuhner [21] in which they found the role of ankle and hip torque in achieving postural balance during standing. Later, Nashner [16] modeled the human body as a simple inverted pendulum to evaluate the vestibular function in the human body during motion. Soames and Atha [20] studied the human sway behavior in motion using an inverted pendulum. Koozekanani *et al.* [18]

studied the center of gravity and pressure by a mathematical model of their four-mass sagittal plane linkage model. Shimba [19] used a mathematical model to estimate the center of gravity in space. Pasteurella and Huston [22] modeled the human body by a ten-bodied system and studied attitude control in space using the principle of conservation of angular momentum.

In kinesiology, human walking has been described as an alternating loss and recovery of balance [23] which is accomplished by the alternating action of the body's lower extremities. Nashner [16] studied the postural balance when walking started. His EMG experiments showed that posture undergoes a loss of balance when the forward motion started. From physical principles, under conditions of the coefficient of friction being less than one, the translational acceleration of the center of mass cannot exceed the acceleration of gravity. Research shows that the maximum speed a human can achieve in normal walking is approximately 2.5 m/sec [24]. The switching speed of human motion is 2.5 m/sec; after that walking gives way to a run. The running speed is dependent upon the type of run, and is in the range of 3 to 10 m/sec.

During normal walking the center of gravity passes from heel to toe in a short time within which the postural balance deviates from the balanced position. Winter [25] emphasized that the balance task was the primary one as compared to the tasks that propel the body forward. An adjustment system is required to maintain the center of gravity within the controllable region. Nashner [16] recommended an algorithm to control the adjustment of posture during normal walking. His EMG responses elaborated the adjustment of the center of gravity so that the posture remains within the region of control.

The direction of gravity on a horizontal surface is assumed to be constant. Balancing the body posture on such a surface is easy because of the non-changing angle to gravity. In contrast, the line of gravity on changing terrain is varying, with respect to the terrain. Balancing on a changing surface requires the determination of the gravity direction rather than the actual terrain. According to the response obtained by Nashner, the body attitude control mechanism requires some time to activate the control

muscles. Balancing during motion on a unknown terrain is difficult since the body orientation in the inertial frame is changing. Finding the orientation is the key to the control of balance in changing terrain. The vision sensory system provides the orientation of the body in many environments, but this is not sufficient in all cases. The vestibular system is needed to cope with different types of environment. Thus, this orientation sensor can be considered as the primary sensor for postural balance.

2.3 REVIEW OF MACHINE BALANCE

2.3.1 Inverted Pendulum

The inverted pendulum is a classic example of a highly nonlinear, coupled, and inherently unstable dynamic system. The center of gravity must be kept directly above the hinging point or point of support of the system. The system dynamics are basic to understanding tasks involving the postural control in humans with an unstable equilibrium at the upright position. A single linked inverted pendulum has often been used to represent the human standing posture. Many researchers [2][18][20] have used the model of an inverted pendulum, of various degrees of freedom, to study the basic balance control in humans.

There have been many experiments performed on inverted pendulums to understand the balancing act in the human biological system. The earliest mathematical work on the dynamics of postural control was based on a single link inverted pendulum [18]. Soames *et al.* [20] studied the relationship between the sway and torque about the human ankle in unbalance using a single link inverted pendulum. Raibert *et al.* [2] showed the balancing of a single leg hopping robot based on the inverted pendulum. Humans can be modeled by a three link inverted pendulum corresponding respectively to the leg, thigh and the trunk. Hemami *et al.* [26] proposed the method of controlling postural stability using a three links inverted pendulum with physical parameters chosen to correspond to those of an average human. The attitude control of a multi-linked inverted pendulum is

similar to the attitude control of human posture. Furuta *et al.* [27] studied the balance of a triple inverted pendulum by applying forces on each of the links.

The standing posture of an inverted pendulum can be used to model the human standing posture. In balanced posture, the center of gravity of the inverted pendulum, which is somewhere above the point of support, has to be maintained. The reaction force generated by the pendulum with the ground has to be made equal to the weight force of the inverted pendulum. The goal of postural stability is to maintain the inverted pendulum directly above the ground support point where the total moment becomes zero.

The pendulum remains balanced while its position is aligned with the line of gravity passing through the center of mass and the point of hinging. Normally, the point of hinging is not like that of human feet. Thus the inverted pendulum becomes more unstable than the human posture. In the upright condition, the moment about the hinging point becomes zero because the reaction force and gravity forces become equal and aligned in the opposite direction. Any force acting externally on the inverted pendulum contributes a non-zero moment that causes destabilization of the inverted pendulum; a control force is required to correct such destabilization. The unstable system dynamics requires a dynamic balance controller to adjust the sway of the pendulum by driving the pendulum in the opposite direction to the sway. Many experiments have been performed on balance control of inverted pendulums of single link [28][29], and multiple link [26][27][30] design.

The basic idea of balance is shown in the broom balancing technique. The method of balancing a broom dynamically on a finger is to move the finger back and forth, depending upon the direction of the tipping. This translational motion results in a torque about the point of contact that causes deceleration in the broom's motion. When the force applied becomes more than enough for the broom's angular motion, the broom changes its direction of acceleration and eventually accelerates towards the vertical. The magnitude of the force depends upon the angular position, and its derivatives, of the broom with the vertical. Thus a variable magnitude of

force is required to adjust the postural imbalance.

The first machines that balanced actively were automatically controlled inverted pendulums. Claude Shannon [31] was probably the first researcher to use the idea of broom balancing to balance a iron rod, an inverted pendulum hinged on top of a truck. He used the same technique as a human uses in balancing the broom on a finger by making truck motions back and forth. Figure 2.2 shows the basic cart-pole model.

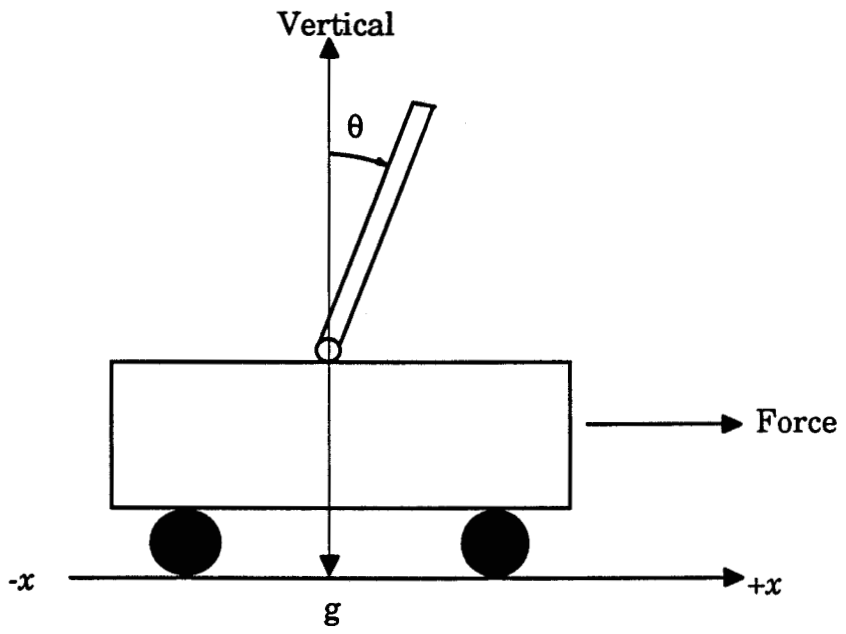

Figure 2.2: The cart pole system [from [32], Fig. 1].

Cannon [33] studied the effect of a single applied force in Shannon's experiments. Cannon was interested to know how a single force that drove the cart motion could control the angle of two pendulums and the position of the cart. The region of controllability of the inverted pendulum is a deterministic factor depending upon the length of the pendulum. A long pendulum has a larger inertia about the point of support than a short pendulum. Thus, the region of controllability of the long pendulum is close to the vertical, whereas the short pendulum has a wider region of controllability. A long pendulum is more stable about the vertical than a short pendulum. The region from where the pendulum can be brought back

into the original position was studied at the Computer Science department, Massachusetts Institute of Technology (MIT) by Connel and Utgoff [32]. They set up an experiment for balancing a pendulum within the region of ± 12 degrees, $\theta(t)$ for particular system parameters. Their experiment showed that the controllability declines if the tipping is more than 12 degrees.

The cart-pole experiments have been a very popular area of research into balance. The cart-pole experiments are basically the same as balancing a broom by applying a translational force at the axis of rotation, or the point of contact. The control force is applied in response to pendulum postural destabilization. The instability occurs when the line of gravity does not pass through both the center of gravity and the point of support. Any sway in posture causes the center of gravity to deviate from the equilibrium which causes the center of mass to accelerate towards the ground. Thus, an active controller is needed to sense the sway and apply a reversing force to counter the force of gravity. This has been a very popular experiment in control engineering. The control systems tested in these experiments determine the ability of the controller to control such a very unstable non-linear system. Pfeiffer *et al.* [7] used a walking stick insect model to study balance control. Hemami and Jaswa [26] studied nonlinear feedback in the inverted pendulum to achieve postural stability where the first and higher derivative components all become zero.

The traditional approach in balance control is the linearization approach. The force applied is a linear function of four state variables, $\theta(t)$, $\dot{\theta}(t)$, $x(t)$, and $\dot{x}(t)$ with constant coefficients [32]. This linearization approach provides the stability of the inverted pendulum for a certain limited range of operation. Anderson [28] suggested the control force, in the same problem, required using a different approach, rather than linearizing the problem. Lin and Sheu [29] studied the balance of an inverted pendulum from the rest (pendant) position, 180 degrees to the vertical unstable equilibrium. Mori *et al.* [34] also proposed a control method to bring the inverted pendulum to the unstable vertical position from its stable pendant position.

In all experiments discussed above, the inverted pendulums were balanced on a plane where terrain is constant or horizontal, i.e., no changing slopes. Balancing in such an environment does not require information about the direction of gravity. The vertical y axis was taken as the reference from which the tipping angle of the pendulum was measured. However, bringing the pendulum about the y-axis, vertical, is only one objective of the work. The maintenance of attitude in a changing terrain is another problem. The system dynamics become very unstable in this case because the direction of gravity with the terrain is not fixed but changing. This changing causes the center of mass of the inverted pendulum to deviate from the direction of the gravity.

Now many mobile robots are required to be operated in an uneven terrain where the terrain is not flat. While the direction of gravity is constant, despite the geographical conditions, in horizontal terrain the direction of gravity is orthogonal to the plane of the terrain, while in changing terrain the line of gravity does not align with the orthogonal axis to the terrain. Balancing is required to bring the inverted pendulum towards the line of gravity, not vertical to the terrain. Hence, the direction of gravity has to be determined to make the inverted pendulum upright in such a changing environment. In a variant of this case, Furuta *et al.* [30] showed the balance of a double inverted pendulum on a constant inclined surface.

2.3.2 Walking Machine

The balancing problem is very important in walking [35]. The control algorithm required is quite different from the algorithm used in postural balance during the standing condition. Walking is the mechanical process of propelling the body's center of gravity forward with the aid of the legs. Many walking machines have been developed in the last two decades. The first machine, Phony Pony, with four legs was built at the USC [36]. Mosher's group [37] at General Electric built a quadruped walking machine that operates purely upon a static balancing technique. Sutherland [2] built the first six-legged, semi automated crawling machine. This machine was statically balanced on three legs while in motion on a smooth terrain. The

realization of such semi-automatic machines in a changing terrain environment was difficult because of the complex control system required to allow the machine to walk on unstructured terrain.

Developed static machines had limitations in their application. The stability of such machines defined only in a known terrain causes the machines to be unable to work in the environment where the terrain is not constant. Another very important factor is the cost of operation of such heavy machines which require large amounts of energy to perform the desired work. The speed of these machines was limited by their large body mass. Because of these situations, researchers decided to work in the area of active balance [2][36]. The importance of active balance in walking robots had been widely recognized, but progress in building physical legged systems that employ active balance was retarded by the perceived difficulty of the task. It was not until the late 1970s that experimental work on balance in legged systems began [12].

Raibert and Sutherland [2] studied the role of active balance in running and walking. Raibert [12] at CMU built a one legged hopping machine that runs like a kangaroo in a series of leaps. This machine consists of two main parts, a body and a springy leg. It was the first successful statically unstable but dynamically stable machine that balanced dynamically on a single pneumatically driven leg. Later Raibert [12] developed a quadruped machine based on the hopping principle.

2.3.3 Biped

The developments on legged machines inspired the scientific community to do research on a human like walking machine; a biped robot [12][36][38] has larger applications than multi-legged machines. Kato *et al.* [39] built one of the earliest biped robots. It was a statically stable machine relying on keeping its center of gravity always above one of its large feet. Miura and Shimoyama [13] built a biped that employed a dynamic balancing technique by allowing the robot to depart from the line of gravity. This robot uses a continuous stepping method to maintain the body attitude within the equilibrium or upright position. After the successful operation of

a one legged hopping machine that balanced dynamically, Raibert [12] built a biped robot that could run with the speed of 4 m/s keeping the machine balanced. It applied the principle used by Miura, leaning the robot in the direction of motion to keep the posture within the region from where the robot body could be brought back into an upright position.

Kajita *et al.* [40] studied the active control of biped robots. They introduced a trajectory, called a potential energy conserving orbit to maintain postural stability during walking. Postural regulation within the balanced region is very important during walking since external disturbances cause the biped to be unstable and lose balance. Zheng [38] proposed an acceleration compensation method to improve the postural adjustments due to perturbations.

Early walking biped robots [13][39] were successful human-made machines that walked on a flat floor. The problem of balancing a walking robot on a difficult terrain was realized by many researchers. Unlike in standing, the center of gravity in walking bipeds moves between the two legs when walking takes place. When terrain is not flat, the center of gravity may move outside the boundary of the two legs causing the system to become unstable. Zheng and Shen [41] studied the balance problem of a biped robot on a slope. The controller they have used works on the information obtained from force sensors, which detect the slope from different points, especially, the heel and toe.

2.4 REVIEW OF INERTIAL SYSTEM

Every particle in the universe has a reference frame; the motion and displacement of the point are measured with respect to this frame. Newton's laws provide the basic laws of mechanics in inertial frames in which bodies with no net force acting on them move in straight lines at constant speed or stay at rest. According to Newton's first law, every particle has an inertia that allows it to be at rest or in constant motion until an external force acts on it. Connected group of particles free from external forces always project their center of mass towards the origin of the inertial frame passing through the vertical or line of gravity.

Inertial systems have universal applications ranging from the science laboratory to a commercial wall clock. Humans today live on the outer surface of planet earth, and are held there by gravitational forces pulling towards the earth center. Each activity performed by humans is based on the inertial frame, including the balancing of their own body upright against gravity. A human obtains inertial information from the vestibular system of the inner ear [42], which finds the point of reference, the vertical in the inertial frame.

Inertial systems have also been used in the navigation of airplanes, the stabilization of an erected body on a vehicle, motion planning of ships, etc. Because of their self-contained, non-radiating, non-jammable and interference free features, these systems are attractive to the area of modern robotics navigation and stabilization. The needs of the Intelligent Autonomous Vehicles (IAV) to operate in large, unstructured and uncertain domains, for example, fire-fighting, repair and cleaning operation in nuclear plant, have become a main focus in research. The realization of such an autonomous vehicle requires an array of information. The angular orientation in the inertial frame is a part of the important information required to control the stability of the vehicle's body. The main property of an inertial sensing system is its ability to determine the direction of gravity. Thus the vehicle's orientation could be regulated in any terrain by the aid of an inertial sensor.

2.4.1 Physical Pendulum

A physical pendulum is a rigid mechanical body of any shape pivoted at some point other than its center of gravity. The equilibrium point of a pendulum is on the line of gravity passing through the pivot point. Any external force about the pivoted point makes the pendulum oscillate about the vertical. The period of oscillation is determined by physical parameters, mainly the length of the pendulum from the pivoted point to the center of mass, whereas the amplitude of oscillation is determined by the magnitude of the applied forces and the presence of frictional forces. The system transfers energy from potential energy to kinetic energy and vice versa.

Once it is started, it keeps on oscillating until the energy stored becomes zero due to dissipation.

Inertial based instrumentation is used in detecting soil vibration during seismic events. Most seismological instruments are based on a pendulum that transforms seismic events into human readable variables to predict and analyze the appearance of unusual natural forces. Many researchers have used pendulum based seismic instruments to measure the translational and rotational motions of earth segments [43]. The gyroscope is an example of an inertial sensor that has the ability to show the vertical position or earth's reference frame. Navigational systems often use the gyroscope and accelerometers to answer the question " where am I?" in the inertial frame [15].

Like humans, robotic motion can be based on inertial information. There are two types of inertial information to be computed in a mobile robot; one is the orientation of robot attitude and the second is the instantaneous motion of the robot. This information is used in postural adjustment and the stabilization of the robot in different working environments. An autonomous robot requires something other than the postural balance, and that is trajectory planning. An inertial accelerometer can be used to control that task. Thus a complex navigational system is required for autonomous mobile mechanical systems.

2.5 CONCLUDING REMARKS

This chapter has been devoted to a discussion of active postural balance. The acts of postural balance in humans, during standing and walking, have been reviewed in the chapter. A survey of research work carried out in the area of active balance, particularly balance of an inverted pendulum has been conducted. The need for autonomous mobile robots in hostile environments, where humans need to be replaced by an autonomous robot, has been discussed. The importance of active balance in legged, walking robots has been stated; the recent developments of human-like biped robots has also been presented. The importance of sensing the line of gravity in a changing terrain has also been highlighted. The importance

and use of inertial sensing systems and their types were also discussed. The research problem on balancing an inverted pendulum in a changing terrain has been briefly stated.

3. DYNAMICS

3.1 INTRODUCTION

The inverted pendulum is a very unstable system. It has been studied by many researchers as a tool to help understand the control of the human balance system. The balancing task requires the maintenance of the inverted pendulum in an upright position against the pull of gravity. Such a task requires the pendulum to be balanced dynamically, especially in a changing terrain, where the direction of gravity is not easily determined. A dynamic balance controller could be used to balance the inverted pendulum. Past researchers have successfully balanced the inverted pendulum in flat terrain, where the direction of gravity is known, by applying a force in the direction of tipping.

In this project the direction of gravity will be sensed using a simple pendulum pivoted on the hinging axis of the inverted pendulum. This chapter deals with the mechanics and dynamics of inverted pendulums in flat and changing terrains. The dynamic behavior of the inertial element will also be discussed in the chapter.

The first section of this chapter is devoted to mechanics and dynamics. Newton's method of writing the mathematical model of a physical system is complex. Another way to form the differential equation of a system is the Lagrange method. The second section deals with developing the mathematical model of the inverted pendulum in various situations. The dynamic behavior of the inverted pendulum in different conditions will be discussed in section three. The dynamic behavior of a simple pendulum, with a fixed and moving pivoting point will be discussed in the fourth section.

3.2 MECHANICS AND DYNAMICS

Mechanics consists of both static and dynamic approaches; the static case deals with the equilibrium of the system at rest or in constant motion, while the dynamic case deals with the system in non-uniform motion. Rigid body dynamics have been used in the analysis of the mechanical systems. In this approach, the dynamic performance of an n degree of freedom (DOF) system is generally represented by n second order, coupled, non-linear differential equations.

3.2.1 Lagrangian Dynamics

There are a variety of approaches that can be employed to derive the dynamic equations of physical systems such as robots; these are (1) Newtonian method, (2) D'Alembert's principle, (3) Hamilton's equations, and (4) Lagrange's equations.

All are basically equivalent in nature, based on Newton's three laws of motion. Newtonian methods are convenient for the treatment of simple rigid body systems while Hamilton's principles and equations are mostly used in the theoretical analysis of quantum mechanics. The Lagrangian method of writing differential equations of a dynamic system is powerful and often more direct than other methods.

The Lagrangian method is applicable to an n degree of freedom rigid body mechanical system. The advantages of this procedure over conventional methods, like Newton's dynamics, is that this method allows a much simpler way to study the dynamic behavior of a rigid body.

The Lagrangian method uses a generalized coordinate system to form the system dynamic equations. The key idea of forming dynamic equations in the Lagrangian method is to consider the scalar quantities; potential energy, kinetic energy, virtual work and dissipative work. This idea is simple because expressing these scalar quantities is not difficult. The basic form of Lagrange dynamics is given in Eq. 3.1; the derivation of Eq. 3.1 is given in Appendix A. In general,

$$\frac{d}{dt}\left(\frac{\partial T}{\partial \dot{q}_r}\right) - \frac{\partial T}{\partial q_r} + \frac{\partial V}{\partial q_r} + \frac{\partial D}{\partial \dot{q}_r} = F_{qr}\,, \tag{3.1}$$

where T is the kinetic energy of the system, V is the potential energy, D is the total dissipative energy, q_r is a generalized coordinate and F_{qr} is a non-conservative force or torque appearing externally in the coordinate of interest.

3.2.2 Inverted Pendulum

The inverted pendulum is an inherently unstable mechanical system that has an unstable equilibrium at the vertical position. An inverted pendulum appears in many physical forms that have the center of mass well above a narrow base of support. The system dynamic is also very non-linear.

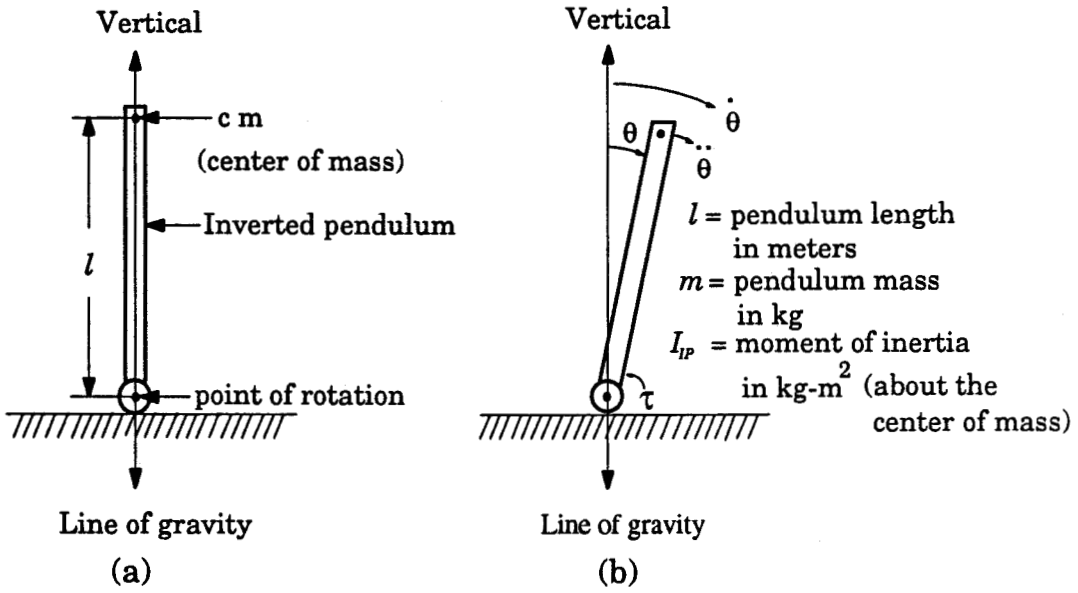

Figure 3.1: Inverted pendulum in horizontal terrain (a) balanced, and (b) unbalanced.

Fig. 3.1(a) shows an inverted pendulum standing or balanced on a horizontal surface whereas Fig. 3.1(b) shows the pendulum in an unbalanced condition where the center of mass is accelerating towards the ground.

Throughout this analysis all of the mass of the inverted pendulum is assumed to be concentrated at the end opposite to the support point. Theta (θ) is the angle of the inverted pendulum with the vertical or line of gravity, g is the acceleration of gravity, 9.8 m / sec^2 and its direction is orthogonal or $\pi/2$ to the terrain surface, m is the mass of the body in kg, l is the distance (meters) of the center of mass from the axis of rotation assumed to be the base of pendulum, and I_{IP} is the moment of inertia of the inverted pendulum about the axis of rotation or base of support in kg-m^2.

The equation of planar motion of the inverted pendulum, Fig. 3.2, has been derived using the Lagrangian method, assuming a fixed axis of rotation,

$$mgl\sin(\theta) - (ml^2 + I_{IP})\ddot{\theta} = \tau. \tag{3.2}$$

Balancing of the inverted pendulum in the vertical position requires bringing it to upright, $(\theta = 0, \dot{\theta} = 0)$, against the gravitational force. This task also involves maintaining the center of mass directly over the base of support. Any angular departure of the center of gravity from the upright position makes the inverted pendulum accelerate towards the ground, which is the only stable equilibrium position.

Displacement of the inverted pendulum from the upright position requires, for restitution, a counter force of the same magnitude as the displacing force. The magnitude of the restitution force depends upon the θ and $\dot{\theta}$ for a given set of parameters of the inverted pendulum. In Eq. 3.2, the left side of the equation shows the unbalanced torques appearing at the base that makes the center of mass accelerate towards the minimum energy point, that is, the ground. An external torque needs to be applied about the base of support, to oppose the gravity force. The direction of this restitution torque is in the opposite direction to the tipping of the pendulum. The control torque, τ, forces the inverted pendulum towards the vertical. Hence, a control torque of a different magnitude, depending upon the state variables, θ and $\dot{\theta}$, is required all the time to keep the inverted pendulum upright. Thus, an active controller is required to control the balance.

In Fig. 3.1 the line of gravity is orthogonal to the terrain surface. The center of gravity and the base of support of the balanced pendulum are aligned with the line of gravity. In horizontal terrain the direction of the line of gravity, passing through the base of support, is known so it is easier to bring and keep the pendulum in the upright position since the angle to the surface can be measured and used to ascertain the direction of gravity. The situation will be different if the terrain or surface is not horizontal but changing. Fig. 3.2 shows the inverted pendulums in balanced and unbalanced positions in a changing terrain. The pendulum is in a balance condition when the line of gravity passes through the base of support and passes through the center of mass.

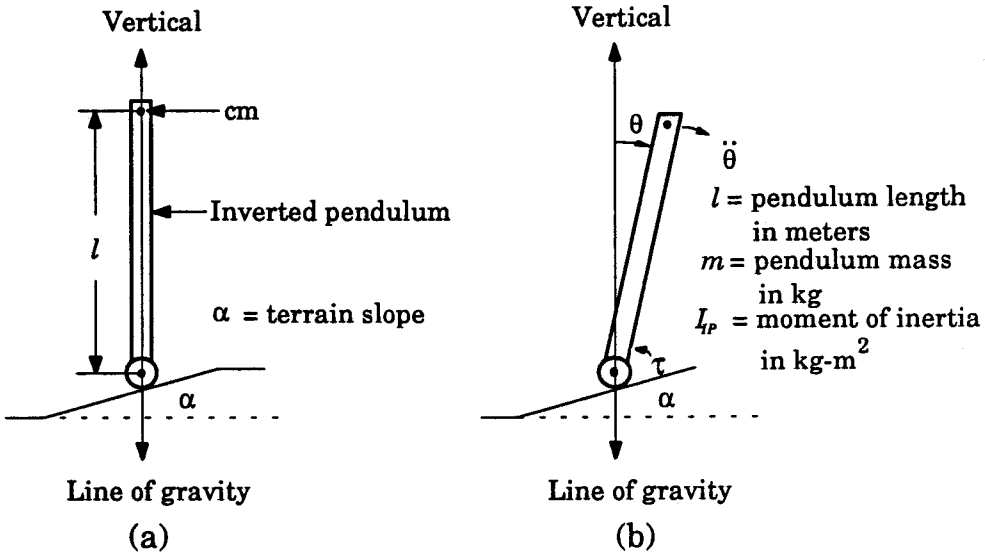

Figure 3.2: Inverted pendulum in changing terrain (a) balanced and (b) unbalanced

The direction of gravity is assumed inertially constant despite geographical changes. This constant is always orthogonal to the terrain surface in horizontal terrain. Unlike in horizontal terrain, (Fig. 3.1), the direction of gravity is not necessarily orthogonal to the surface in changing terrain. Hence, the line of the gravity is at an angle $\pi/2 \pm \alpha$ with the terrain surface. Balancing the inverted pendulum against gravity requires the determination of the direction of gravity. The slope, or the terrain gradient, that determines the offset of the vertical with the terrain surface must be

known to balance the inverted pendulum in changing terrain if the control is with respect to the supporting structure. Hence, the angle, α, determines the terrain dynamics and the angle, α, in the system equation is the key factor in positioning the inverted pendulum upright.

3.2.3 Inverted Pendulum with Moving Support in Horizontal Terrain

When the point of support of the inverted pendulum is allowed to move the dynamic behavior of the inverted pendulum will be different from that in the standing position. The system becomes more unstable and the required control torque will depend upon the angular position and the linear position of the inverted pendulum. The system dynamics become more non-linear, and coupled. Eq. 3.3(a) and Eq. 3.3(b) represent the system dynamics of the inverted pendulum in linear motion.

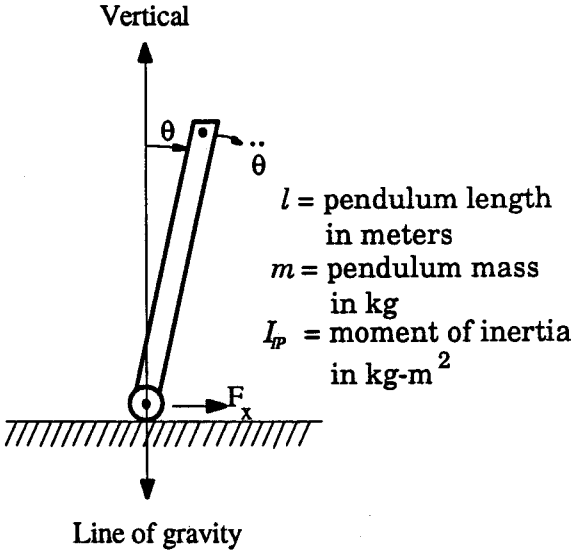

Figure 3.3: Inverted pendulum with linear motion in horizontal terrain.

Fig. 3.3 shows the inverted pendulum with linear motion of the point of rotation. This system has two degrees of freedom, the angular position, θ and the linear position of the support, x. System dynamics have been formed using the Lagrange method; two dynamic equations represent the system,

$$m\ddot{x} + ml\cos(\theta)\ddot{\theta} - ml\sin(\theta)\dot{\theta}^2 = F_x, \text{ and} \tag{3.3-a}$$

$$ml\cos(\theta)\ddot{x} + (ml^2 + I_{IP})\ddot{\theta} - mlg\sin(\theta) = 0. \tag{3.3-b}$$

Solving,

$$\ddot{x} = \frac{\{F_x + m\,l\,[\sin(\theta)\dot{\theta}^2 - \cos(\theta)\ddot{\theta}]\}}{m}, \tag{3.4-a}$$

and

$$\ddot{\theta} = \frac{ml\,g\sin(\theta) - l\cos(\theta)[F_x + m\,l\sin(\theta)\dot{\theta}^2]}{(ml^2 + I_{IP}) - m\,l^2\cos^2(\theta)}. \tag{3.4-b}$$

The forward motion is represented by $\ddot{x}$ and the rotational motion of the inverted pendulum about the point of hinging by $\ddot{\theta}$ in the equations of motion. Many researchers [27][40][44] have used these mathematical equations, Eq. 3.3, to study the dynamic balance of the most unstable, non-linear, and coupled dynamic system; the cart-pole is an example of this system. The balance task requires the forced acceleration of the point of hinging in the forward or the reverse direction. The resulting effective torque, about the point of hinging, decelerates the inverted pendulum. The necessary acceleration depends upon the initial state (θ_0, $\dot{\theta}_0$, x_0 and $\dot{x}_0$) of the inverted pendulum, so the angular acceleration vector of the inverted pendulum with the vertical can be written as a function of $(\theta, \dot{\theta}, x, \dot{x})$.

3.2.4 Inverted Pendulum with Moving Support in Changing Terrain

The balancing of an inverted pendulum in changing terrain is a more complex task. Since the terrain is changing, the direction of gravity with respect to the terrain surface is not known. The terrain slope, α, is the only determining factor of the terrain. Since the terrain is not known, another degree of freedom is added to the system dynamics.

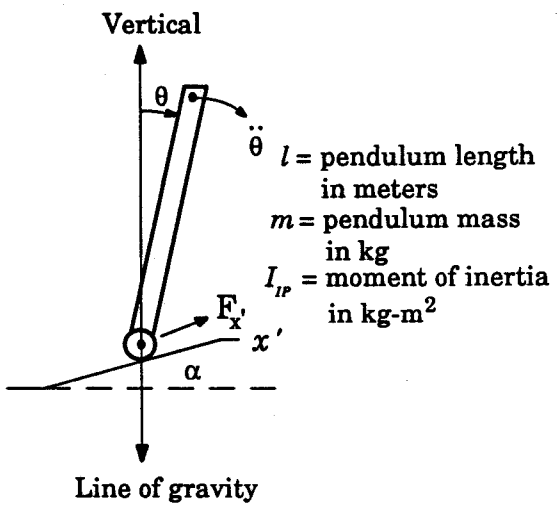

Figure 3.4: Inverted pendulum with linear motion in changing terrain.

Fig. 3.4 shows the inverted pendulum with motion in a changing terrain. As shown in Fig. 3.4, the direction of the gravity with the terrain is not orthogonal to the surface. The system dynamics become very complex, as shown in Eq. 3.5(a) and Eq. 3.5(b),

$$m_2 l\cos(\theta+\alpha)\ddot{x}' + (m_2 l^2 + I_{IP})\ddot{\theta} - m_2 l x' \sin(\theta+\alpha)\ddot{\alpha} - 2m_2 l \sin(\theta+\alpha)\dot{\alpha}\,\dot{x}' - m_2 l x' \cos(\theta+\alpha)\dot{\alpha}^2 - m_2 \lg \sin(\theta) = 0, \tag{3.5-a}$$

$$(m_1+m_2)\ddot{x} + m_2 l\cos(\theta+\alpha)\ddot{\theta} - m_2 l \sin(\theta+\alpha)\dot{\theta}^2 - (m_1+m_2)x'\dot{\alpha}^2 - (m_1+m_2)g\sin(\alpha) = F_{x'}. \tag{3.5-b}$$

The above two equations show the system dynamics of the inverted pendulum in Fig. 3.4. The equations are non-linear and coupled. The angle θ is measured with the true vertical. The direction of the gravity reference is not available in this case so the terrain gradient α is not known. These equations show that balancing of the inverted pendulum in the upright position is possible only if the vertical reference is known.

3.3 INERTIAL ELEMENT

The direction of the force of gravity is generally assumed constant for small changes in location. This constant, the direction of gravity, could be detected by the aid of an enclosed inertial element, such as in systems that have been used in the navigation of ships, airplanes, and other vehicles. Most commercially available inertial system are very expensive. The gyroscope is an example of an inertial system. A less expensive alternative is a simple pendulum. The simple pendulum is an example of an inertial element that experiences a simple harmonic motion (SHM) and comes to rest on the line of gravity that passes through the pivoting point and the center of mass.

3.3.1 Simple Pendulum

The simple pendulum is a mechanical object of arbitrary shape pivoted at some point other than its center of gravity. The pendulum will deviate from equilibrium when it is excited by an external force. Once it is excited, it will go into SHM. The pendulum may exist as a simple, mass less string with a bob or as a rigid rod that acts like a pendulum. Fig. 3.5 shows a simple pendulum having a mass or bob attached to the free end of a mass-less string.

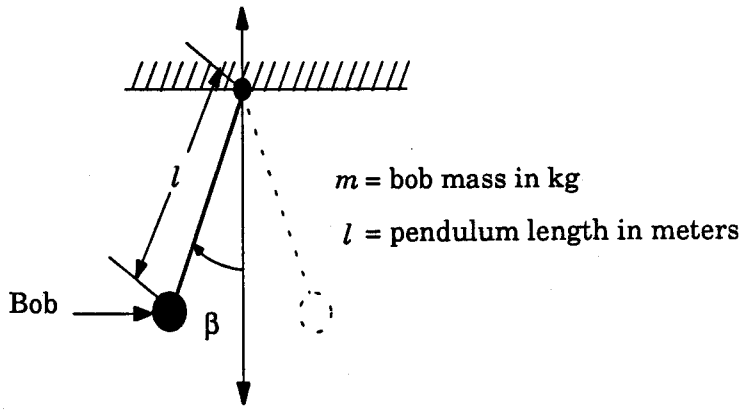

Figure 3.5: Simple pendulum.

The pendulum makes an angle with the vertical, β, in the presence of an external force. The magnitude of this angle depends upon the amplitude

of the initial push on the bob by the external force. The pendulum continues swinging back and forth about the vertical as defined by the direction of gravity for an indefinite time if the damping friction is zero. Friction at the pivoting point results in a damped SHM about the vertical, and the pendulum will come to rest at the vertical position. Thus the direction of gravity can be determined from the dynamic behavior of the pendulum.

The dynamic equation of a simple pendulum is given in Eq. 3.6. This equation has been formed using Lagrangian dynamics,

$$m l^2 \ddot{\beta} + m g l \sin(\beta) = 0. \tag{3.6}$$

The period of the SHM can be expressed by the following series [45],

$$T = 2\pi\sqrt{\frac{l}{g}}\left(1+\frac{1^2}{2^2}\sin^2\varphi+\frac{1^2\times3^2}{2^2\times4^2}\sin^4\varphi+.....\right),$$

where φ is half the maximum angle of β. The period depends upon the amplitude of the swing indicating that the system is non-linear. For, a small swing, β, the second and third terms become negligible. Thus, the period T, can be written as,

$$T \approx 2\pi\sqrt{\frac{l}{g}}. \tag{3.7}$$

3.3-2 Rigid Simple Pendulum

The rigid pendulum has a distributed mass that is centered at some point other than the point of support. The analysis of the period of swing of a rigid pendulum is different from that of a simple pendulum. The moment of inertia of the pendulum body affects the period of SHM. Fig.3.6 shows the physical pendulum having mass m centered at a distance l from the pivot point.

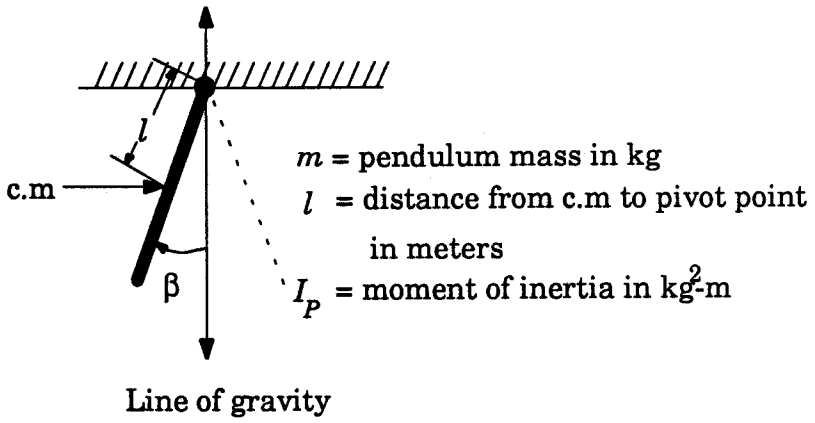

Figure 3.6: Rigid Simple pendulum.

The dynamic equation and the period of SHM are given in Eq.3.8 and Eq.3.9 respectively using the Lagrangian method. I_P is the moment of inertia of the pendulum about the pivot point and f_c is the velocity dependent friction at the pivoting point,.

$$(m\,l^2 + I_p)\,\ddot{\beta} + f_c\,\dot{\beta} + m\,g\,l\sin(\beta) = 0. \tag{3.8}$$

The period of SHM, for small angles is given as,

$$T \approx 2\pi\sqrt{\frac{(ml^2 + I_p)}{m\,g\,l}}. \tag{3.9}$$

Fig. 3.7 shows the SHM of a friction-less rigid simple pendulum, physical parameters listed in Table 3.1, when it is left oscillating from an initial point β_0=1 degree,

Table 3.1: System Parameters

m_2	0.1 kg
l	0.1 meter
Ip	0.001 kg-m^2

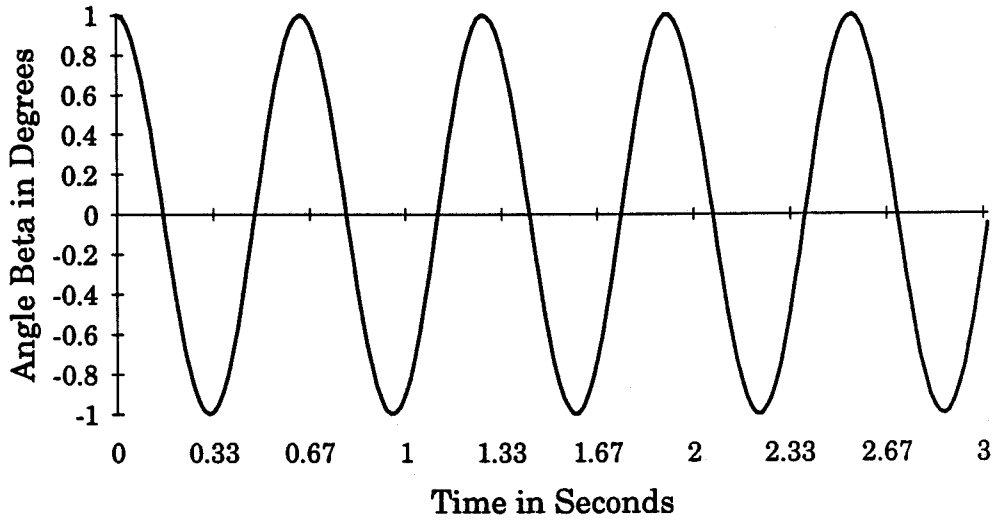

Figure 3.7: Simple harmonic motion of undamped simple pendulum.

The vertical axis in Fig. 3.7 is the angular offset of the simple pendulum from the line of gravity, i.e., zero. The offset is periodic because the pendulum is not damped. A small friction at the pivoting point results in damped SHM of the pendulum and eventually the pendulum comes to rest at the line of gravity, as shown in Fig. 3.8. The time required to come to rest or become aligned with the line of gravity after the initiation of motion depends upon the coefficient of friction at the pivoting point and the magnitude of the smallest observable motion.

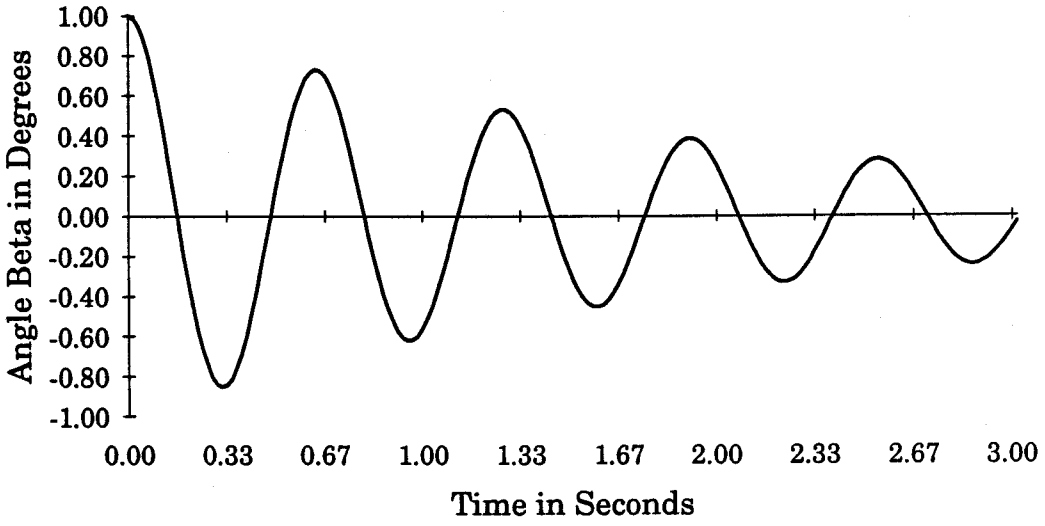

Figure 3.8: Simple harmonic Motion of damped pendulum.

3.3.3 Rigid simple Pendulum with Dynamic Support

The dynamic behavior of a pendulum will be different when its point of support moves. Fig. 3.9 shows the rigid pendulum with an accelerated point of support. The linear acceleration of the pivoting point effectively contributes a torque about the support of the pendulum that forces it to deviate from the SHM about the reference vertical line. Normally, a pendulum oscillates about the line of gravity, however if the pivoting point has a linear acceleration, the reference line about which the pendulum oscillates in response to an external disturbance will be offset from the line of gravity. Thus the reference line about which the pendulum oscillates depends upon the linear acceleration of the pivoting point. The direction of this offset also depends upon the direction of the linear acceleration of the pivoting point.

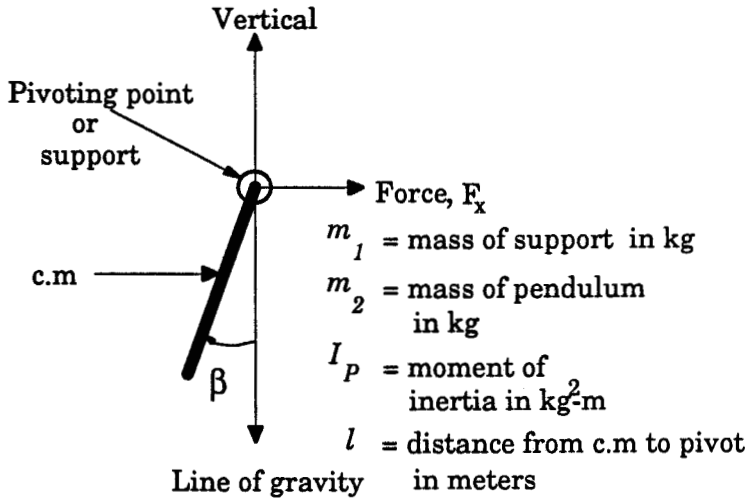

Figure 3.9: Rigid pendulum with moving pivoting point.

System dynamic equations for a horizontal acceleration of the pivot point and a rigid pendulum have been formed using the Lagrangian method and are given in Eqs. 3.10.

$$m_2 l\cos(\beta)\ddot{x} - (m_2 l^2 + I_p)\ddot{\beta} - m_2 lg\sin(\beta) - f_c\dot{\beta} = 0, \qquad (3.10\text{-a})$$

and,

$$(m_1 + m_2)\ddot{x} - m_2 l\cos(\beta)\ddot{\beta} + m_2 l\sin(\beta)\dot{\beta}^2 = F_x. \qquad (3.10\text{-b})$$

The relation between the linear acceleration of the pivoting point, $\ddot{x}$ and the angular acceleration of the pendulum, $\ddot{\beta}$ is shown by Eq. 3.10(c),

$$\ddot{\beta} = \frac{m_2 l \cos(\beta)\ddot{x} - m_2 l g \sin(\beta) - f_c \dot{\beta}}{(m_2 l^2 + I_p)}. \qquad (3.10\text{-c})$$

The solution of Eq. 3.10(c) has been carried out by using Euler's numerical integration method (given in Appendix B.). Fig. 3.10 to Fig. 3.18 shows the simulation of Eq. 3.10(c) for different linear acceleration functions and different amounts of friction. The system parameters are listed in Table 3.1.

Fig. 3.10 shows the acceleration function of the pivoting point. The acceleration increases linearly for $0 < t \leq 4$, constant for $4 < t \leq 6$, decreases linearly for $6 < t \leq 10$, and zero for $t > 10$.

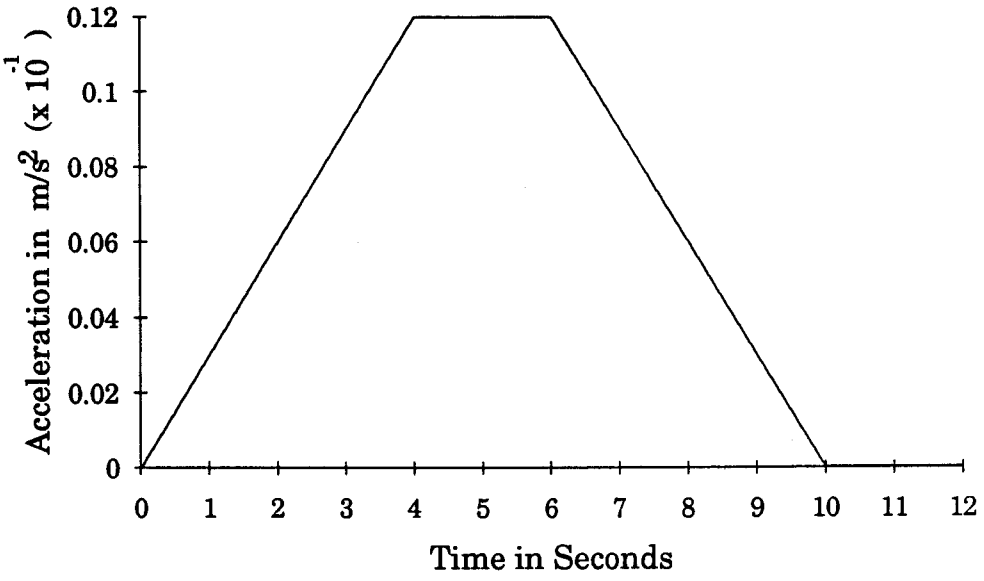

Figure 3.10: Linear Acceleration function of pivoting point.

The angular offset of the reference line about which the pendulum swings follows the acceleration function of the pivoting point, as shown in Fig. 3.11. The amplitude of the oscillation in this case increases at the discontinuities in the acceleration of the pivoting point.

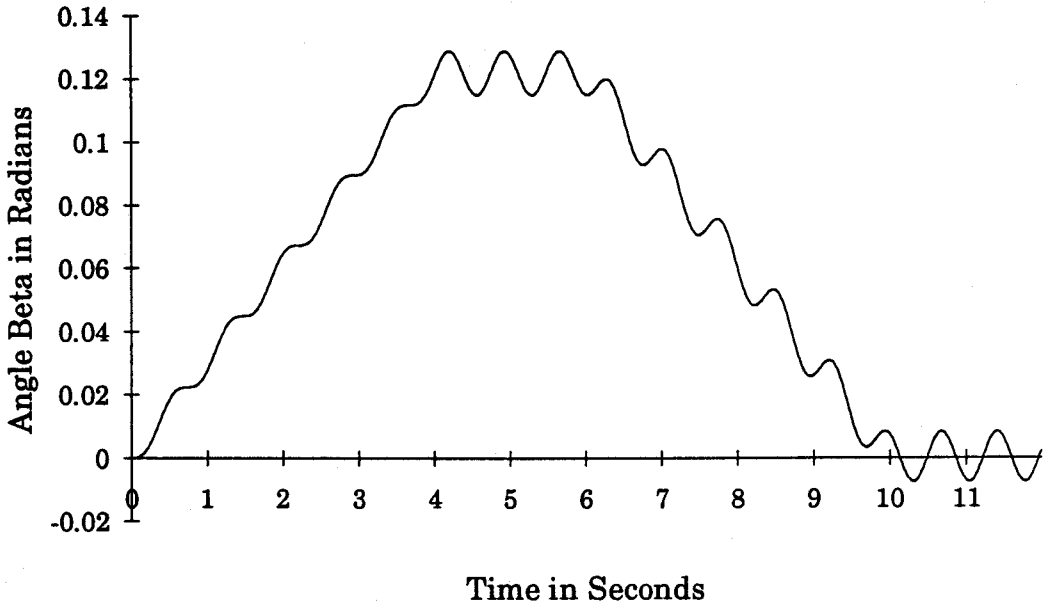

Figure 3.11: Angular offset of the reference without damping friction.

Small, velocity dependent, friction at the pivoting point damped the SHM of the pendulum as shown in Fig. 3.12. Thus, it may be possible to measure the offset of the reference line from the vertical position, if the pendulum is sufficiently damped.

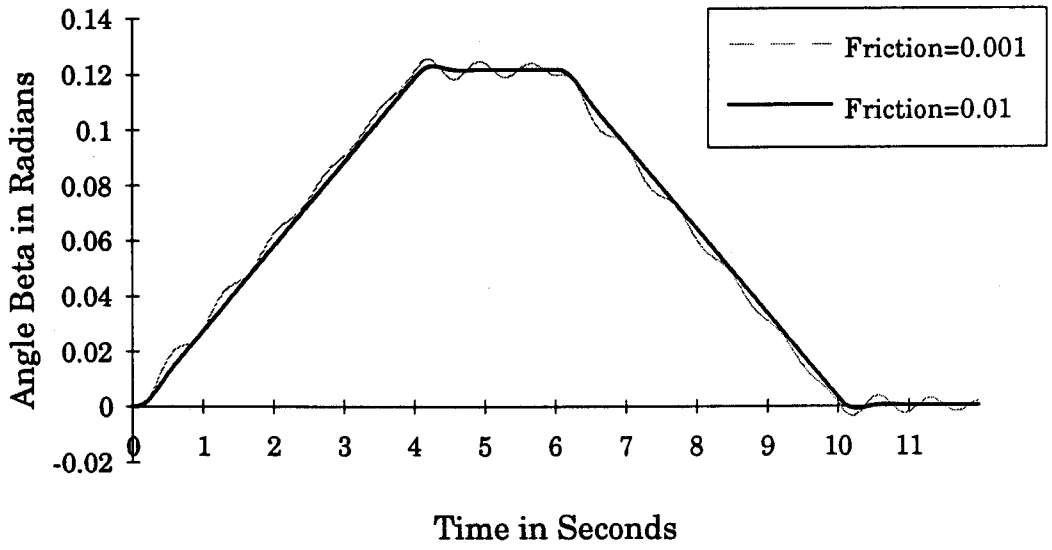

Figure 3.12: Offset of the damped pendulum.

Fig. 3.13 shows a quadratic acceleration function of the pivoting point. For $0 < t \leq 4$ acceleration is increasing, for $4 < t \leq 6$ constant acceleration, for $6 < t \leq 10$ decreasing acceleration, and for $t > 10$ acceleration is zero,

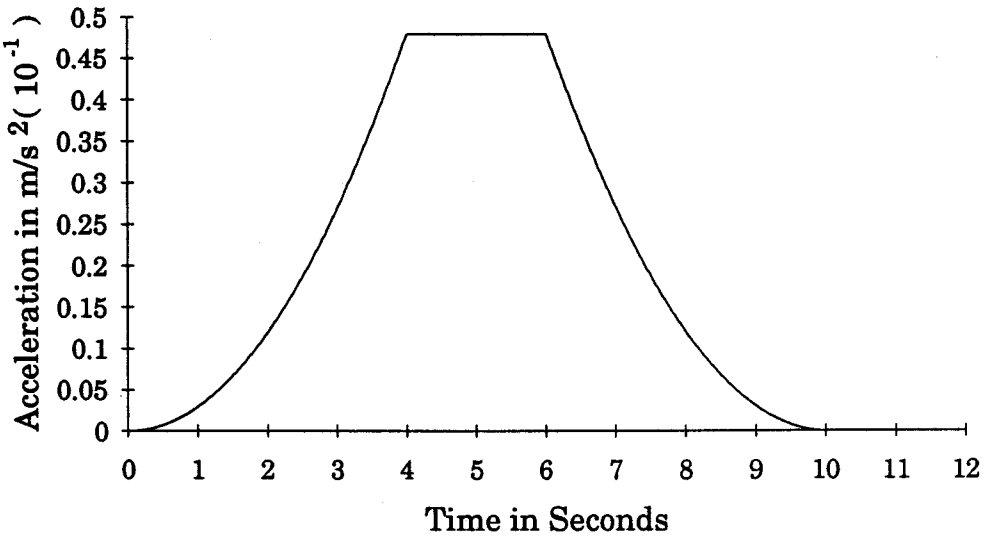

Figure 3.13: Quadratic acceleration function of pivot point.

Fig. 3.14 shows the angular offset of the pendulum. The dynamic behavior of the pendulum is similar to the acceleration function from 0 to 4 seconds, though the pendulum is not damped.

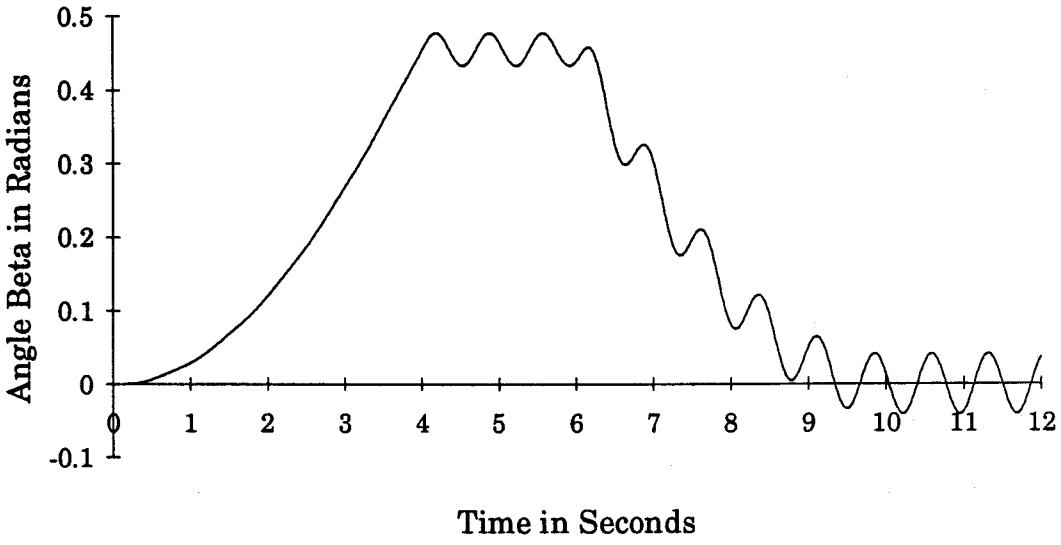

Figure 3.14: The behavior of the pendulum for the acceleration of pivoting point shown in Fig 3.13.

Fig. 3.15 shows the behavior of the pendulum for the acceleration function shown in Fig. 3.13, when the pendulum is damped,

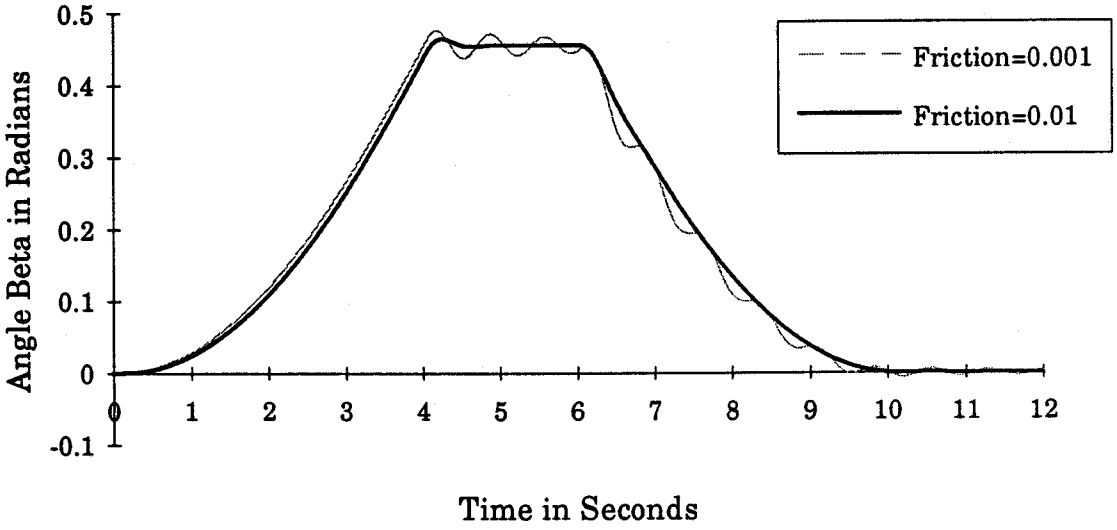

Figure 3.15: Angular offset of the pendulum with damping friction for Fig. 3.13.

Fig 3.17 shows the behavior of the pendulum when the pivoting point is oscillating at a frequency significantly lower than the natural frequency of the pendulum, Fig. 3.16, without damping friction at pivoting point. The pendulum experiences a SHM about the reference line that has been sinusoidally offset from the vertical position.

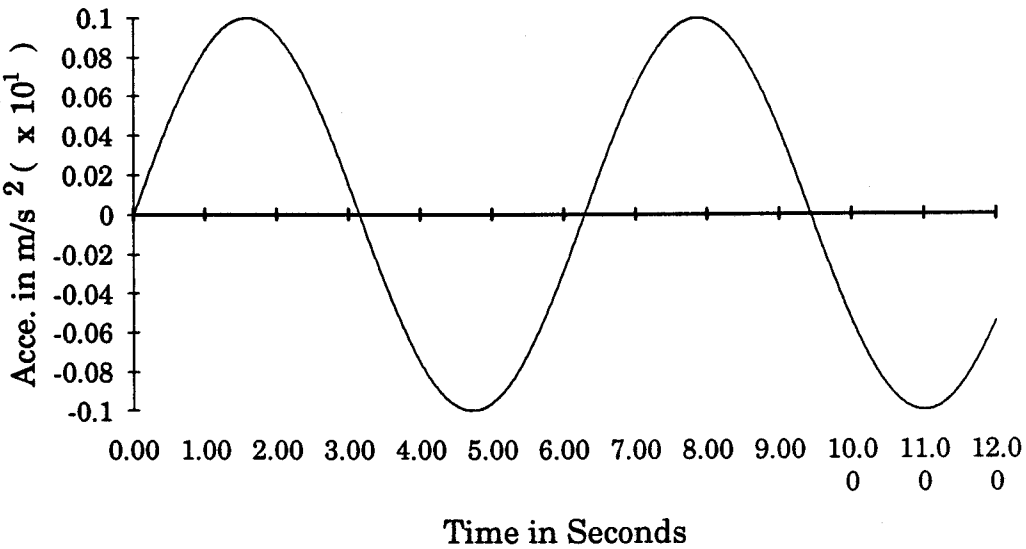

Figure 3.16: Sinusoidal acceleration of pivoting point.

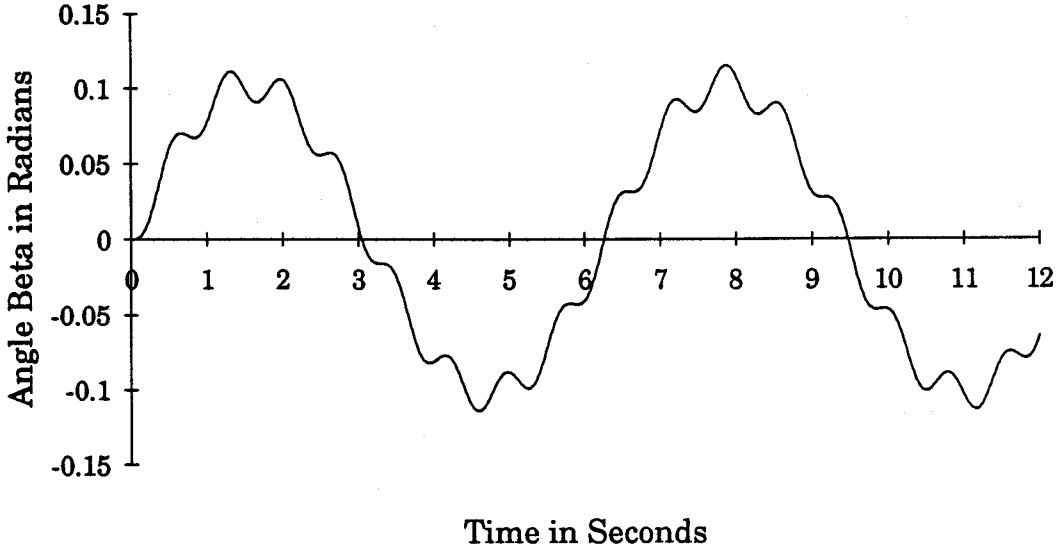

Figure 3.17: Angular offset of the pendulum with undamped SHM.

The SHM dies out after one period of the pivoting point when there is a sufficient velocity dependent friction at the pivoting point. The wave form of the pendulum's offset is a exact replica of the acceleration function, as shown in Fig. 3.18,

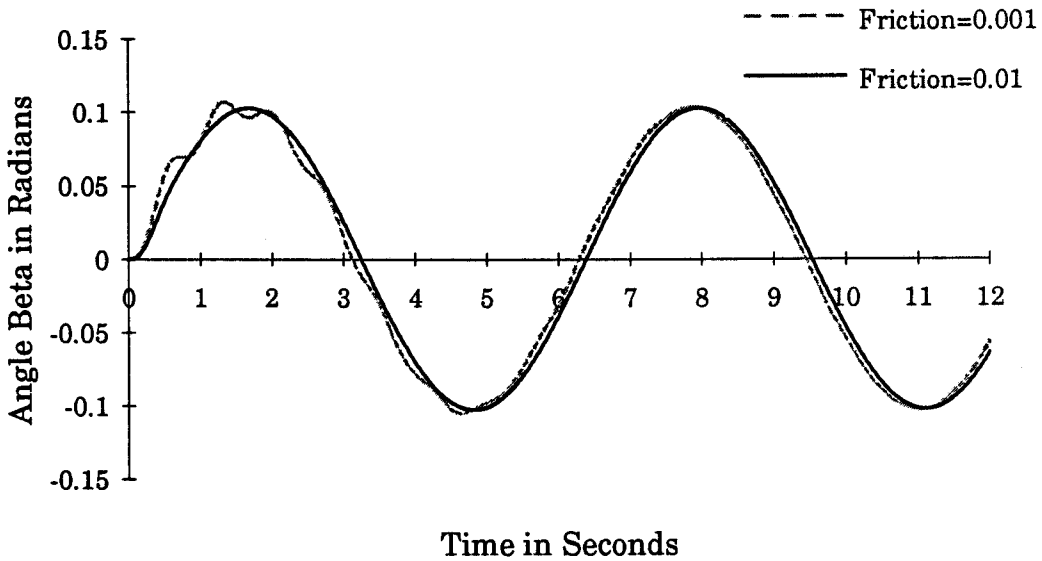

Figure 3.18: The offset of the pendulum with damping friction for Fig. 3.16.

From above results, it is evident that a relation between the acceleration function of the pivoting point and the offset angle can be made.

3.4 CONCLUDING REMARKS

This chapter has been devoted to the development of the mathematical model of the dynamic system. The importance of gravity direction in balance and the relationships between the terrain and the line of gravity were also shown and discussed. The dynamic behavior of a simple pendulum has been discussed. The behavior of a damped and undamped rigid pendulum has been shown. The new reference line used by the pendulum is offset, from the line of the gravity, when its pivoting point goes into motion. That makes the pendulum oscillate about a new reference line other than the line of gravity. The offsets of the pendulum from the vertical for various accelerations have been shown and discussed.

The next chapter uses the behavior of the simple pendulum and selects a model to achieve the dynamic balance of the inverted pendulum regardless of terrain conditions.

4. DESIGN OF INVERTED PENDULUM SYSTEM

4.1 INTRODUCTION

Balancing an inverted pendulum requires a reference; this reference is the line of gravity that passes through the point of hinging and the center of gravity of the inverted pendulum. The direction of gravity in horizontal terrain is orthogonal to the terrain surface; the gravity direction in a constant slope is fixed with respect to the terrain. The line of gravity in changing terrain is not necessarily orthogonal to the terrain surface, and the angle with the surface depends upon the terrain gradients. Thus, the balance task in horizontal terrains is to bring the inverted pendulum into an orthogonal position. This requires a control torque which is applied in the opposite direction of the pendulum's angular acceleration. On the other hand, the balancing of the inverted pendulum in changing terrains requires the detection of the line of gravity.

The dynamic behavior of a simple pendulum could be used to detect the line of gravity in changing terrain. As described in Chapter 3, a simple pendulum with velocity dependent friction at the pivoting point always returns to rest on the line of gravity. The inertial information obtained from the simple pendulum could be employed to locate the direction of gravity in a changing terrain. Hence, the balancing of the inverted pendulum in changing terrain could be carried out by using an enclosed inertial element.

This chapter deals with the design of an inverted pendulum system which balances itself in a changing terrain.

4.2 DESIGN OF AN ACTIVELY BALANCED INVERTED PENDULUM SYSTEM

4.2.1 Purpose

Robot carts, which have stable posture, have been in used for decades in automated factories and other highly-structured environments. Most of the automated carts in present use, however, are not really autonomous but rely on "tracks" imbedded in or painted on the floor for navigation. These carts have a stable attitude on four wheels or tripod systems which gives a static stability. Their mobility has been confined to a pre-planned, structured trajectory, and the statically stable cart is mobile only in structured terrains. Thus, these carts can not be operated safely in an environment where the terrain is changing and unstructured.

Environmental uncertainties dominate the problem domain of the autonomous mobile robot; the terrain is one of the uncertainties that limit the operation of these robots. Researchers have realized the importance of an autonomous mobile robot that acts like a human or other higher animal in dealing with unstructured and hostile environments where statically stable robots might not be suitable.

Balancing the body attitude of an unstable autonomous mobile vehicle is a primary task. The body is required to be balanced in the vertical position regardless of the terrain shape and structure. The body of such robots can be considered like an inverted pendulum hinging at the support.

The purpose of this design is to test a method of detecting the direction of gravity so that the balancing of an inverted pendulum could be achieved regardless the terrain conditions. This design could be employed to solve the balance problem of an unstable autonomous mobile robot.

4.2.2 The Inverted Pendulum System

Generally, a single link inverted pendulum system consists of a distributed mass rigid pole hinging on a free support. The center of mass, above the point of hinging, causes the pole to be very unstable about the vertical. The inverted pendulum becomes more unstable if the point of hinging is dynamic. In this condition, the system has two degrees of freedom. The angular position of the inverted pendulum with the vertical can be considered to be a function of the first and second derivatives of the angular position of the inverted pendulum and the linear position of the hinging point. The system could be represented by two degrees of freedom and two dynamic equations. The cart-pole system is an example of an inverted pendulum with a dynamic point of hinging.

4.2.3 Design Consideration

An important consideration in the design of an inverted pendulum system is the mode of operation. An inverted pendulum system can be made to operate in a constrained or structured environment where the direction of gravity is known. Only a control torque is then needed about the point of hinging of the inverted pendulum to regulate the body position about the balanced position. The inverted pendulum system in this study is required to be mobile in an unstructured environment. Four wheel carts may not always be suitable in changing terrains since without adjustments they may fall over. A single wheel mobile system, a unicycle, is better than a multi-wheel system and can make various types of motion.

The second consideration in the design is the orientation of the inverted pendulum in the inertial frame. The angular position of the inverted pendulum should be measured from the vertical in the inertial frame. Thus, a reference line is required to measure the angular position of the inverted pendulum with the vertical, regardless of terrains.

The third consideration in the design is sensing the direction of gravity. The direction of gravity is always orthogonal to the surface in

horizontal terrain because of the zero gradient, but not orthogonal to the surface of terrain in changing terrains.

4.2.4 Sensor

The balance task for the inverted pendulum is to keep it in the vertical position against the pull of gravity and other perturbing forces appearing externally. As discussed and shown in the third chapter, a simple pendulum behaves like an inertial element to detect the vertical. Its dynamic behavior could be used to detect the direction of the gravity in a changing terrain.

The pendulum experiences a SHM about the line of gravity when it is excited and eventually comes to rest at the line of gravity if damping is present at the pivoting point. The pendulum with a dynamic pivoting point will experience this SHM about a new reference line which is offset from the line of gravity. The angular position of this new reference line with the vertical, about which the pendulum oscillates, depends upon the linear acceleration of the pivoting point. This important dynamic behavior will be used in this design to detect the direction of gravity.

The dynamic behavior of the simple pendulum, represented by Eq. 3.8 shows the offset of the pendulum from the vertical position. This offset can be estimated by measuring the acceleration of the pivoting point, as shown in Fig. 3.10 through Fig. 3.18. The relationship between the offset angle and the acceleration of the pivoting point can be established within the constrained motion.

Two types of sensing techniques are required to locate the vertical; the accelerometer for translational motion of the hinging point and the inertial sensor for the angular position of the inverted pendulum. The information extracted from these systems, is used to find the vertical in a changing terrain, where the direction of the gravity is not necessarily constant with respect to the terrain surface.

4.3 SYSTEM MODELING AND DESCRIPTION

An inverted pendulum system hinging at the axle of a wheel has been used to study the balance problem in changing terrain. A simple rigid pendulum is used as a sensor to detect the direction of gravity. The proposed system has been studied in flat and unknown terrains.

4.3.1 The Inverted Pendulum System in a Horizontal Terrain

The mathematical model of the inverted pendulum system that is being used consists of the following mechanical components:

i) a distributed mass, m_{IP}, inverted pendulum. The center of mass is located at the distance l_{IP}, measured from the point of support

ii) a wheel of mass, m_C , concentrated in a ring at radius r,

iii) an inertial element, basically a rigid simple pendulum of mass, m_P, located at l_P (measured from pivot point) pivoting at the axle of the wheel.

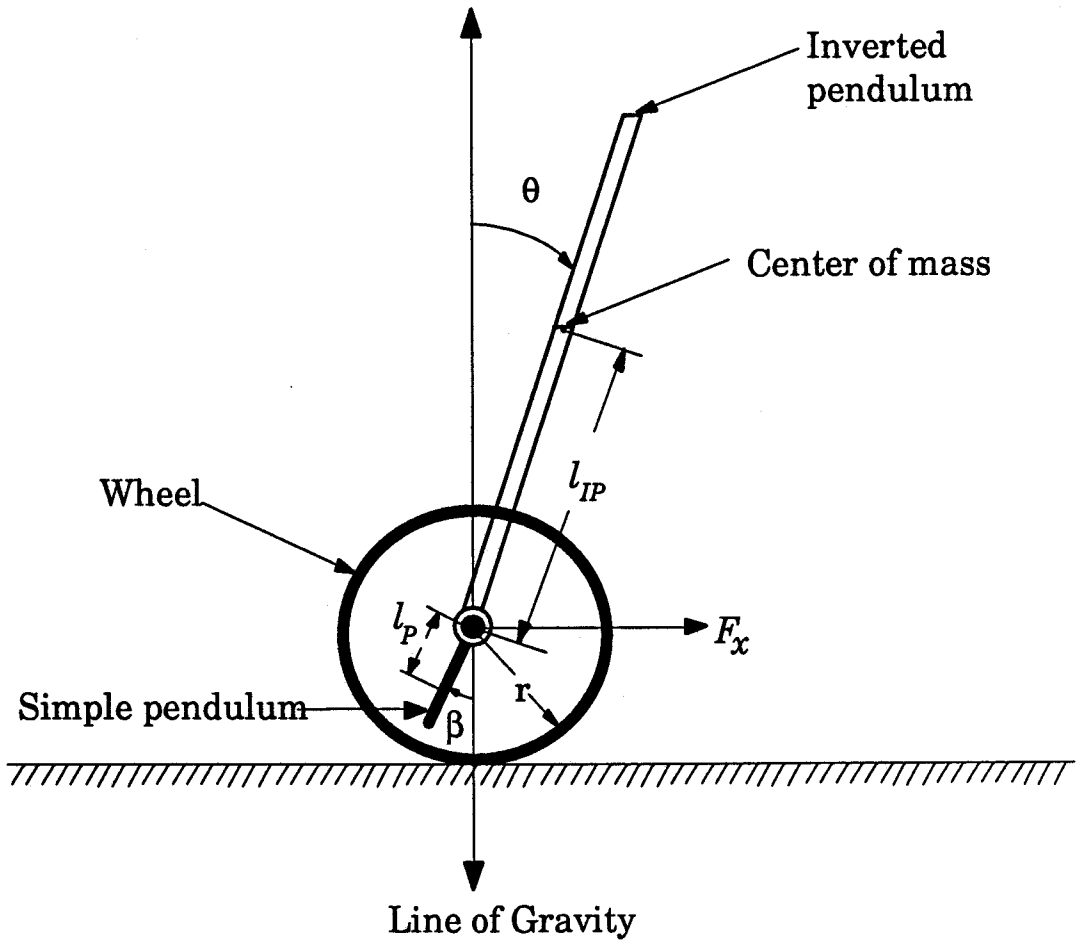

Figure 4.1: Model of an inverted pendulum system with an inertial element.

The mathematical model of the system, shown in Fig. 4.1, in a horizontal terrain is represented by three non-linear coupled differential equations. These equations have been constructed using the Lagrangian method under the following assumptions:

i) All mechanical parts are rigid and the system is two dimensional.

ii) The driving torque about the point of hinging of the inverted pendulum has been applied between the axle and the inverted pendulum. Thus a single driving system is used.

iii) A velocity dependent damping force has been used to damp the SHM of the simple pendulum (inertial element).

iv) Friction force is exerted by the ground, and the friction force generated at the pivot of the simple pendulum is velocity dependent.

v) Three generalized coordinates θ, β, and x represents the three degrees of freedoms in the system.

vi) The system parameters are defined in the Table 4.1.

Table 4.1 Nomenclature for the system, Fig. 4.1

Symbol	Description	Unit
x	distance traveled by cart	*meter*
θ	angular offset of inverted pendulum from vertical	*radian*
β	angular offset of simple pendulum from vertical	*radian*
m_{IP}	mass of inverted pendulum	*kg*
m_P	mass of simple pendulum	*kg*
m_C	mass of cart, wheel	*kg*
J_{IP}	moment of inertia of inverted pendulum	$kg\text{-}m^2$
J_P	moment of inertia of simple pendulum	$kg\text{-}m^2$
J_w	moment of inertia of wheel	$kg\text{-}m^2$
l_{IP}	distance of center of mass from point of hinging	*meter*
l_P	distance of center of mass from pivot	*meter*
r	radius of wheel	*meter*
g	gravity acceleration	$9.8\ meter/sec^2$
c_1	friction coefficient of inverted pendulum	$kg\text{-}m^2/sec$
c_2	friction coefficient at pivoting point of regular	$kg\text{-}m^2/sec$
c_3	friction coefficient exerted by ground on wheel	$kg\text{-}m^2/sec$
$\dot{x}$	linear velocity of cart	*meter/sec*
$\dot{\theta}$	angular velocity of inverted pendulum	*radian/sec*
$\dot{\beta}$	angular velocity of simple pendulum	*radian/sec*

Mathematical Model

The mathematical model of Fig. 4.1 is shown in Eq. 4.13. The kinetic, potential, and dissipative energies are given for the inverted pendulum, simple pendulum, and for the cart as follows:

1) *for the inverted pendulum,*

kinetic energy,

$$T_1 = \frac{1}{2} J_{IP} \dot{\theta}^2 + \frac{1}{2} m_{IP} \left\{ \left[\frac{d}{dt} \left(x + l_{IP} \sin(\theta) \right) \right]^2 + \left[\frac{d}{dt} \left(l_{IP} \cos(\theta) \right) \right]^2 \right\}, \qquad (4.1\text{-a})$$

potential energy,

$$P_1 = m_{IP} \; l_{IP} \; g \cos(\theta), \qquad (4.1\text{-b})$$

dissipation energy,

$$D_1 = \frac{1}{2} c_1 \dot{\theta}^2, \qquad (4.1\text{-c})$$

where c_1 is the coefficient of friction of the inverted pendulum on the axle as defined in Table 4.1.

2) *for the simple pendulum,*

kinetic energy,

$$T_2 = \frac{1}{2} J_P \dot{\beta}^2 + \frac{1}{2} m_P \left\{ \left[\frac{d}{dt} \left(x - l_P \sin(\beta) \right) \right]^2 + \left[\frac{d}{dt} \left(l_P \cos(\beta) \right) \right]^2 \right\}, \qquad (4.2\text{-a})$$

potential energy,

$$P_2 = -m_P \; l_P \; g \cos(\beta), \qquad (4.2\text{-b})$$

dissipation energy,

$$D_2 = \frac{1}{2} c_2 \dot{\beta}^2, \qquad (4.2\text{-c})$$

where c_2 is the coefficient of friction of the simple pendulum at the pivot as defined in Table 4.1.

3) *for the wheel,*

kinetic energy,

$$T_3 = \frac{1}{2} m_c \dot{x}^2 + \frac{1}{2} J_w \omega^2,$$

where the subscript *IP* and *P* denote the inverted pendulum and simple pendulum respectively:

If the wheel is rolling on the ground and the ground is exerting sufficient static friction to avoid slip, the linear acceleration of the wheel is limited by the relation:

$$F_x \leq \mu_s N,$$

where μ_s is the coefficient of static friction, and N is the normal force.

If the wheel is rolling without slip, the relation between the linear acceleration of the axle and the angular acceleration of the wheel can be given as,

$$\dot{x} = r\dot{\phi}_w = r\omega, \quad \therefore \quad \omega = \frac{\dot{x}}{r},$$

$$\ddot{x} = r\ddot{\phi}_w = r\dot{\omega}, \quad \therefore \quad \ddot{\phi}_w = \frac{\ddot{x}}{r},$$

where $\dot{\phi}_w$ or ω is the angular velocity of the wheel in rad/sec.

Therefore,

$$T_3 = \frac{1}{2} m_c \dot{x}^2 + \frac{1}{2} J_w \left(\frac{\dot{x}}{r}\right)^2 \tag{4.3-a}$$

potential energy, $P_3 = 0$

Total kinetic energy T,

$$T = \sum_{i=1}^{3} T_i ,$$

$$\begin{aligned} &= \frac{1}{2}\left(m_{IP} + m_p + m_c + \frac{J_w}{r^2}\right)\dot{x}^2 + \frac{1}{2}\left(m_{IP}\ l^2{}_{IP} + J_{IP}\right)\dot{\theta}^{\,2} + \\ &\frac{1}{2}\left(m_p\ l^2{}_P + J_P\right)\dot{\beta}^{\,2} + m_{IP}\ l_{IP}\cos(\theta)\dot{x}\dot{\theta} - m_p\ l_p\cos(\beta)\dot{x}\dot{\beta}. \end{aligned} \tag{4.4}$$

Total potential energy P,

$$\begin{aligned} P &= \sum_{i=1}^{3} P_i , \\ &= m_{IP}\ l_{IP}\ g\cos(\theta) - m_P\ l_P\ g\cos(\beta). \end{aligned} \tag{4.5}$$

Total dissipation energy D,

$$\begin{aligned} D &= \sum_{i=1}^{3} D_i , \\ &= \frac{1}{2}\left(c_1\dot{\theta}^{\,2} + c_2\,\dot{\beta}^{\,2}\right). \end{aligned} \tag{4.6}$$

From the Lagrangian method, Appendix A, the system equations can be written as:

$$\begin{aligned} &\left(m_{IP} + m_P + m_c + \frac{J_w}{r^2}\right)\ddot{x} + m_{IP}\ l_{IP}\cos(\theta)\ddot{\theta} - m_P\ l_P\cos(\beta)\ddot{\beta} \\ &- m_{IP}\ l_{IP}\sin(\theta)\dot{\theta}^{\,2} + m_P\ l_P\sin(\beta)\dot{\beta}^{\,2} = F_x , \end{aligned} \tag{4.7}$$

$$m_{IP}\ l_{IP}\ \cos(\theta)\ddot{x}+\left(m_{IP}\ l^2{}_{IP}+J_{IP}\right)\ddot{\theta}-m_{IP}\ l_{IP}\ g\sin(\theta) +c_1\dot{\theta}=-\tau, \tag{4.8}$$

$$m_P\ l_P\ \cos(\beta)\ddot{x}-(m_P\ l^2{}_P+J_P)\ddot{\beta}-m_P\ l_P\ g\sin(\beta)-c_2\ \dot{\beta}=0, \tag{4.9}$$

In Eq. 4.7 the force F_x is the resultant reaction force appearing in x coordinate. Similarly, τ is the applied torque between the inverted pendulum and the axle.

The above three equations, (4.7), (4.8), and (4.9) can be written in matrix form as:

$$K_1[\ddot{q}]=K_2[\dot{q}]+K_3[\dot{q}^2]+K_4, \tag{4.10}$$

where,

$q=[x\ \ \theta\ \ \beta]^T$, and

$$K_1=\begin{bmatrix}\left(m_{IP}+m_P+m_c+\frac{J_w}{r^2}\right) & m_{IP}\ l_{IP}\ \cos(\theta) & -m_P\ l_P\ \cos(\beta)\\ m_{IP}\ l_{IP}\ \cos(\theta) & \left(m_{IP}\ l^2{}_{IP}+J_{IP}\right) & 0\\ m_P\ l_P\ \cos(\beta) & 0 & -\left(m_P\ l^2{}_P+J_P\right)\end{bmatrix},$$

$$K_2=\begin{bmatrix}0 & 0 & 0\\ 0 & -c_1 & 0\\ 0 & 0 & c_2\end{bmatrix},$$

$$K_3=\begin{bmatrix}0 & m_{IP}\ l_{IP}\ \sin(\theta) & -m_P\ l_P\ \sin(\beta)\\ 0 & 0 & 0\\ 0 & 0 & 0\end{bmatrix},$$

$$K_4 = \begin{bmatrix} F_x \\ m_{IP}\ l_{IP}\ g\sin(\theta) - \tau \\ m_P\ l_P\ g\sin(\beta) \end{bmatrix}.$$

The mathematical model of the inverted pendulum system, Fig. 4.1, in horizontal terrain is given by,

$$[\ddot{q}] = K_1^{-1}\left[K_2[\dot{q}] + K_3[\dot{q}^2] + K_4\right]. \tag{4.11}$$

4.3.2 Relation Between The Control Torque and Linear Force

The system is driven by a control torque about the pivot point. This control torque, applied to the axle with respect to the inverted pendulum, produces a force that causes the axle to move, as shown in Fig. 4.2,

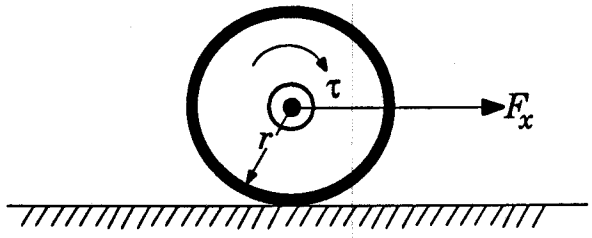

Figure 4.2: Wheel.

The relationship between the control torque, τ, and the translational force, F_x can be written as,

$$\tau = J_w\ddot{\phi}_w + F_x\ r,$$

or,

$$F_x = \frac{\tau}{r} - \frac{J_w}{r}\ddot{\phi}_w,$$

since,

$$\ddot{\phi}_w = \frac{\ddot{x}}{r},$$

therefore,

$$F_x = \frac{\tau}{r} - J_w \frac{\ddot{x}}{r^2}. \tag{4.12}$$

Eq. 4.7 and Eq. 4.8 can be modified considering single torque applied between the inverted pendulum and the axle appears in Eq. 4.7. Thus the torque component in the Eq. 4.8 is zero, because a single torque is applied in the system.

Hence, Eq. 4.7 and Eq. 4.8 can be rewritten as,

$$\begin{aligned}&\left(m_{IP} + m_P + m_c + 2\frac{J_w}{r^2}\right) r\,\ddot{x} + m_{IP}\, l_{IP}\, r\cos(\theta)\ddot{\theta} - m_P\, l_P\, r\cos(\beta)\ddot{\beta} \\ &\quad - m_{IP}\, l_{IP}\, r\sin(\theta)\dot{\theta}^2 + m_P\, l_P\, r\sin(\beta)\dot{\beta}^2 + c_3\, r\,\dot{x} = \tau.\end{aligned}, \tag{4.7}'$$

and

$$\begin{aligned}&m_{IP}\, l_{IP}\cos(\theta)\ddot{x} + \left(m_{IP}\, l^2{}_{IP} + J_{IP}\right)\ddot{\theta} - m_{IP}\, l_{IP}\, g\sin(\theta) \\ &\quad + c_1\dot{\theta} = 0,\end{aligned} \tag{4.8}'$$

4.3-3 Inverted Pendulum System in Changing Terrain

The system dynamics are different in a changing terrain where the slope angle, α, is included in the system characteristics,

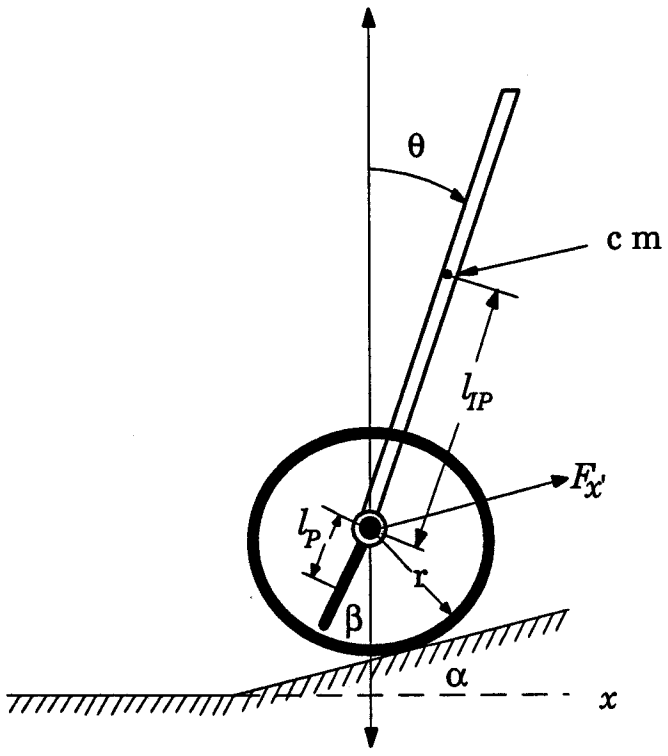

Figure 4.3: Inverted pendulum system in slope.

Fig. 4.3 shows the inverted pendulum system, Fig. 4.1, on a slope or in changing terrain.

Mathematical Model

The mathematical model of above system, Fig. 4.3, is similar to the mathematical model of Fig. 4.1 except the slope angle, α, can be included as,

$$\left(m_{IP}+m_P+m_c+\frac{J_w}{r^2}\right)\ddot{x}'+m_{IP}\ l_{IP}\ \cos(\theta+\alpha)\ddot{\theta}-m_P\ l_P\ \cos(\beta+\alpha)\ddot{\beta}$$
$$-m_{IP}\ l_{IP}\ \sin(\theta+\alpha)\dot{\theta}^{\,2}+m_P\ l_P\ \sin(\beta+\alpha)\dot{\beta}^{\,2}= \qquad (4.13)$$
$$F_x'-\left(m_{IP}+m_P+m_c\right)\ g\sin(\alpha),$$

$$m_{IP}\ l_{IP}\ \cos(\theta+\alpha)\ddot{x}'+\left(m_{IP}\ l^2{}_{IP}+J_{IP}\right)\ddot{\theta}-m_{IP}\ l_{IP}\ g\sin(\theta) \qquad (4.14)$$
$$+c_1\dot{\theta}=-\tau,$$

$$m_P\ l_P\ \cos(\beta+\alpha)\ddot{x}' - (m_P\ l^2{}_P + J_P)\ddot{\beta} - m_P\ l_P\ g\sin(\beta) - c_2\dot{\beta} = 0, \qquad (4.15)$$

where $\ddot{x}'$ is the acceleration of axle in slope.

The mathematical model of the inverted pendulum system, Fig. 4.3, is still given by,

$$[\ddot{q}] = K_1^{-1}\left[K_2[\dot{q}] + K_3[\dot{q}^2] + K_4\right], \qquad (4.16)$$

where,

$$K_1 = \begin{bmatrix} \left(m_{IP} + m_P + m_c + \frac{J_w}{r^2}\right) & m_{IP}\ l_{IP}\ \cos(\theta+\alpha) & -m_P\ l_P\ \cos(\beta+\alpha) \\ m_{IP}\ l_{IP}\ \cos(\theta+\alpha) & \left(m_{IP}\ l^2{}_{IP} + J_{IP}\right) & 0 \\ m_P\ l_P \cos(\beta+\alpha) & 0 & -\left(m_P\ l^2{}_P + J_P\right) \end{bmatrix},$$

$$K_2 = \begin{bmatrix} 0 & 0 & 0 \\ 0 & -c_1 & 0 \\ 0 & 0 & c_2 \end{bmatrix},$$

$$K_3 = \begin{bmatrix} 0 & m_{IP}\ l_{IP}\ \sin(\theta+\alpha) & -m_P\ l_P\ \sin(\beta+\alpha) \\ 0 & 0 & 0 \\ 0 & 0 & 0 \end{bmatrix}, \text{ and}$$

$$K_4 = \begin{bmatrix} F_x - \left(m_{IP} + m_P + m_c\right) g\sin(\alpha) \\ m_{IP}\ l_{IP}\ g\sin(\theta) - \tau \\ m_P\ l_P\ g\sin(\beta) \end{bmatrix}.$$

The system equations, Eq. 4.11 and Eq. 4.16, are very non-linear and coupled. The analytical solution of the non-linear coupled equations has been solved using a numerical method.

4.4 EULER-TRAPEZOIDAL NUMERICAL SOLUTION

The Euler-Trapezoidal method is a predictor-corrector numerical method in which an initial prediction of the system variable is corrected by an iterative process to find a new point in the solution. The algorithm for this method is given by [47],

$$y_1^{(r+1)} = y_0 + \frac{h}{2}\left(f(x_0, y_0) + f(x_0 + h, y_1^{(r)})\right). \tag{4.17}$$

The derivation of Eq. 4.17 is given in Appendix B.

4.5 SIMULATION

Several preliminary simulations were carried out for the system in a variety of initial conditions. These simulations were done to help understand the behavior of the inverted pendulum system. They also served as a check on the validity of the models.

Simulations based on the mathematical model Eq. 4.11 have been carried out using the Euler-Trapezoidal numerical integration and Backward-Difference method, given in Appendix C, for numerical differentiation, on a customized software written in C++ on a SUN workstation. This simulation has been carried out in near real time with a time increment of two hardware clock tics, 32 ms of the UNIX workstation. The samples were taken at the rate of 20 samples per period of system characteristics frequency. The simulations have been done during low traffic so that the CPU is involved primarily in the simulation. This consideration satisfied the requirements for real time simulation of the system mathematical model. The simulation results for different initial conditions are given below, with the parameters of the simulation listed in Table 4.2.

This simulation considers the system dynamic behavior when the inverted pendulum starts from an initial state. The inverted pendulum is allowed to fall by only ±5 degrees from the vertical in the simulation program. A control torque has not been used in this simulation.

Table 4.2 System Parameters

m_{IP}	10.0 kg	τ	0.0 N-m
m_P	0.1 kg	J_{IP}	3.33 kg-m^2
m_C	1.0 kg	J_P	3.3 x 10^{-4} kg-m^2
l_{IP}	1.0 m	J_w	5 x10^{-3} kg-m^2
l_P	0.1 m	c_1	0.0 kg-m^2/sec
r	0.1 m	c_2	0.0 kg-m^2/sec

The ground plane provides sufficient amount of static friction, μ_s to avoid wheel slip. All velocity dependent friction coefficients are set to zero in this simulation.

4.5.1 Simulation in Flat / Horizontal Terrain

Simulation 1

The simulation in Fig. 4.4 through Fig. 4.6 has been done using the initial conditions for the system in Fig. 4.1, listed in Table 4.3.

Table 4.3 Initial value

$\theta_0 = 1.7\times10^{-4}$ *radians*
$\dot{\theta}_0 = 0.0$ *radian/sec.*
$\beta_0 = 0.0$ *radians*
$\dot{\beta}_0 = 0.0$ *radian/sec.*
$\dot{x}_0 = 0.0$ *meter/sec.*

The initial angle, θ_0, of the inverted pendulum with the vertical allows it to accelerate towards the ground; the inverted pendulum accelerates rapidly after 0.4 second, as shown in Fig. 4.4,

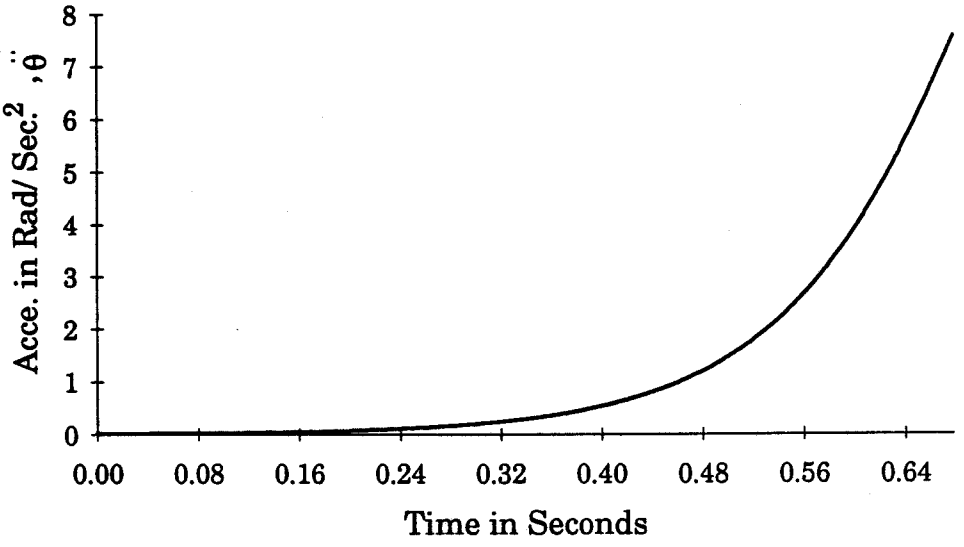

Figure 4.4: Angular acceleration of inverted pendulum with vertical.

Fig. 4.5 shows the angular position of the inverted pendulum with the vertical,

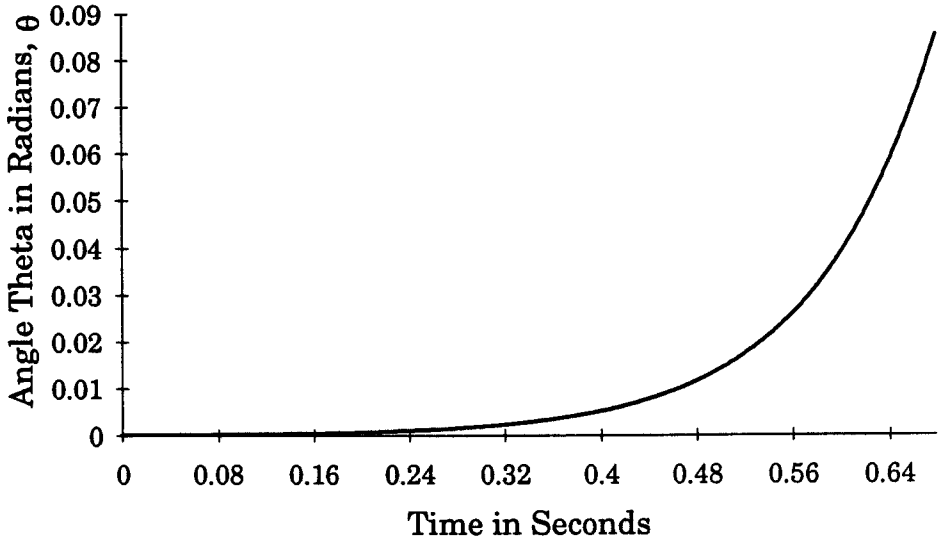

Figure 4.5: Angle of inverted pendulum with vertical.

The acceleration of the inverted pendulum affects the linear acceleration of the axle, as shown in Fig. 4.6,

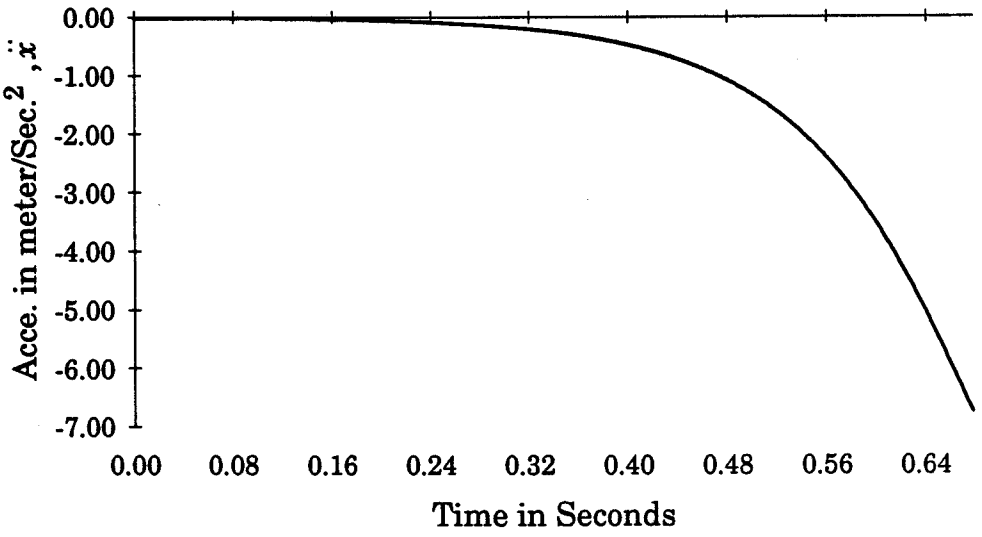

Figure 4.6: Linear acceleration of axle

The two curves, Fig. 4.4 and Fig. 4.6 show that there is close relationships between the dynamics of the inverted pendulum and the axle. This information is necessary for balance control.

Simulation 2

The simulation in Fig. 4.7 through Fig. 4.9 has been done using the initial conditions for the system in Fig. 4.1, listed in Table 4.4,

Table 4.4: Initial value

$\theta_0 = 0.0$ *radians*
$\dot{\theta}_0 = 0.0$ *radian/sec.*
$\beta_0 = 1.7 \times 10^{-3}$ *radians*
$\dot{\beta}_0 = 0.0$ *radian/sec.*
$\dot{x}_0 = 0.0$ meter/sec.

Initially, the angle $\theta_0 = 0$, and the lower pendulum is oscillating about the vertical starting with an initial angle of 0.1 degree. This oscillation

makes the axle to move, as shown in Fig. 4.7, which results in the acceleration of the inverted pendulum, as shown in Fig. 4.8,

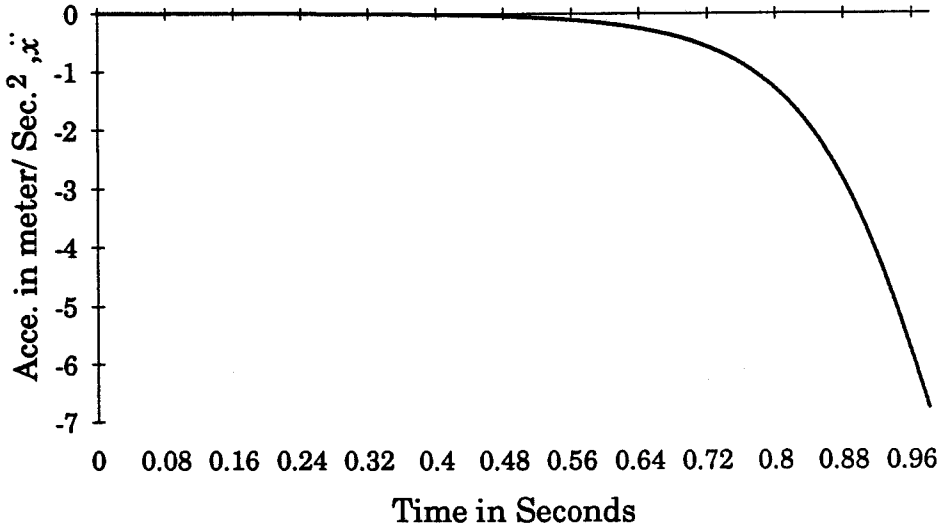

Figure 4.7: Linear acceleration of axle.

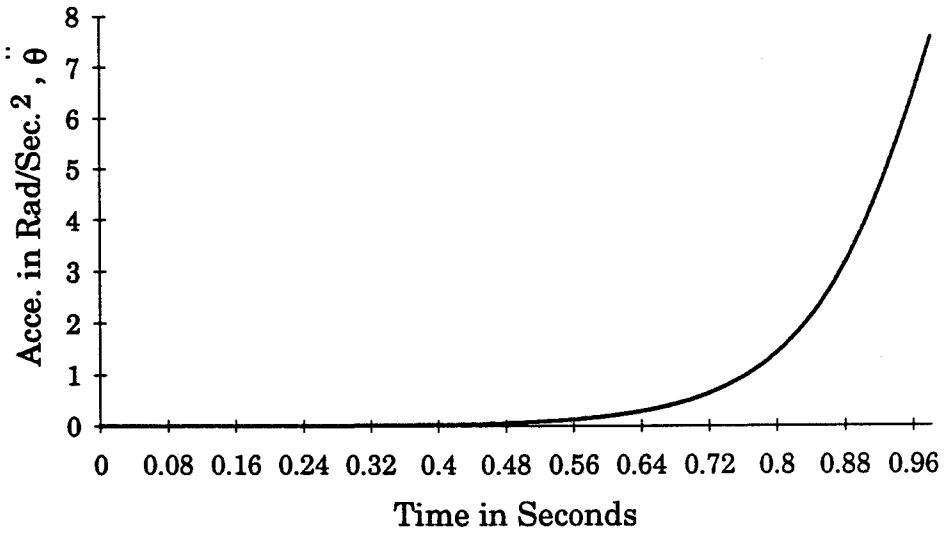

Figure 4.8: Angular acceleration of inverted pendulum with vertical.

Fig. 4.9 shows the angular position of the inverted pendulum with the vertical,

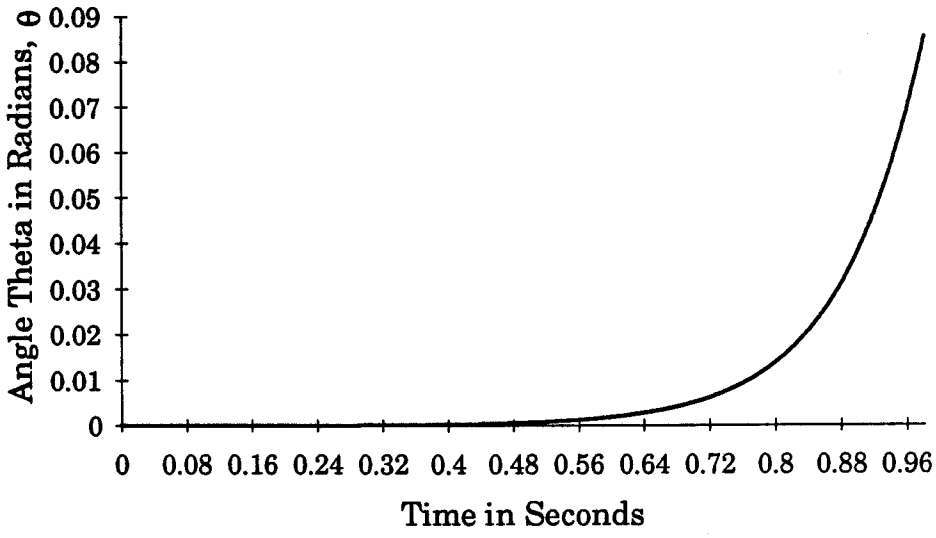

Figure 4.9: Angle of inverted pendulum with vertical.

Hence, from the above results, it can be seen that the acceleration of the inverted pendulum is dependent both upon the initial angular position of the inverted pendulum and the motion of the simple pendulum.

4.5.2 Simulation on a Slope

The dynamic behavior of the inverted pendulum is different when it is operating on a slope, as shown in Fig. 4.3; the terrain gradient is very important as can be seen in the following cases. Simulation of the mathematical model, Eq. 4.16, of Fig. 4.3 has been carried out with the system parameters listed in the Table 4.5. The slope gradient is known in the simulation program.

The simulation in Fig. 4.10 through Fig. 4.12 has been done using the initial conditions for the system in Fig. 4.3, listed in Table 4.5.

Table 4.5 Initial value

$\theta_0 = 1.7 \times 10^{-4}$ *radians*
$\dot{\theta}_0 = 0.0$ *radian/sec.*
$\beta_0 = 0.0$ *radians*
$\dot{\beta}_0 = 0.0$ *radian/sec.*
$\dot{x}_0 = 0.0$ *meter/sec.*
$\alpha = 87.26 \times 10^{-3}$ *radians*

The terrain slope is 5 degrees and the applied control torque is zero. These conditions result in the axle accelerating in the reverse direction, as shown in Fig. 4.10,

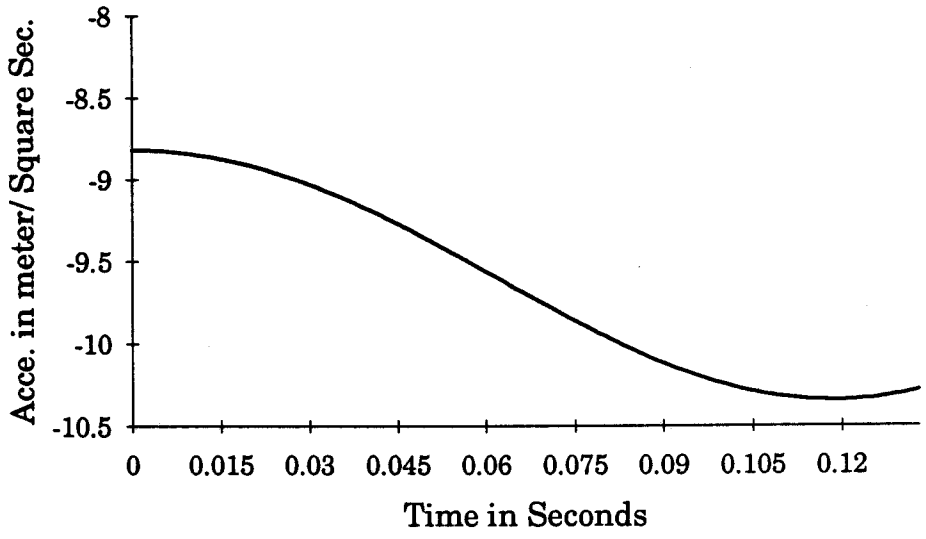

Figure 4.10: Linear acceleration of axle

In this situation the inverted pendulum accelerates towards the forward direction, as shown in Fig. 4.11,

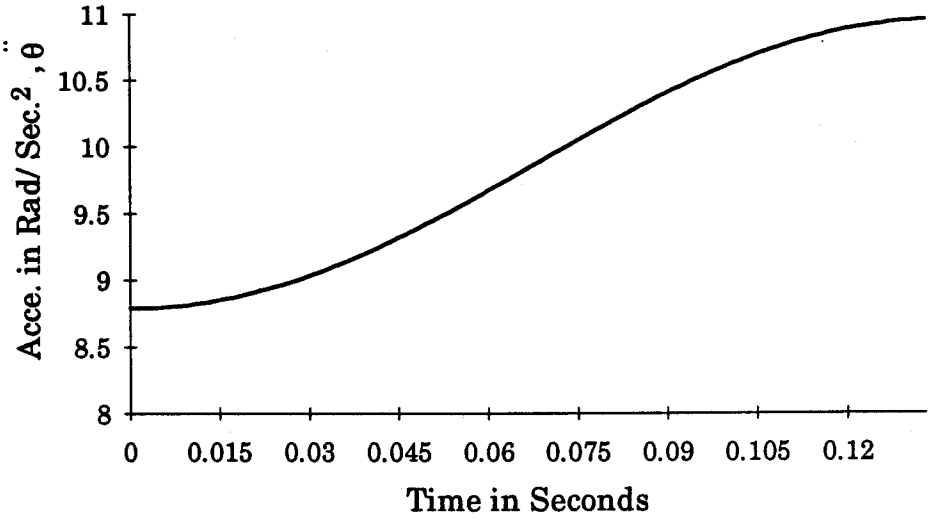

Figure 4.11: Angular acceleration of inverted pendulum with vertical.

Fig. 4.12 shows the angular position of the inverted pendulum with the vertical,

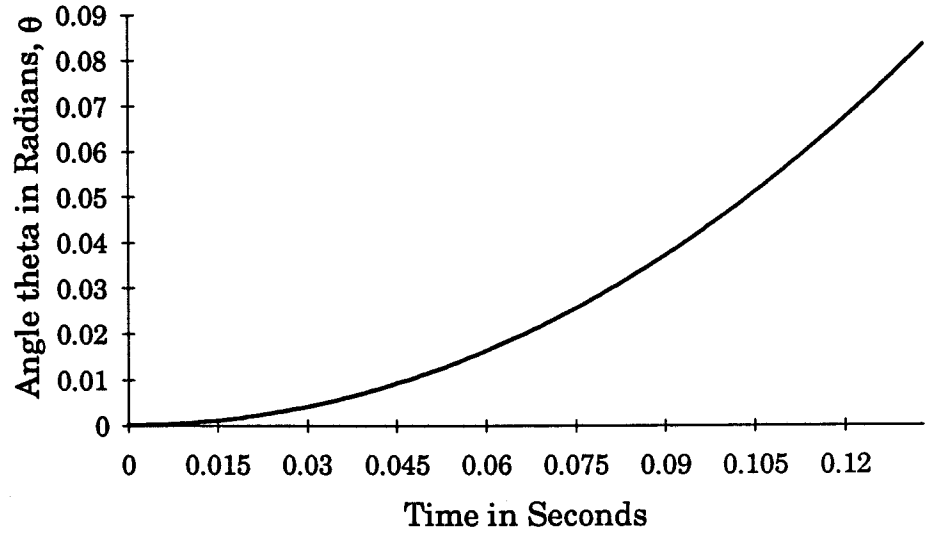

Figure 4.12: Angle of inverted pendulum with vertical.

All the above simulations were carried out taking the known vertical as a reference. This reference is always constant if the terrain is flat. The measurement or localization of this vertical position now has to be done when the system is operating in a changing terrain.

4.6 MEASUREMENT OF POSITION OF THE INVERTED PENDULUM IN CHANGING TERRAIN

The simulation, so far, was carried out on the assumption of α, the terrain gradient. The assumption of this angle is not possible when the terrain gradient is not previously known. The task of balancing the inverted pendulum is to regulate it within a small angular offset from the vertical or upright position. The vertical position or line of gravity, with respect to the terrain, depends upon the terrain gradient, α; this gradient is very important in the balance of the inverted pendulum.

The inertial element, the simple pendulum has been used in the proposed model, Fig. 4.3, to locate the direction of gravity. Hence, the angular offset of the inverted pendulum can be measured, only with the simple pendulum Fig. 4.13.

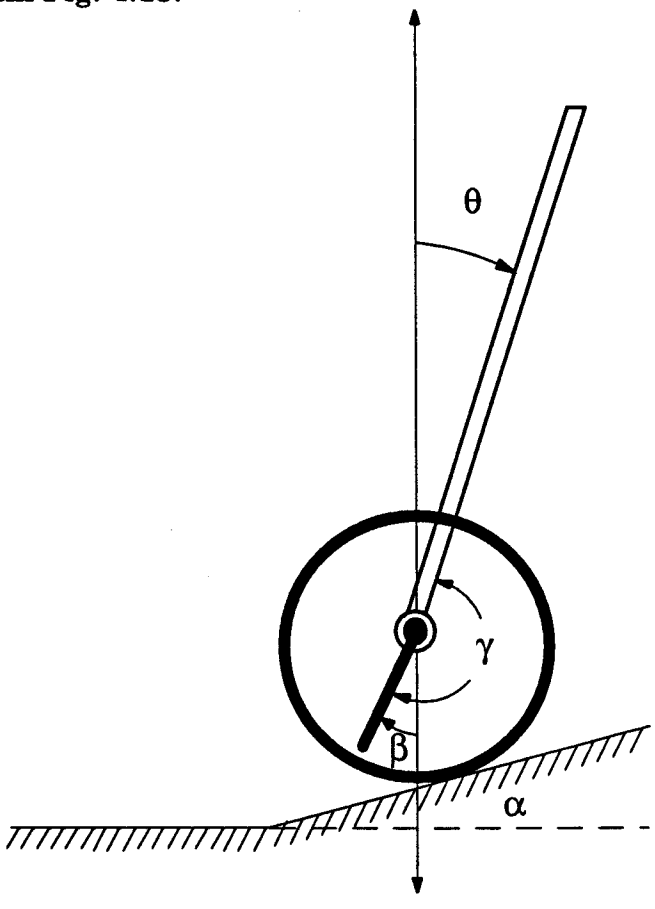

Figure 4.13: Measurement of imbalance of inverted pendulum.

Fig. 4.13 shows the position of the inverted pendulum. The angle θ can be measured by the relation,

$$\theta = 180 + \beta - \gamma \quad \text{degrees} \tag{4.18}$$

where γ is the angle measured between the inverted pendulum and the simple pendulum.

At the rest condition, β=0 degrees, so

$$\theta = 180 - \gamma$$

and in motion, $\beta \neq 0$,

so in general,

$$\theta = 180 + \beta - \gamma. \tag{4.19}$$

4.6.1 Measurement of Gravity Direction in Changing Terrain

It has been assumed here that the direction of gravity on a slope is not perpendicular to the terrain surface but is offset by an angle α. The problem becomes more complex if the angle α is changing, as shown in Fig. 4.14,

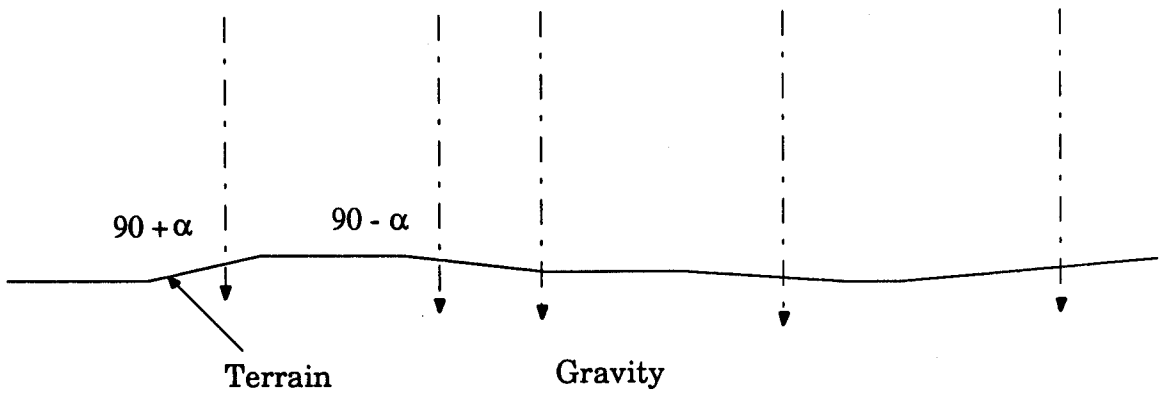

Figure 4. 14: The direction of gravity in changing terrain.

4.6.2 Estimation of Offset Angle, β

The natural behavior of the simple pendulum is to oscillate about the line of gravity that passes through the pivoting point and the center of mass of the pendulum. This behavior will be altered when the pivoting point is in motion, since the motion of the pivoting point causes an offset of the reference line from the vertical position. The pendulum experiences oscillation about the new reference line. The offset angle depends upon the linear acceleration of the pivoting point in the inertial frame, as shown in section 3.3.3 in third chapter.

4.6.3 Estimation of β in Horizontal Terrain

The system behavior of the simple pendulum in flat terrain, Fig. 4.1, is represented by the differential equation, Eq. 4.9,

$$m_P\ l_P\ \cos(\beta)\ddot{x} - (m_P\ l^2{}_P + J_P)\ddot{\beta} - m_P\ l_P\ g\sin(\beta) - c_2\ \dot{\beta} = 0. \qquad (4.9)$$

Eq. 4.9 is nonlinear and coupled with the linear acceleration, $\ddot{x}$. Thus, it can be used to show the relation between the pendulum's offset and the linear acceleration of axle. If the linear acceleration is limited to a maximum of 1 meter/sec^2 then it can be shown that the offset to the vertical will be confined within an acceptable range. Then Eq. 4.9 could be linearized as,

$$m_P\ l_P\ \ddot{x} - (m_P\ l^2{}_P + J_P)\ddot{\beta} - m_P\ l_P\ g\beta - c_2\dot{\beta} = 0. \qquad (4.20)$$

with $\cos(\beta) \cong 1$, $\sin(\beta) \cong \beta$, for $\beta \leq 5$ degrees

If the damping coefficient, c_2, at the pivoting point is sufficient then the pendulum's oscillation will be damped, Fig. 3.9. In order to make pendulum offset a function only of linear acceleration, the condition given below should be satisfied,

$$c_2\ \dot{\beta} = -(m_P\ l^2{}_P + J_P)\ddot{\beta},$$

or $$\frac{\ddot{\beta}}{\dot{\beta}} = -\frac{c_2}{(m_P l^2{}_P + J_P)},$$

then Eq. 4.20 can be written as,

$$m_P\ l_P\ \ddot{x} = m_P\ l_P\ g\beta,$$

$$\therefore \quad \beta \equiv \frac{\ddot{x}}{g}. \tag{4.21}$$

Thus, the ratio of the linear acceleration to the acceleration of gravity is the angular offset of the reference line from the line of gravity. Eq. 4.21 is only valid in flat terrain.

4.6.4 Estimation of β in Changing Terrain

In changing terrains the direction of gravity is not known In order to keep the inverted pendulum in balance position the direction of gravity must be known. The β is measured against the reference line which is the direction of gravity. Since the reference line, the direction of gravity, is not known in changing terrain a method must be used to estimate the β in unknown terrains. The system differential equation, Eq. 4.15, represents the system dynamic behavior of the simple pendulum when on a slope, Fig. 4.3,

$$m_P\ l_P\ \cos(\beta+\alpha)\ddot{x}' - (m_P\ l^2{}_P + J_P)\ddot{\beta} - m_P\ l_P\ g\sin(\beta) - c_2\dot{\beta} = 0. \tag{4.15}$$

After using the conditions used above, Eq. 4.15 can be linearized as shown in the following steps. The value of β is given in Eq. 4.22,

$$\beta \equiv \frac{\cos(\alpha+\beta)\ddot{x}'}{g}, \tag{4.22}$$

so the linear acceleration in changing terrain has two components in the inertial frame, as shown in Fig. 4.15,

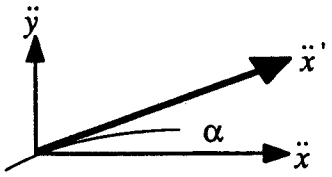

Figure 4.15: Acceleration vector.

In this case,

$$\ddot{x} = \ddot{x}'\cos(\alpha),$$

and,

$$\ddot{y} = \ddot{x}'\sin(\alpha),$$

hence, Eq. 4.22 can be written as,

$$\therefore \qquad \beta \cong \left(\frac{\ddot{x}\cos(\beta) - \ddot{y}\sin(\beta)}{g}\right).$$

With $\cos(\beta) \cong 1$ and $\sin(\beta) \cong \beta$, then,

$$\beta \cong \left(\frac{\ddot{x} - \ddot{y}\beta}{g}\right),$$

therefore,

$$\beta \cong \frac{\ddot{x}}{g + \ddot{y}}. \tag{4.23}$$

The difference between Eq. 4.21 and Eq. 4.23 is the vertical acceleration of the pivoting point appearing in the denominator and the linear horizontal acceleration in the numerator. In order to find the offset angle of the simple pendulum, the linear acceleration $\ddot{x}'$ is needed in terms of acceleration components in the inertial frame, i.e., $\ddot{x}$ and $\ddot{y}$. Since the angle α is unknown, the $\ddot{x}'$ component can not be split into two natural components. Thus, a method is required to separate these components.

4.6.5 Estimation of Vertical Acceleration $\ddot{y}$

The motion of the system, Fig. 4.1, requires some energy to be supplied to a torque generating system, for example, an electric motor. This energy input makes possible the balancing of the inverted pendulum and also the forward motion of the cart. In flat terrain, the system accelerates only in the horizontal direction, while on a slope or in changing terrain additional energy is needed to compensate for the changes in potential energy. The required additional energy depends upon the vertical acceleration of the system in the changing terrain.

$$\text{Energy}_{\text{total}} = \text{Energy}_1 + \text{Energy}_2, \tag{4.24}$$

where, Energy_1 is the energy required for the system in motion on a flat terrain, and Energy_2 is the additional energy for the same system parameters and conditions in the sloped or changing terrain.

The torque, τ_1, causes a displacement of the wheel, ϕ_w, thus the total work done in flat terrain is,

$$W_1 = \tau_1.\phi_w,$$

and the additional work done in unknown terrain is,

$$W_2 = (m_{IP} + m_P + m_c)g\ h,$$

or,

$$W_2 = \tau_2.\phi_w,$$

where τ_2 is the additional torque needed.

The total work required by the system on a slope is,

$$\begin{aligned} W_{\text{Total}} &= W_1 + W_2, \\ &= \tau_1.\ \phi_w + (m_{IP} + m_P + m_c)g\ h, \\ \therefore \quad W_{\text{Total}} &= (\tau_1 + \tau_2)\ \phi_w. \end{aligned} \tag{4.25}$$

The power, P, is the rate of change of work,

$$P = \frac{d}{dt}(W_{Total}),$$

$$= \frac{d}{dt}\left[\tau_1 . \phi_w + (m_{IP} + m_P + m_c) g\ h\right],$$

$$= \tau_1\ \dot{\phi}_w + (m_{IP} + m_P + m_c) g\ \dot{h}.$$

Since $\dot{y} = \dot{h}$, the rate of change in vertical distance,

therefore,

$$P_{total} = \tau_1\ \dot{\phi}_w + (m_{IP} + m_P + m_c) g\ \dot{y}, \quad \text{and} \tag{4.26}$$

$$\dot{y} = \left(\frac{P_{total} - \tau_1 \dot{\phi}_w}{(m_{IP} + m_P + m_c) g} \right). \tag{4.27}$$

The simulation results for the calculation of the additional torque, τ_2 in Eq. 4.25 is shown in Fig. 4.16 through Fig. 4.18.

Fig 4.16 shows the terrains in which the simulations have been carried out.

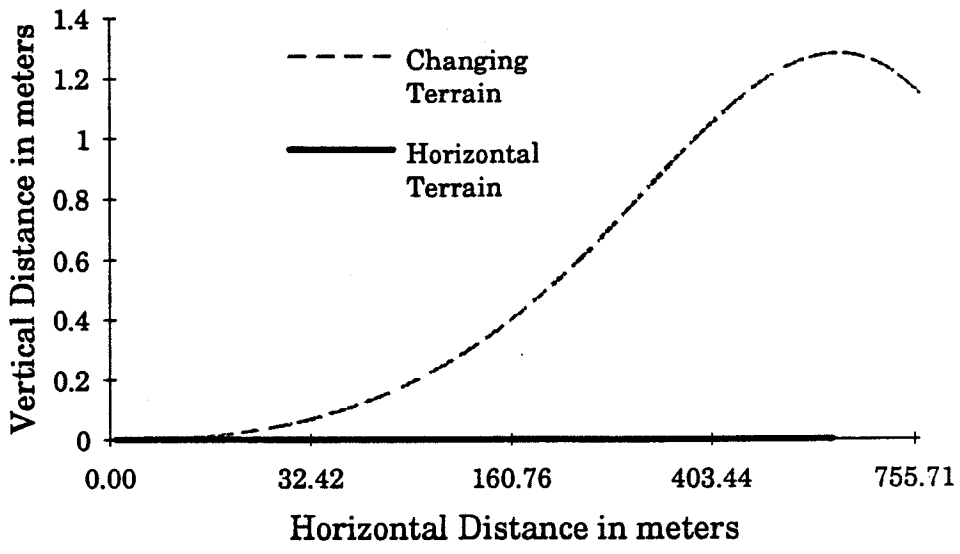

Figure 4.16: Terrains.

Fig. 4.17 shows the additional torque required to move the inverted pendulum in the terrains shown in Fig. 4.16.

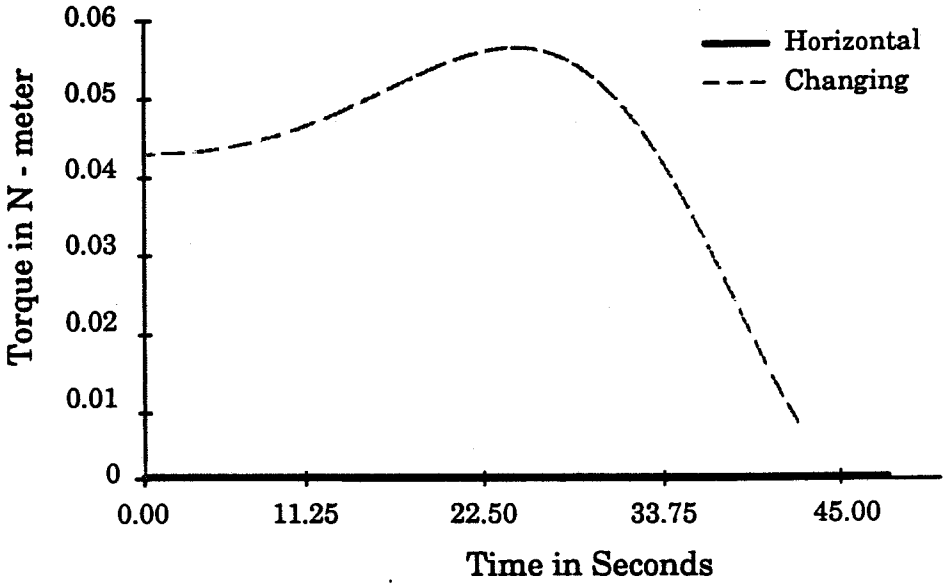

Figure 4.17: Additional torque.

Fig. 4.18 shows the total control torque that is required to move the inverted pendulum system in changing terrains, shown in Fig. 4.16,

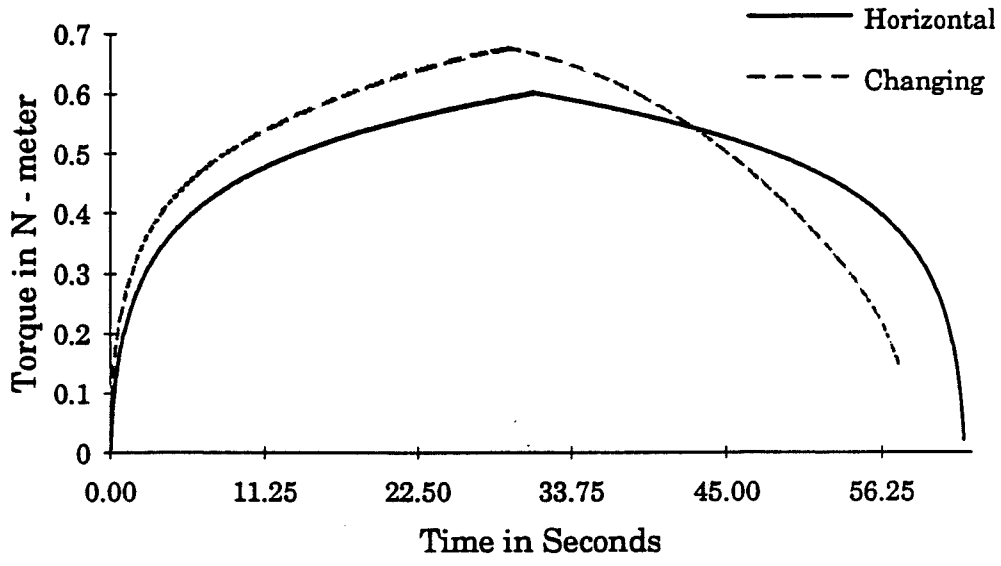

Figure 4.18: Total control torque.

4.6.6 Calculation of $\ddot{x}$

In order to estimate the offset angle, β, the linear acceleration of the cart, in the inertial frame is also required.

From Fig. 4. 15,

$$\bar{\ddot{x}}' = \bar{\ddot{x}} + \bar{\ddot{y}},$$

where $\bar{\ddot{x}}', \bar{\ddot{x}}, and\ \bar{\ddot{y}}$ are vector representation of the acceleration components,

$$\therefore \qquad \bar{\ddot{x}} = \bar{\ddot{x}}' - \bar{\ddot{y}},$$

therefore the magnitude of acceleration, $\ddot{x}$, is,

$$|\ddot{x}| = \sqrt{\ddot{x}'^2 - \ddot{y}^2}, \tag{4.28}$$

also, the angle, α,

$$\alpha = \sin^{-1}\left[\frac{\ddot{y}}{\ddot{x}}\right]. \tag{4.29}$$

With all above expressions and results the β vector can be estimated. Some results of these calculations are given in section 4.6.8 of this chapter.

4. 6.7 Calculation of Linear Acceleration, $\ddot{x}'$

Assuming that the terrain surface provides enough static friction to avoid slip, the relation between the linear acceleration and the angular acceleration of the wheel is given as,

$$\ddot{x}' = r\ddot{\phi}_w,$$

where *r* is the radius of the wheel.

The measurement of the angular acceleration of the wheel thus gives the linear acceleration of the axle. The measurement of acceleration of the

wheel needs a reference. Since the reference is unknown as the wheel rolls over changing terrain, one possible way of measuring the angular acceleration of the wheel is a measurement relative to the angular position of the inverted pendulum which is almost always vertical. This measurement gives a angular acceleration between the wheel and the inverted pendulum. An opto-sensor could be used to measure this difference.

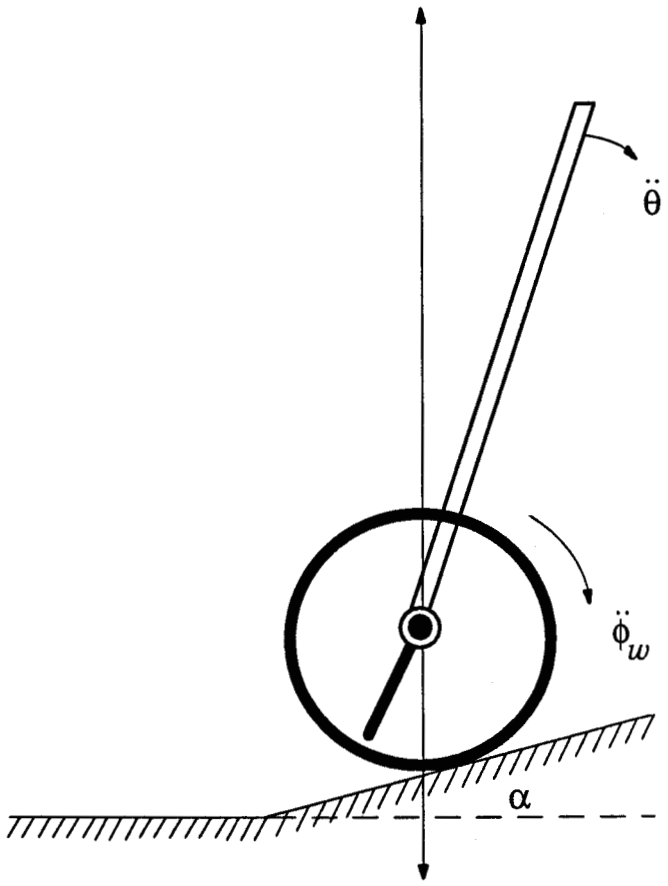

Figure 4.19: Measurement of angular acceleration.

From Fig. 4.19,

$$\ddot{\varphi} = \ddot{\phi}_w - \ddot{\theta},$$

therefore,

$$\ddot{\phi}_w = \ddot{\varphi} + \ddot{\theta}, \tag{4.30}$$

where, $\ddot{\varphi}$ is the difference angular acceleration between the inverted pendulum and the wheel.

Thus Eq. 4.19 can be solved to a close approximation to find the imbalance of the inverted pendulum,

$$\theta = 180 + \beta - \gamma, \tag{4.19}$$

since

$$\beta \cong \frac{\ddot{x}}{g + \ddot{y}}, \tag{4.23}$$

from Eq. 4.28 and 4.29,

$$\beta \cong \frac{\sqrt{\ddot{x}'^2 - \ddot{y}^2}}{g + \ddot{y}}, \tag{4.31}$$

$$\therefore \quad \beta \cong \frac{\sqrt{\ddot{x}'^2 - \left[\frac{d}{dt}\left\{\left(\frac{P_{total} - \tau_1 \dot{\phi}_w}{(m_{IP} + m_P + m_c)g}\right)\right\}\right]^2}}{g + \frac{d}{dt}\left\{\left(\frac{P_{total} - \tau_1 \dot{\phi}_w}{(m_{IP} + m_P + m_c)g}\right)\right\}},$$

therefore, the final expression for angle β can be written as,

$$\beta \cong \frac{\sqrt{\left\{r\left(\ddot{\varphi} + \ddot{\theta}\right)\right\}^2 - \left[\frac{d}{dt}\left\{\left(\frac{P_{total} - \tau_1 (\dot{\varphi} + \dot{\theta})}{(m_{IP} + m_P + m_c)g}\right)\right\}\right]^2}}{g + \frac{d}{dt}\left\{\left(\frac{P_{total} - \tau_1 (\dot{\varphi} + \dot{\theta})}{(m_{IP} + m_P + m_c)g}\right)\right\}} \tag{4.32}$$

4.6.8 Simulation of β Estimation, Eq. 4. 31

The method of finding the vertical offset of the simple pendulum has been shown in Eq. 4.31. This equation has been simulated in near real time, sample taken every after 32 ms, in the SUN workstation. The simulation results are shown in Fig. 4.20 through Fig. 4.25. This simulation uses the same parameters as used in previous simulations.

Fig. 4.20 shows the type of terrain profile in which the simulation has been carried out,

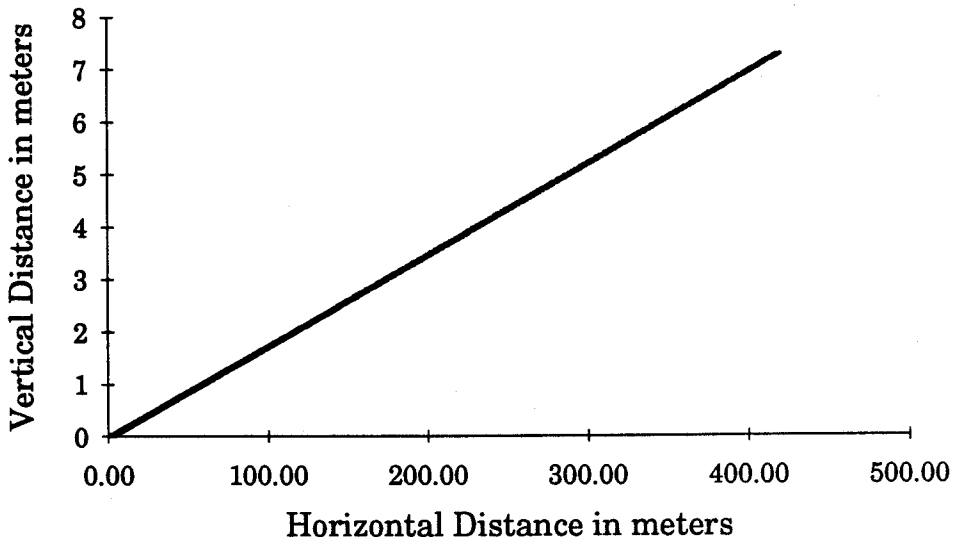

Figure 4.20: Terrain profile.

Fig. 4.21 shows the calculated angle β,

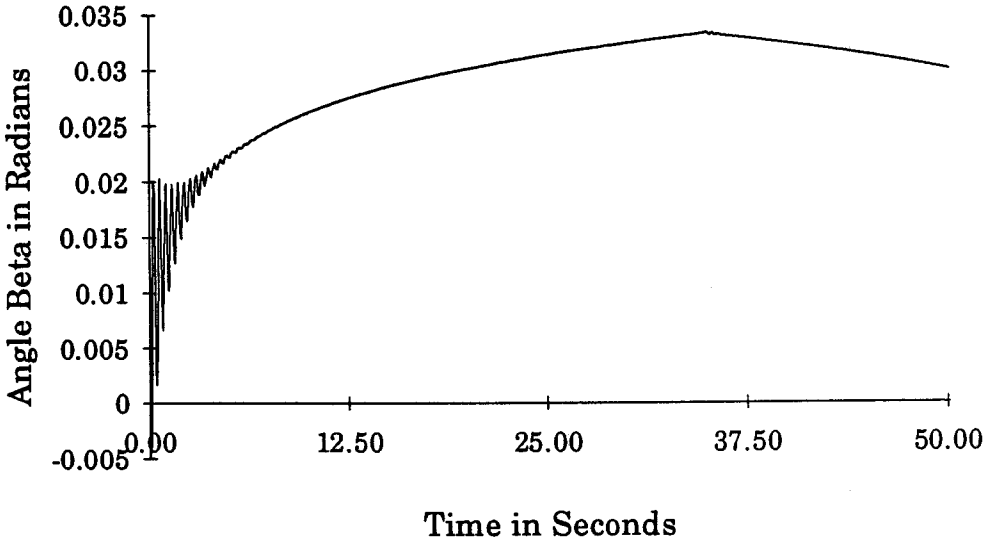

Figure 4.21: Calculated angle β.

The estimated angle β using the Eq. 4.31 is shown in Fig. 4.22,

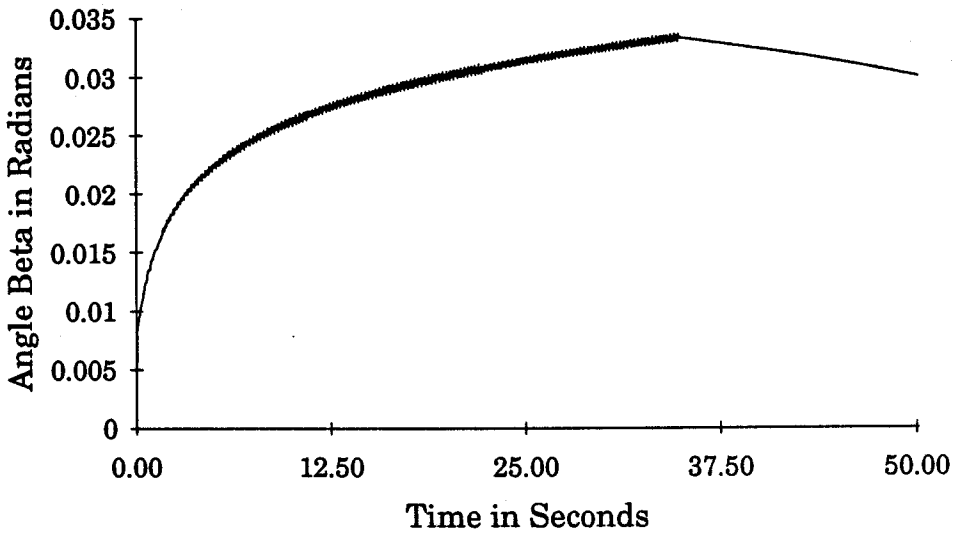

Figure 4.22: Estimated angle β.

A similar simulation has been carried out in a changing terrain (Fig. 4.23). Fig 4.23 shows a changing terrain in which the simulation has been carried out

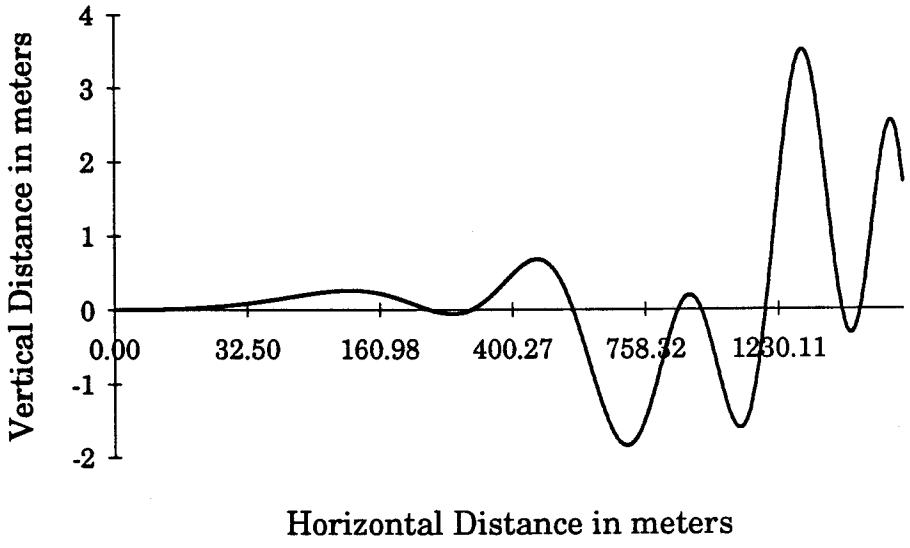

Figure 4.23: Terrain profile.

Fig. 4. 24 shows the calculated angle β

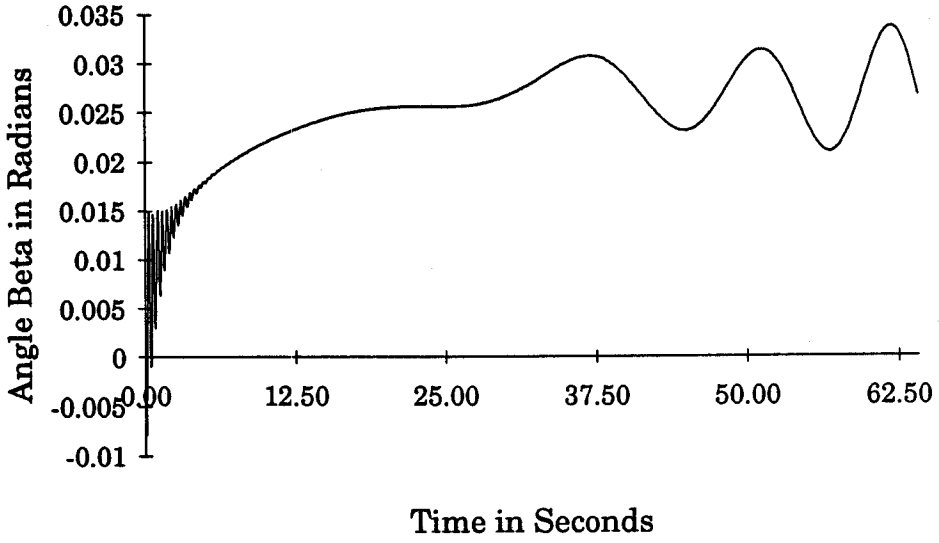

Figure 4.24: Calculated angle β.

The estimated angle β using the Eq. 4.31 is shown in Fig. 4. 25

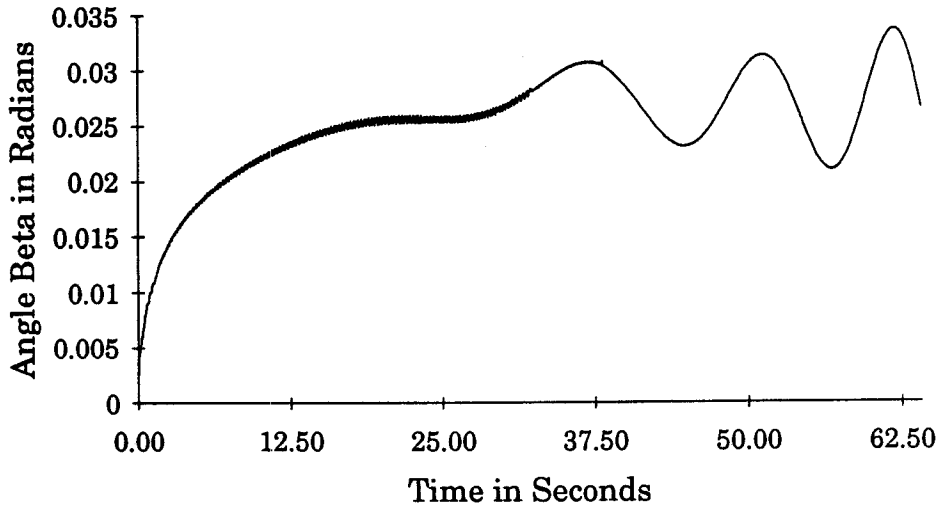

Figure 4. 25: Estimated angle β.

The results of simulation indicate that the value of β can be obtained with this estimation technique. Thus the method of finding the direction of gravity, Eq. 4.31, can be employed to find the imbalance of the inverted pendulum, Eq. 4.19, in changing terrain where the terrain is not always orthogonal to the line of gravity.

4.6.9 Error Between Calculated and Estimated β

The simulation result shows that the required angle, β, for the estimation of the imbalance of the inverted pendulum could be found by the estimation method. The velocity dependent friction at the pivoting point causes the suppression of SHM of the simple pendulum. This suppression eliminates the uncertainty which could cause the wrong estimation of θ, and give the estimated offset angle within an acceptable value.

The error angle, between the calculated and the estimated value β is very small, as shown in Fig. 4.26. The error is high at the discontinuity in the acceleration but is very small during continuous motion. The average difference between calculated and estimated β during continuous motion is about 2% of the calculated value.

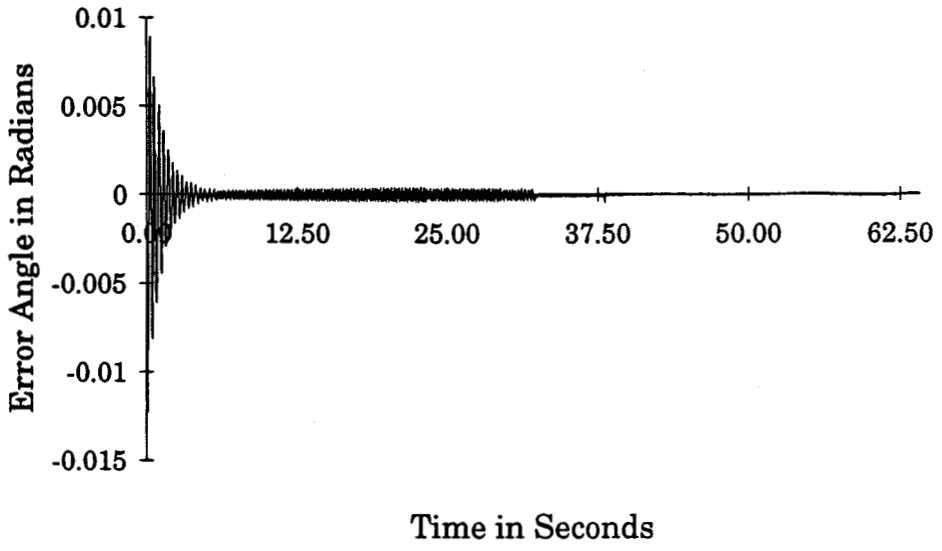

Figure 4.26: Error between calculated and estimated β

4.7 CONCLUDING REMARKS

This chapter has been devoted to the design of an inverted pendulum system that can be balanced in changing terrains. The design considerations for a proposed model have been highlighted, followed by the necessary sensory systems. Simulations of the mathematical model of the proposed system have been carried out. The necessity of a gravity sensor has been

highlighted. The inertial sensor, used for gravity sensing, and its dynamic behavior in motion and at rest are also shown. An estimation method that can be used to find the direction of gravity was formulated. The simulation results of the proposed method and the comparison of the simulated result with the calculated value has been developed.

5. MOTION PLANNING AND CONTROL

5.1 INTRODUCTION

Motion planning in robotics is one of the important problems one has to solve in order to create a truly autonomous robot. This motion plan chooses the type of motion which is required to meet the goal. This task involves the generation of task oriented motion strategies. The motion required by the robot must be coordinated with the control system.

Humans usually plan their motion ahead of the required task. The type of motion depends upon the objective of the task. Humans propel their body in the desired direction by unbalancing the body in the direction of motion and balancing the body in the vertical position at the end of the motion. Thus the human body is in balance and unbalance condition during motion. The biological controller regulates the body's center of mass within the acceptable region from where the body can be brought back into the balanced position at the end of the motion.

A similar idea could be used to plan the motion of the inverted pendulum system. This chapter deals with the motion planning of an inverted pendulum system which has been described in the previous chapter. A preliminary examination of a controller that controls the system in motion and stabilizes the system at rest will be presented in this chapter.

5.2 MOTION PLANNING IN HUMANS

The attitude of the human body is in an unbalanced and balanced position during motion. To accomplish motion the human generates a motion plan before the motion task starts. Generally, this motion plan consists of three phases, unbalanced, constant, and balanced. The motion controller executes the plan to achieve the desired motion in the desired time. The unbalancing phase, known as the initial phase, starts before the motion by leaning the body's center of mass in the direction of the desired motion. The duration and degree of unbalance depends upon the motion plan. During constant motion, the angular position of the body's center of mass, in the inertial frame, remains unchanged. The balancing phase starts when the desired task is nearly over and the desired distance is about to be covered. When the goal is about to be reached the controller stabilizes the body in a vertical balance position.

The actions of unbalance and balance in motion can be understood by analyzing the reaction forces developed by the body's center of mass which push the body in the direction opposite to the motion. This could cause the fall of the body in the opposite direction beyond the control range. To avoid a fall, the body's center of mass needs to be unbalanced in the direction of the motion to cancel the reaction force, that pushing the body in reverse, with the gravitational force. When these two forces become equal, there will be a constant motion of the body's center of mass. Balancing is required when the magnitude of motion decreases which causes the decrease in reaction force so a smaller amount of gravitational force is needed to cancel the reaction force. This will stabilize the center of mass.

Fig. 5.1 shows the position of the human body during the motions,

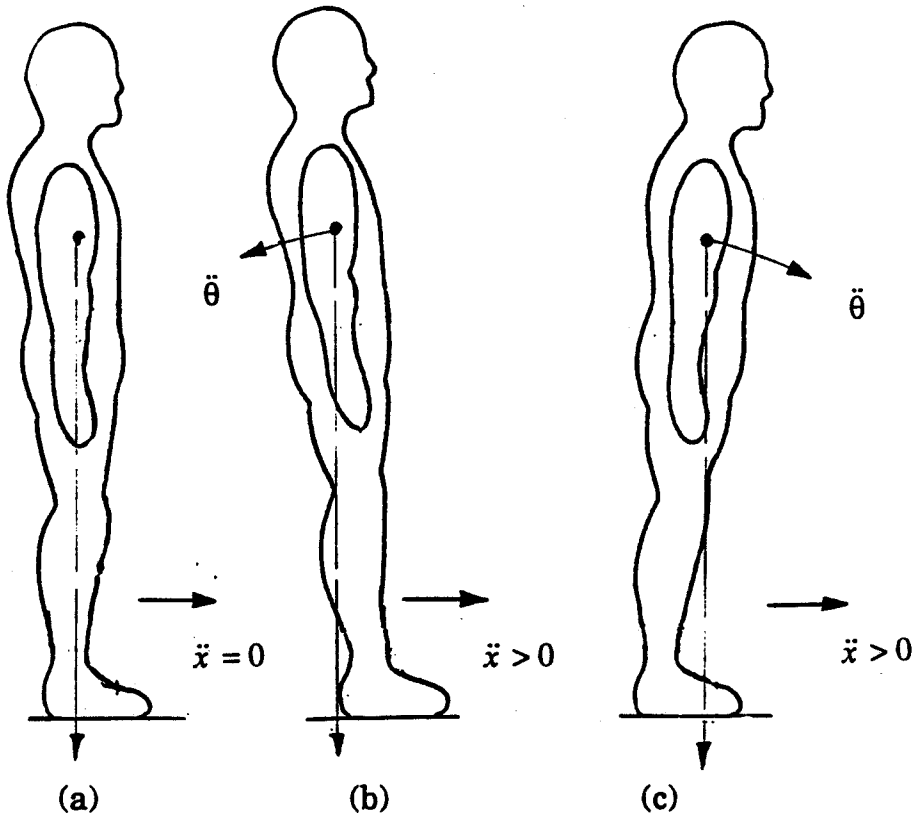

Figure 5.1: Human in Motion.

In the balanced position (zero motion) the reaction force at the center of mass is zero and the gravitational force is through the body's point of support and center of mass, Fig. 5.1(a). Thus the body is in a balanced position. When forward motion starts from this position, Fig. 5.1(b), the reaction force developed at the center of mass pushes the body in a reverse direction. This unbalances the body's center of mass in the reverse direction of motion. To prevent the body from falling, the body's center of mass must lean forward before the motion is started, Fig. 5.1(c). Thus the angular offset of the body's center of mass from the vertical position depends upon the magnitude of the motion.

5.3 MOTION PLANNING OF INVERTED PENDULUM SYSTEM

The inverted pendulum has been considered as a single link human posture hinging about the ankle. A similar idea to that used by humans to plan motion could be employed to plan the motion of an inverted pendulum system. A similar algorithm, unbalance and balance action, could be used to achieve the motion of the system. Fig. 5.2 shows the behavior of the inverted pendulum in the various motions,

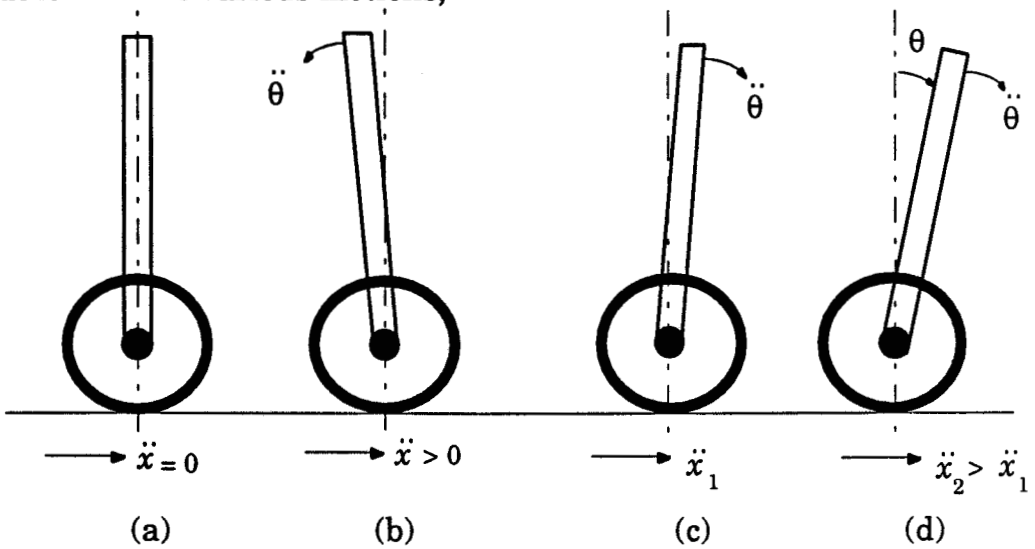

Figure 5.2: The position of inverted pendulum in various motion.

The inverted pendulum is initially in a balanced position with zero motion, Fig. 5.2(a). The inverted pendulum starts to fall in the opposite direction of the motion when linear acceleration starts, Fig. 5.2(b). Similar to the case of human motion, the inverted pendulum should be unbalanced in the direction of motion before the motion starts, Fig. 5.2(c). The imbalance of the inverted pendulum starts when the linear acceleration of the axle starts. This causes the stabilization of the inverted pendulum against the rapid fall due to gravity. An algorithm is required to control the motion of the inverted pendulum system.

5.3.1 Piece Wise Motion Planning

Fig. 5.3 shows a graphical representation of a motion plan to achieve the distance, x_d, covered in the desired time, t_d,

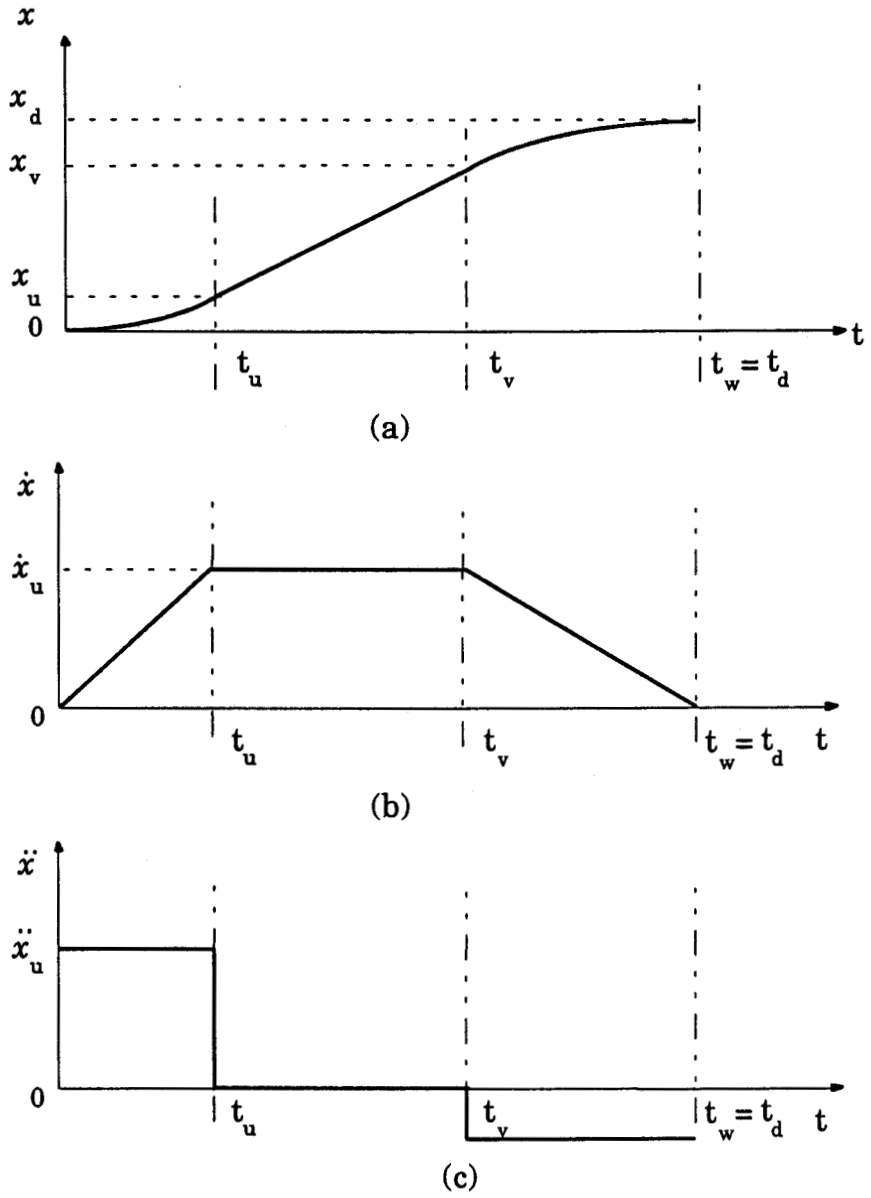

Figure 5.3: Motion planning (a) the distance traveled profile, (b) the desired velocity profile, and (c) acceleration of axle.

A servo control on the linear velocity could be used to cover the desired distance. Piece-wise velocity functions have been shown in Fig. 5.3(b) and the corresponding distance traveled in Fig. 5.3(a). The velocity function has been

divided into three segments, (1) linear increasing, (b) constant, and (c) linear decreasing, as shown in Fig. 5.3(b). Fig 5.3(c) shows the required acceleration function of the axle for the above plan.

The ideal angular position of the inverted pendulum with the vertical is linearly dependent on the axle acceleration, as shown in Fig. 5.4(a). The corresponding ideal angular velocity and accelerations are shown in Fig. 5.4(b) and Fig. 5.4(c) respectively.

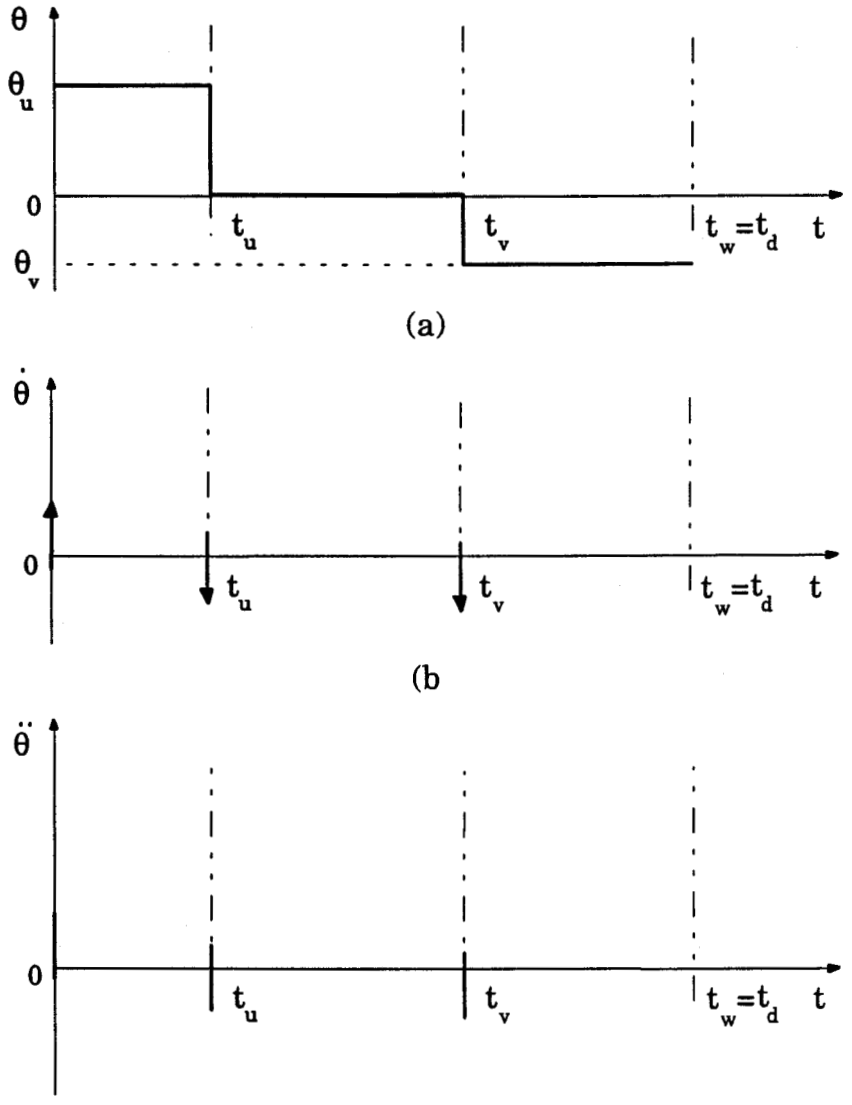

Figure 5.4: Angular profile of the inverted pendulum with the vertical (a) angular position,(b) the angular velocity, and (c) angular acceleration.

In the motion plan, as shown in Fig. 5.3 and Fig. 5.4, the acceleration of the axle is abrupt which causes a stability problem for the inverted pendulum. Thus the above plan is physically not possible. Hence a plan which is close to the plan shown in Fig. 5.3 and Fig. 5.4, except at the transitions, could be employed to achieve the desired motion. Such a plan is shown in Fig. 5.5 and Fig. 5.6.

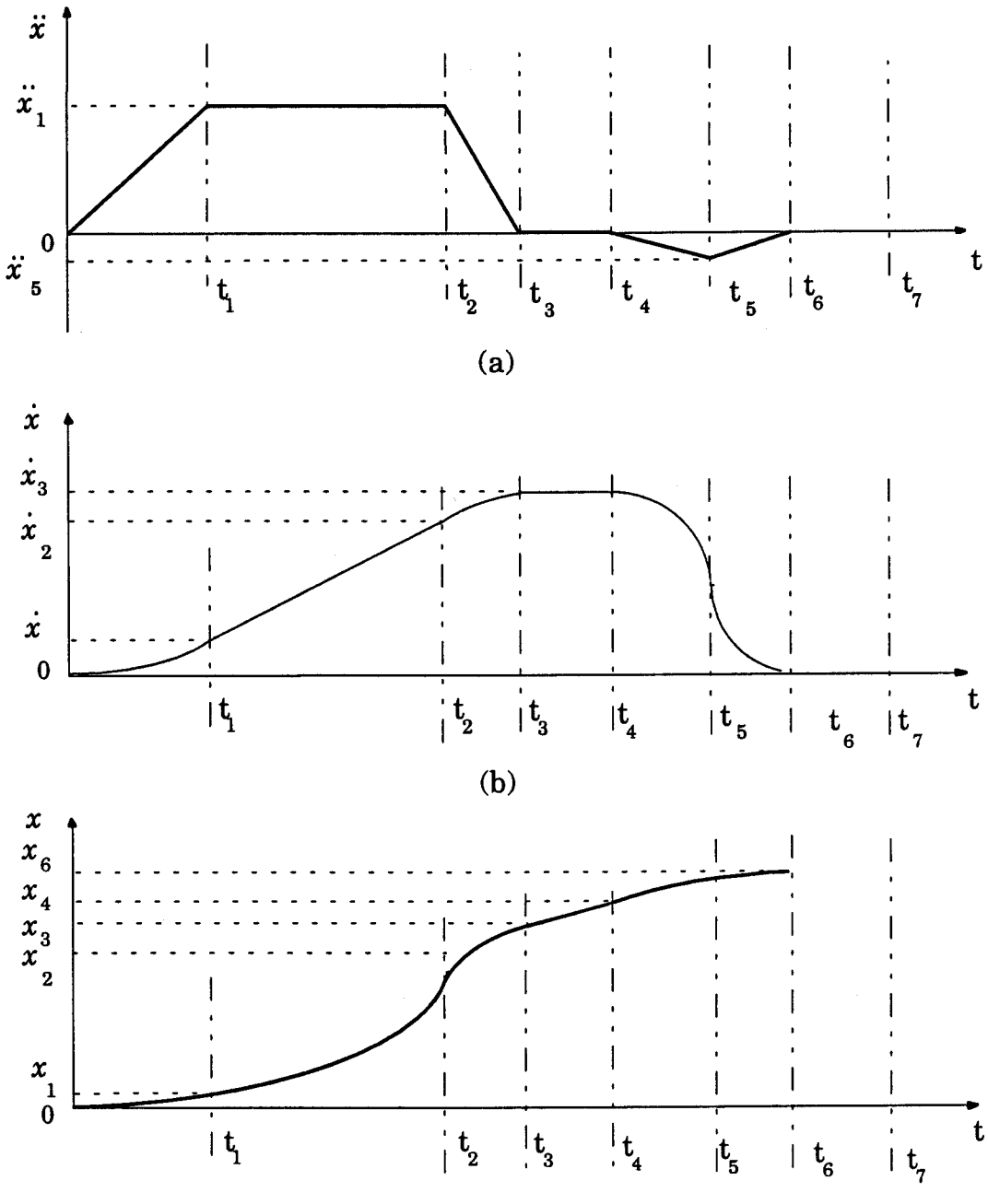

Figure 5.5: Motion planning (a) acceleration of axle, (b) the velocity profile, and (c) the distance traveled.

Fig. 5.6 shows the angular position, velocity and acceleration of the inverted pendulum.

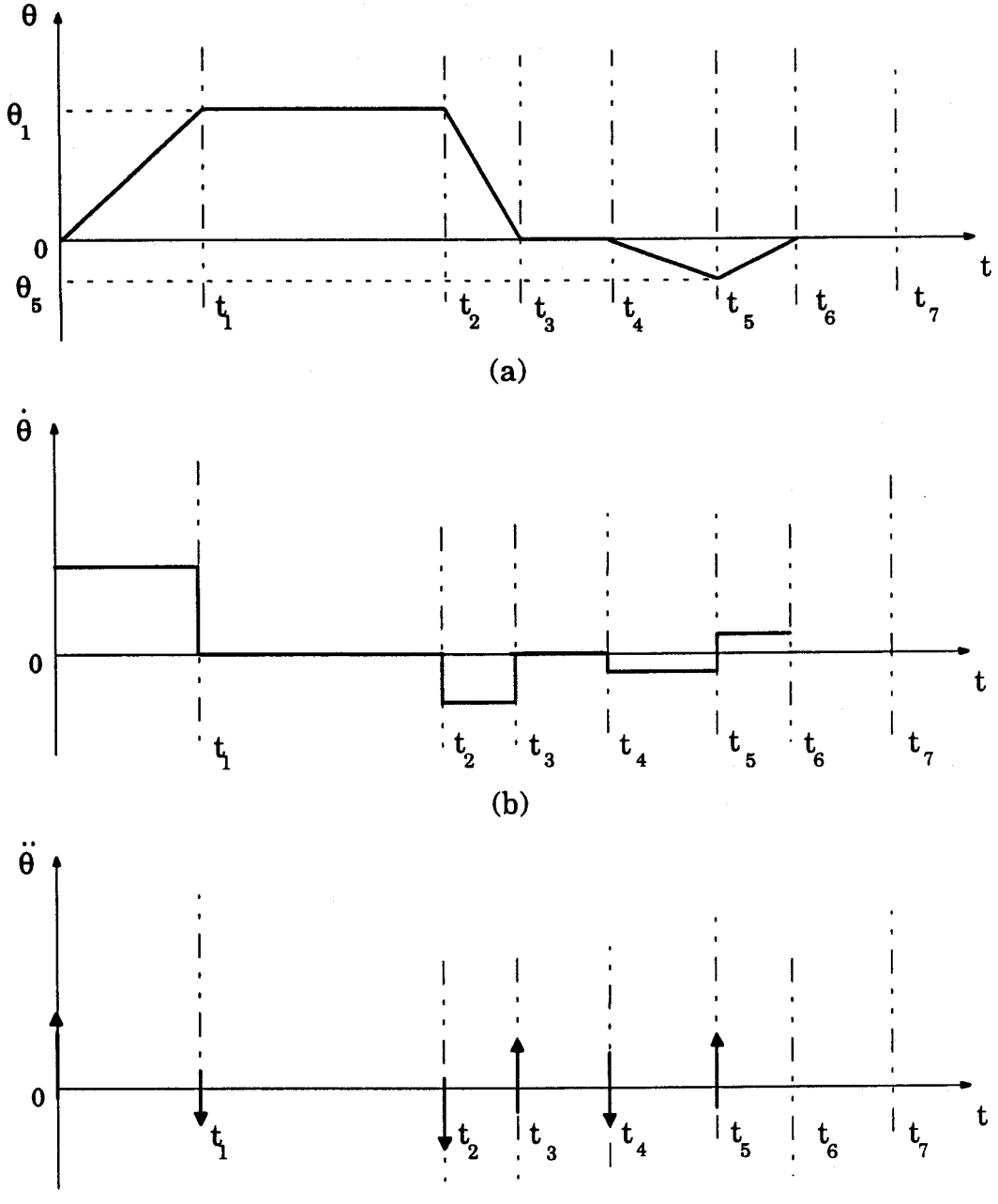

Figure 5.6: Angular profile of the inverted pendulum with the vertical (a) angular position,(b) the angular velocity, and (c) angular acceleration.

The entire motion plan can be expressed in the seven piece-wise terms, (1) unbalance in forward direction, (2) constant unbalance, (3) recovering, (4)

balanced, (5) unbalance in reverse direction of motion, (6) recovering, and (7) stabilization.

(1) **Unbalance in forward direction:-** In order to start the motion of the inverted pendulum system, the axle must be accelerated in the forward direction. The magnitude of the acceleration depends upon the angular displacement of the inverted pendulum from the vertical in the direction of the motion. The inverted pendulum must be unbalanced. This phase starts at $t=0$ and ends at $t = t_1$, Fig. 5.6(a).

(2) **Constant unbalance:-** The velocity or speed of the axle depends upon the acceleration. A constant acceleration develops a linear velocity with time, as shown in Fig. 5.5(b). The required speed can be achieved by keeping the acceleration constant. The angular position of the inverted pendulum remains unchanged when the acceleration of the axle is constant, thus in this phase, $t=t_1$ to $t=t_2$, the unbalance of the inverted pendulum is constant. The degree of unbalance depends upon the magnitude of the constant acceleration of the axle.

(3) **Recovering:-** The angular offset of the inverted pendulum decreases as the time advances. This phase recovers the inverted pendulum from the unbalance position, phase2, towards the balanced position, $t=t_2$ to $t=t_3$.

(4) **Balanced:-** In this phase, $t=t_3$ to $t=t_4$, the acceleration of the axle is zero thus the inverted pendulum remains in the balanced position.

(5) **Unbalance in reverse direction:-** When the distance is about to be covered, the forward speed of the axle must be reduced so that the system can stop at the desired position. In order to accomplish this, a braking force is required on the axle. This brake force decelerates the axle. Since the braking force is applied to the axle with respect to the inverted pendulum, the inverted pendulum must be unbalanced in the reverse direction of the motion for a duration, $t=t_4$ to $t=t_5$. The degree of unbalance depends upon the amount of braking force. Generally, the inverted pendulum must remain near the vertical to stabilize it in the balance position at the end of the motion. Thus a

small unbalance of the inverted pendulum corresponds to a small braking force. This small braking force, applied on the axle decreases the speed of axle. Thus the duration of this phase depends upon the speed of the axle and the magnitude of the braking force.

(6) **Recovering:-** In this phase, $t=t_5$ to $t=t_6$, inverted pendulum comes towards the balanced position. The speed of the axle also continuously decreasing in this phase.

(7) **Stabilization:-** In this phase, the inverted pendulum is stabilized in the vertical balanced position. A small correction of angular offset will be done. The inverted pendulum remains balanced all the time until a new motion cycle is started.

Fig. 5.7 shows the motion plan of the system. The entire motion cycle has been divided into seven phases,

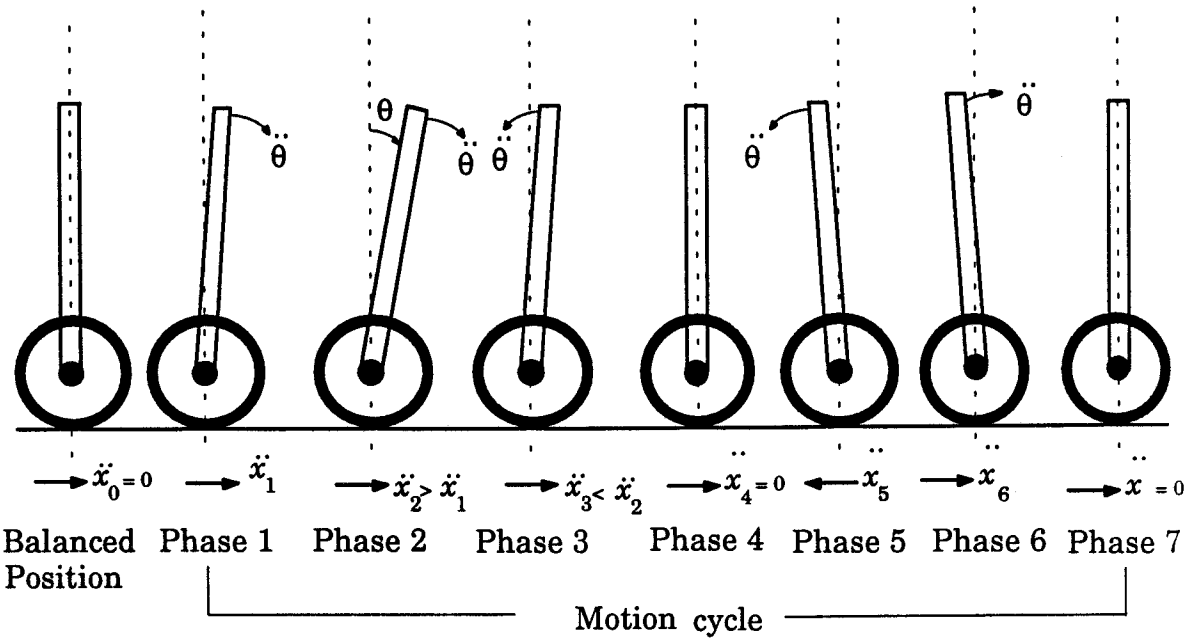

Figure 5.7: Position of the inverted pendulum in different phases.

Fig. 5.7 shows the inverted pendulum in different phases during the motion. Phase1 represents the unbalance of the inverted pendulum for

$0 \le t < t_1$, Fig. 5.6(a). The inverted pendulum is in constant imbalance position in phase2, $t_1 \le t < t_2$, Fig. 5.6(a). The recovering, phase3, $t_2 \le t < t_3$, brings the inverted pendulum towards the vertical position, Fig. 5.6(a). During phase 4, $t_3 \le t < t_4$, the inverted pendulum remains in the balanced position. Phase 5, $t_4 \le t < t_5$, represents the inverted pendulum in the unbalance position in the reverse direction of the motion. The recovering phase, $t_5 \le t < t_6$, brings the inverted pendulum towards balanced position. The stabilization phase $t_6 \le t < t_7$ balances the inverted pendulum in the vertical position. This stabilization will end the motion cycle. The inverted pendulum will be in the balanced position until a new motion cycle is started.

Phase1	$0 \le t < t_1$
Phase2	$t_1 \le t < t_2$
Phase3	$t_2 \le t < t_3$
Phase4	$t_3 \le t < t_4$
Phase5	$t_4 \le t < t_5$
Phase6	$t_5 \le t < t_6$

The acceleration function, in Fig. 5.5(b), can be written as,

$$\left.\begin{array}{ll} \ddot{x}_1 = K_1 t & 0 \le t < t_1 \\ \ddot{x}_2 = K_2 & t_1 \le t < t_2 \\ \ddot{x}_3 = K_2 - K_3(t - t_2) & t_2 \le t < t_3 \\ \ddot{x}_4 = 0 & t_3 \le t < t_4 \\ \ddot{x}_5 = -K_4(t - t_4) & t_4 \le t < t_5 \\ \ddot{x}_6 = -K_4(t_5 - t_4) + K_5(t - t_4) & t_5 \le t < t_6 \end{array}\right\} \quad (5.1)$$

Eq. 5.1 can be written in matrix form, as shown below,

$$\begin{bmatrix} \ddot{x}_1 \\ \ddot{x}_2 \\ \ddot{x}_3 \\ \ddot{x}_4 \\ \ddot{x}_5 \\ \ddot{x}_6 \end{bmatrix} = \begin{bmatrix} K_1 & 0 & 0 & 0 & 0 \\ 0 & K_2 & 0 & 0 & 0 \\ 0 & (K_2 + K_3 t_2) & -K_3 & 0 & 0 \\ 0 & 0 & 0 & 0 & 0 \\ 0 & K_4 t_4 & 0 & -K_4 & 0 \\ 0 & -(K_4 t_5 - K_4 t_4 + K_5 t_4) & 0 & 0 & K_5 \end{bmatrix} \begin{bmatrix} t \\ 1 \\ t \\ t \\ t \end{bmatrix}$$

therefore,

$$[\ddot{x}] = [K][t'] \tag{5.2}$$

where, $[\ddot{x}] = [\ddot{x}_1 \quad \ddot{x}_2 \quad \ddot{x}_3 \quad \ddot{x}_4 \quad \ddot{x}_5 \quad \ddot{x}_6]^T$, $[t'] = [t \quad 1 \quad t \quad t \quad t]^T$

and $[K] = \begin{bmatrix} K_1 & 0 & 0 & 0 & 0 \\ 0 & K_2 & 0 & 0 & 0 \\ 0 & (K_2 + K_3 t_2) & -K_3 & 0 & 0 \\ 0 & 0 & 0 & 0 & 0 \\ 0 & K_4 t_4 & 0 & -K_4 & 0 \\ 0 & -(K_4 t_5 - K_4 t_4 + K_5 t_4) & 0 & 0 & K_5 \end{bmatrix}$

5.3.2 Simulation of motion plan in Horizontal Terrain

The simulation of the piece-wise motion planning for a horizontal terrain uses Eq. 4.7' and Eq. 4.8'. The system physical parameters and coefficients for Eq. 5.2 are listed in Table 5.1 and Table 5.2 respectively. This simulation has been carried out to understand the behavior of the inverted pendulum during a piece-wise motion of the axle.

Table 5.1: System parameters

Mass, m_{IP}	10 kg
Mass, m_P	0.1 kg
Length, l_{IP}	1.0 m
Length, l_P	0.1 m
Inertia, J_{IP}	3.33 kg-m^2
C_1	0.0
C_2	0.005

Table 5.2: Coefficients for Eq. 5.2

t_1	1.0 seconds
t_2	3.0 seconds
t_3	5.0 seconds
t_4	7.0 seconds
t_5	19.2497 seconds
t_6	41.9767 seconds
K_1	0.5
K_2	0.5
K_3	0.25
K_4	-0.008163
K_5	0.004704
Distance covered, x_d	35.85 meters
Time taken, t_d	41.98 seconds

Fig. 5.8 shows the resultant acceleration of the axle during the motion. The coefficients for Eq. 5.2 for the simulation have been used from Table 5.1 and Table 5.2.

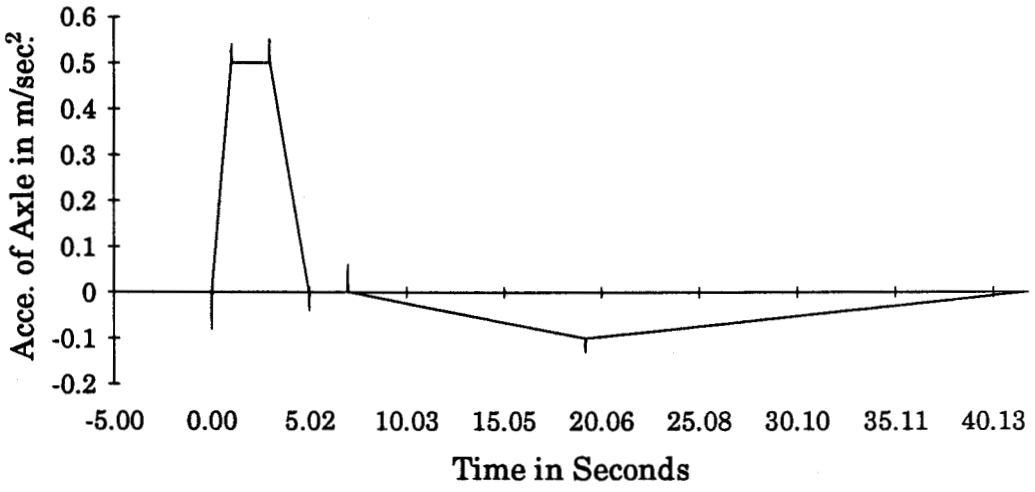

Figure 5.8: Acceleration of Axle.

In Fig. 5.8 the initial acceleration is very high and is in the opposite direction of the motion. This acceleration is required to initiate the angular

motion of the inverted pendulum in the forward direction from the rest position. The relationship between the acceleration of the axle and the angular position of the inverted pendulum is assumed to be linear for the motion planning. Thus the angular position of inverted pendulum follows the acceleration function of the axle, as shown in Fig. 5.9. At discontinuities, the accelerations of the axle is very high. This is the acceleration which is required to change the motion of the inverted pendulum from one state to the next state.

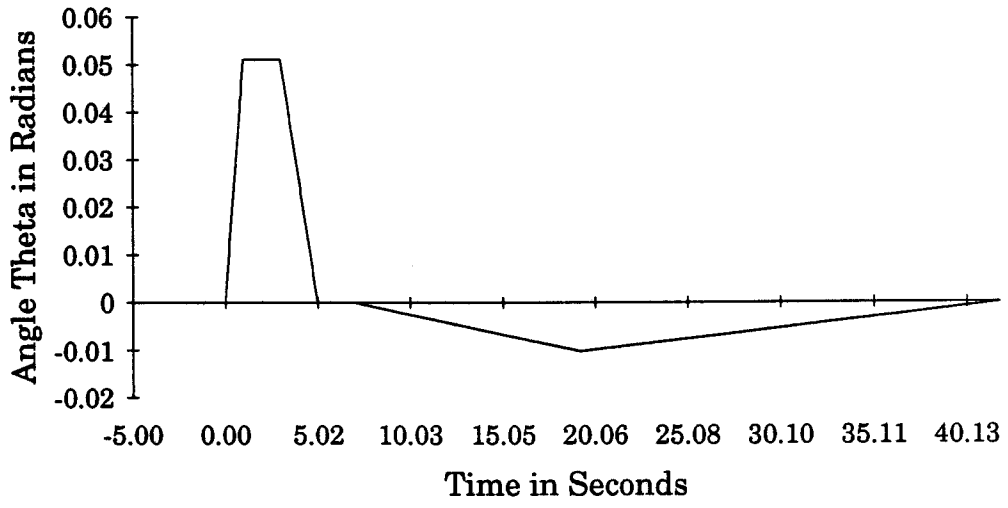

Figure 5.9: Angular position of Inverted Pendulum during motion.

The resultant velocity of the axle is as shown in Fig. 5.10,

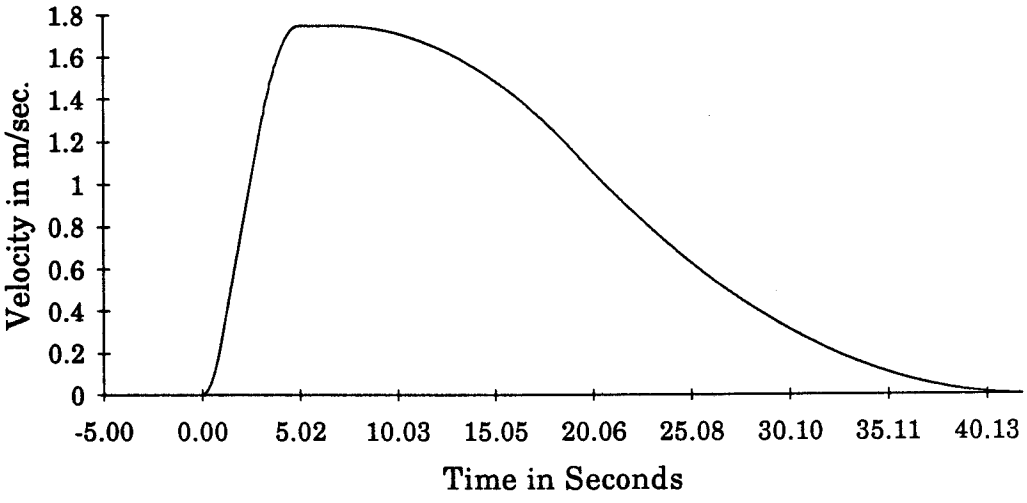

Figure 5.10: Axle Speed.

Fig. 5.11 shows the distance traveled by the inverted pendulum system during the motion task.

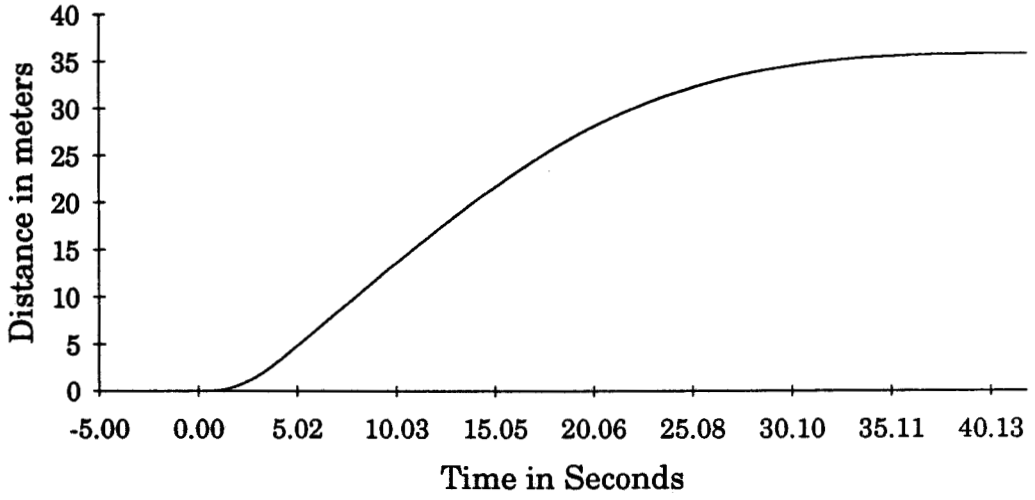

Figure 5.11: Distance traveled by the Inverted Pendulum system.

Fig. 5.12 and Fig. 5.13 show the angular velocity and acceleration of the inverted pendulum during this motion plan.

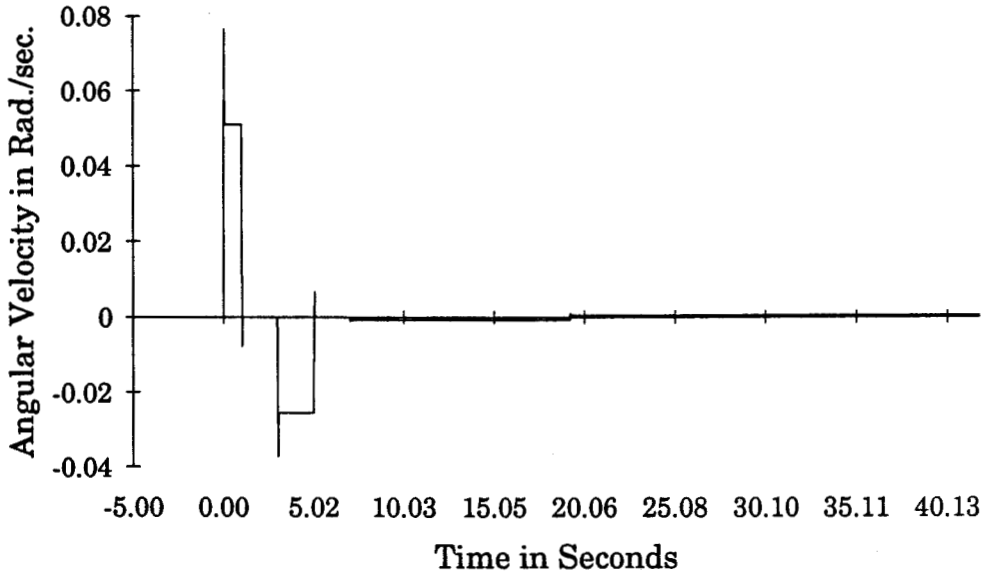

Figure 5.12: Angular velocity of Inverted Pendulum during motion.

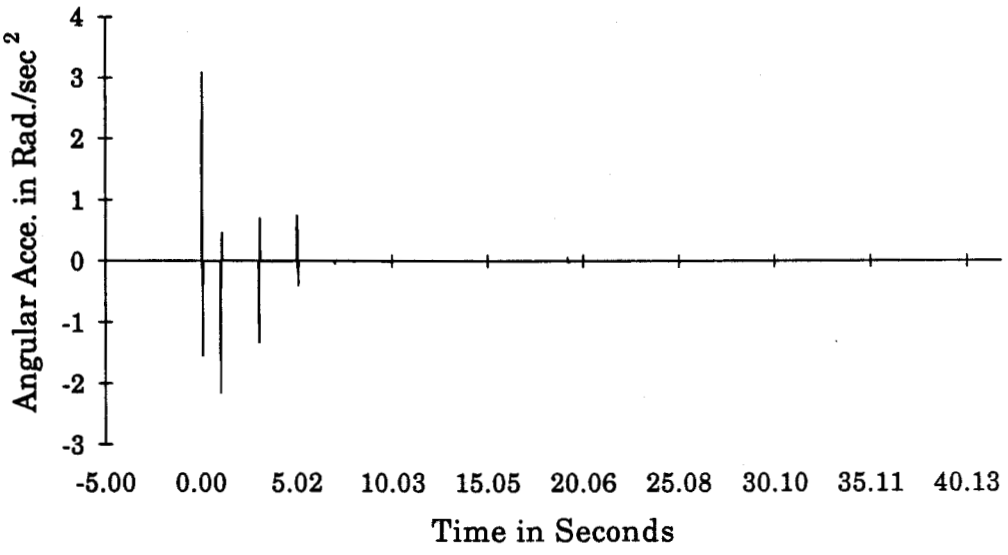

Figure 5.13: Angular acceleration of Inverted Pendulum during motion.

Fig. 5.13 shows that the angular acceleration of the inverted pendulum at the discontinuities is very high. This higher acceleration could make the inverted pendulum to become more unstable than in continuous motion.

As expressed in Eq. 4.9, the dynamic equation of the lower pendulum, the resultant offset β of the pendulum, in this situation, from the vertical position is shown in Fig. 5.14,

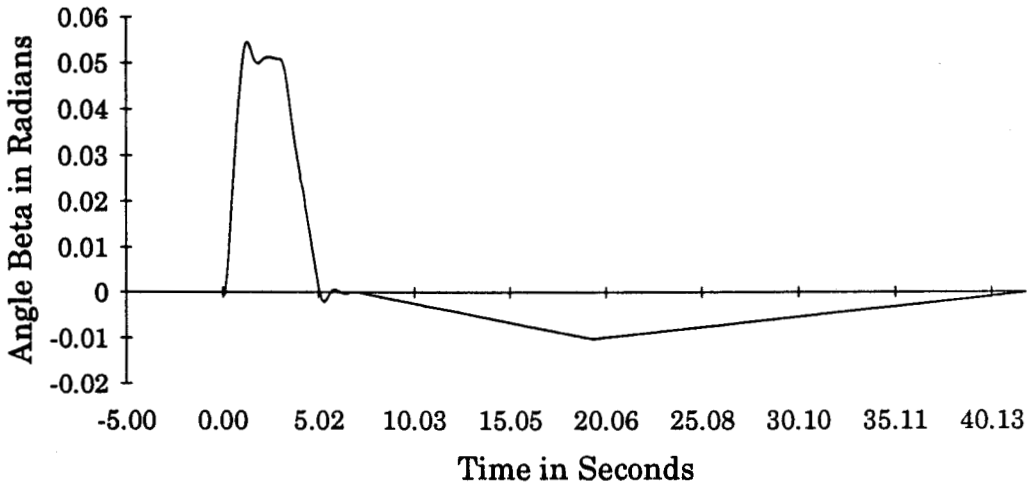

Figure 5.14: Angular offset of the simple pendulum from vertical.

The error angle between calculated, solving Eq. 4.9, and the estimated, solving Eq. 4.32, β for the motion plan shown in Fig. 5.8 is as shown in Fig. 5.15

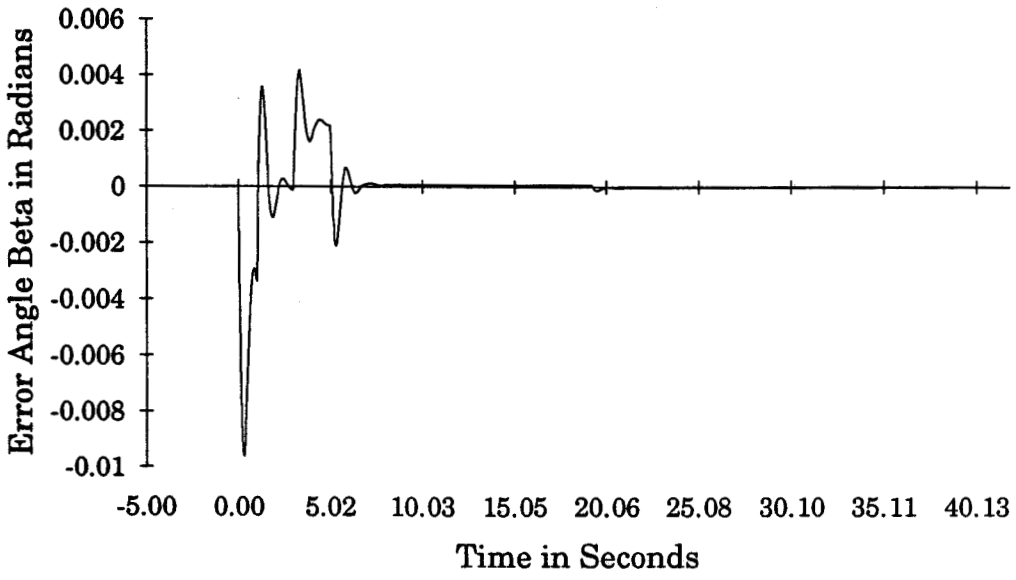

Figure 5.15: Error Angle between Calculated and Estimated β.

In Fig. 5.15 the error of the estimated β at the discontinuities is high. The magnitude of the error depends upon the magnitude of accelerations at the discontinuities.

The drawback of the above planning is the sharp change in the angular velocity of the inverted pendulum at discontinuities, as shown in Fig. 5.12, which could cause a problem of stability. The angular offset of the simple pendulum has been used to estimate the location of direction of gravity, however due to the abrupt change in the motion, the simple pendulum experiences a SHM. This oscillation has been damped by velocity dependent friction at the pivoting point, but the settlement of the oscillation of the pendulum, even though it is damped, takes a considerable time, as shown in Fig. 5.14. Thus the estimation of the angle β at the discontinuity results in some error, as shown in Fig. 5.15. This gives an inaccurate estimation of the direction of gravity.

The discontinuity in the motion should be avoided to make the system more stable and to make a better estimation of the direction of gravity. Thus, a continuous motion plan could be considered for the motion planning.

5.3.3 Continuous Motion Planning

Fig. 5.16 shows a graphical representation of a improved piece-wise motion plan.

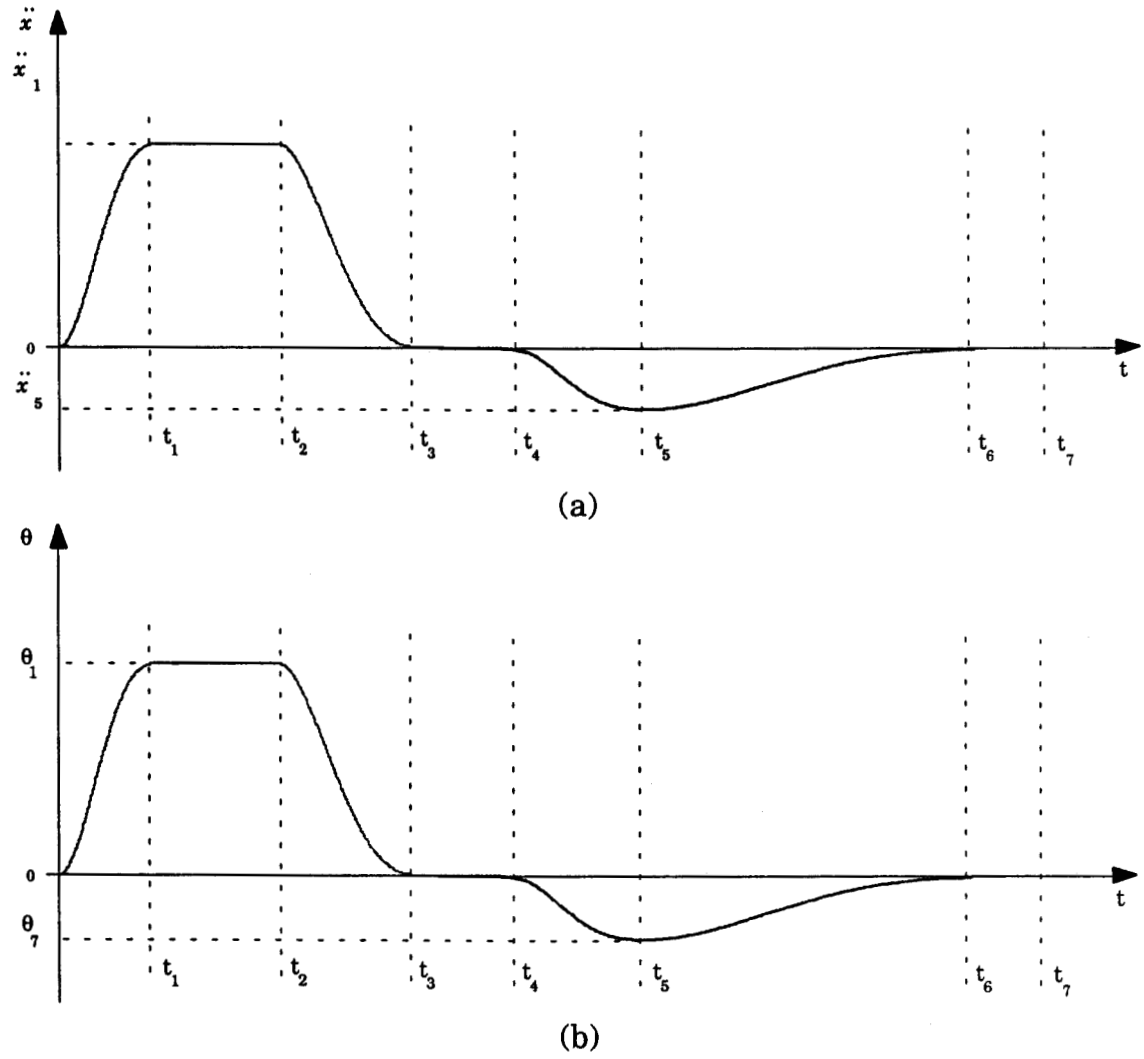

Figure 5.16: Continuous motion plan (a) linear acceleration of axle, and (b) the angular position of inverted pendulum.

The plan, shown in Fig. 5.16, is similar to a theoretical continuous motion plan. The acceleration function, Fig. 5.16(a), has been chosen for each time interval so that the boundaries of adjacent intervals meet closely. This assumption assures continuity in the acceleration of the axle. Since the angular position of the inverted pendulum is linearly related to the acceleration of the axle, the angle θ is also continuous with time, as shown in Fig. 5.16(b).

The above plan can be expressed in mathematical equations.

$$\left.\begin{aligned}
\ddot{x}_1 &= K_{11}t^2 + K_{12}t^3 + K_{13}t^4 && 0 \le t < t_1 \\
\ddot{x}_2 &= K_{11}t_1^{\,2} + K_{12}t_1^{\,3} + K_{13}t_1^{\,4} && t_1 \le t < t_2 \\
\ddot{x}_3 &= \ddot{x}_2 - [K_{31}(t-t_2)^2 + K_{32}(t-t_2)^3 + K_{33}(t-t_2)^4] && t_2 \le t < t_3 \\
\ddot{x}_4 &= 0 && t_3 \le t < t_4 \\
\ddot{x}_5 &= -[K_{51}(t-t_4)^2 + K_{52}(t-t_4)^3 + K_{53}(t-t_4)^4] && t_4 \le t < t_5 \\
\ddot{x}_6 &= \ddot{x}_5 + [K_{61}(t-t_5)^2 + K_{62}(t-t_5)^3 + K_{63}(t-t_5)^4] && t_5 \le t < t_6
\end{aligned}\right\} \quad (5.3)$$

5.3.4 Simulation of Continuous Motion Plan in Horizontal Terrain

This simulation uses the system parameters and coefficients listed in Table 5.3 and Table 5.4 respectively.

Table 5.3: System parameters

Mass, m_{IP}	10 kg
Mass, m_P	0.1 kg
Length, l_{IP}	1.0 m
Length, l_P	0.1 m
Inertia, J_{IP}	3.33 kg-m^2
C_1	0.0
C_2	0.005

Table 5.4: Coefficients for Eq. 5.3

t_1	4.0 seconds
t_2	4.2 seconds
t_3	9.0 seconds
t_4	9.2 seconds
t_5	22.76 seconds
t_6	59.033 seconds
K_{11}	0.1875
K_{12}	-0.0625
K_{13}	0.0059
K_{31}	0.1302
K_{32}	-0.0362
K_{33}	0.0028
K_{51}	0.0033
K_{52}	-0.0003
K_{53}	0.0
K_{61}	0.0005
K_{62}	-0.00002
K_{63}	0.0
Distance covered, x_d	51.97 meters
Time taken, t_d	59.033 seconds

Fig. 5.17 shows acceleration function of the axle using Eq. 5.3 with system parameters and coefficients listed in Table 5.3 and Table 5.4 respectively,

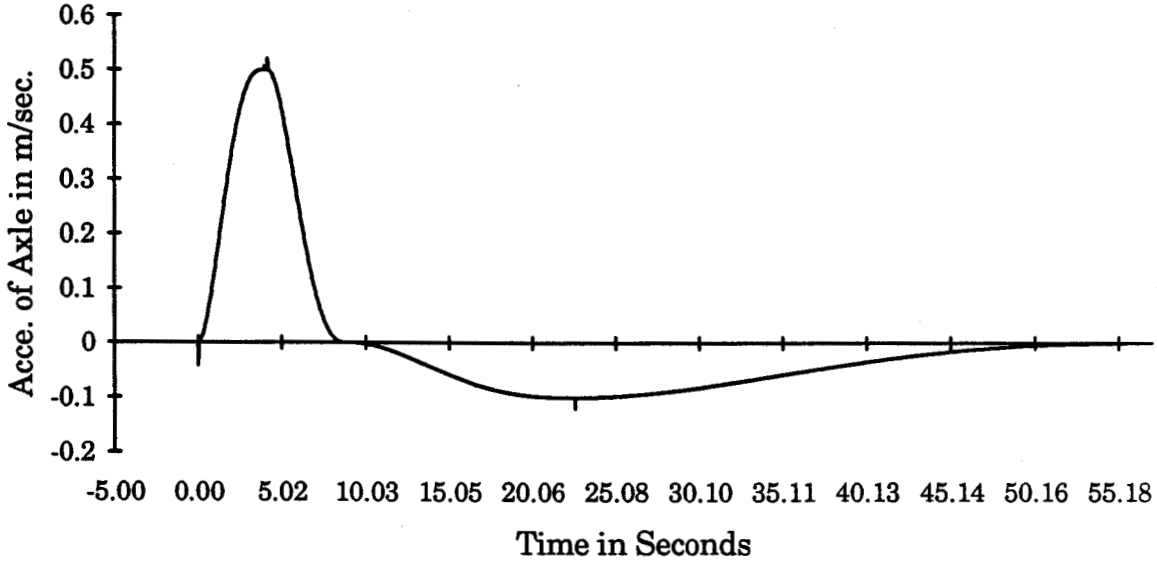

Figure 5.17: Axle acceleration.

The velocity and position of the axle during motion are shown in Fig. 5.18 and Fig. 5.19,

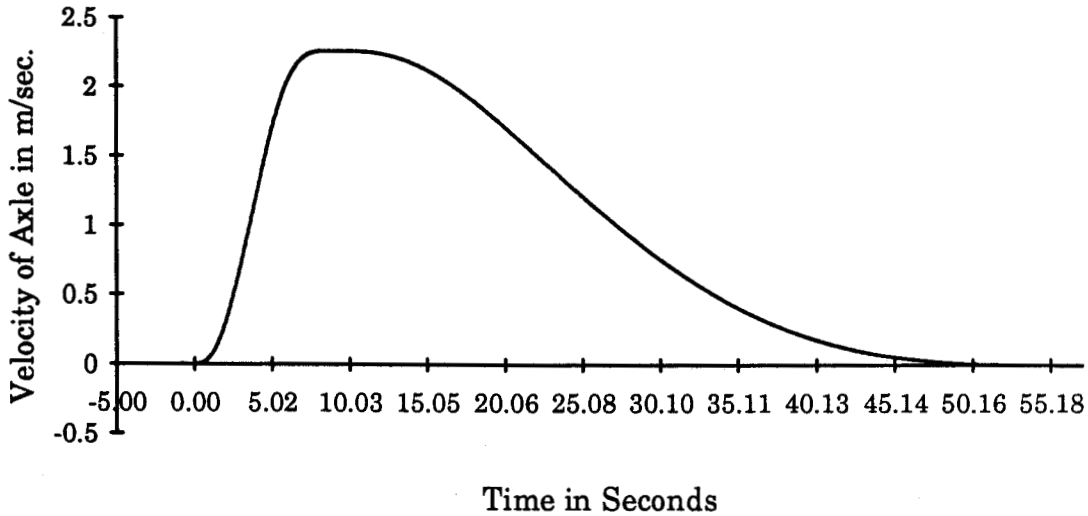

Figure 5.18: Axle speed during motion.

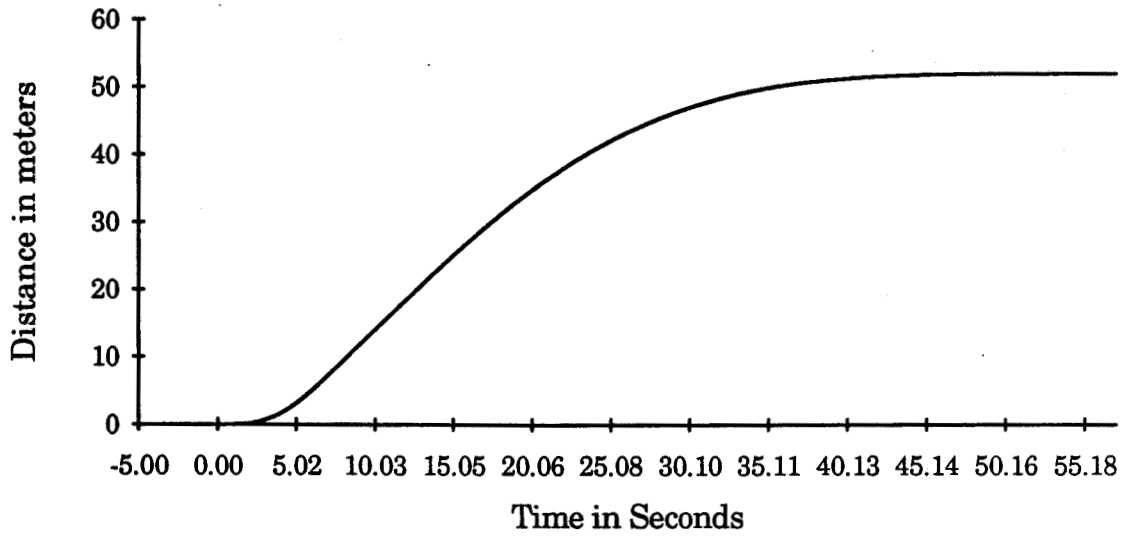

Figure 5.19: Distance covered.

The angular position of inverted pendulum during the motion is shown in Fig. 5.20,

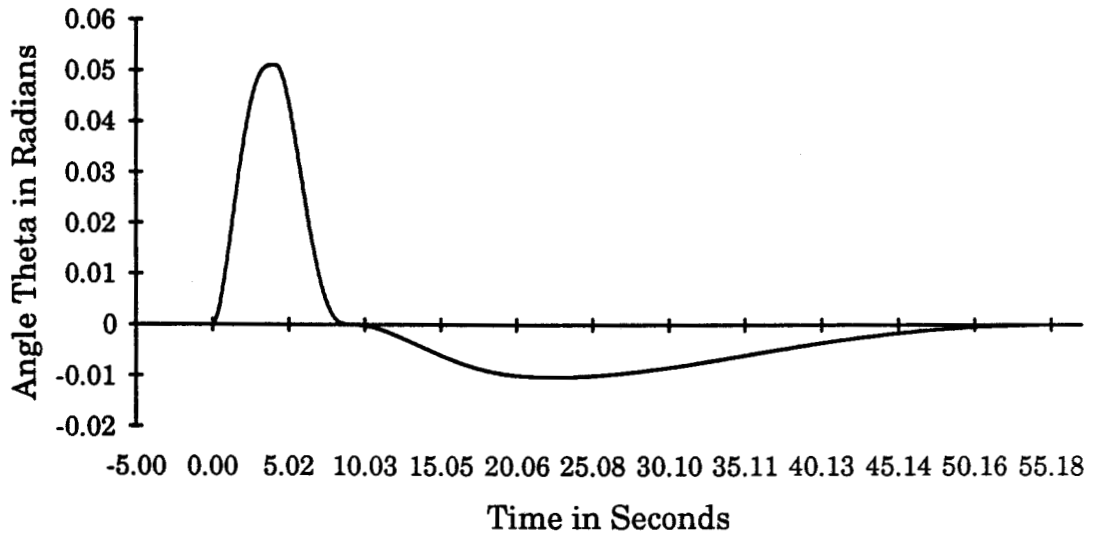

Figure 5.20: Angular position of Inverted Pendulum.

The angular velocity and acceleration are shown in Fig. 5.21 and 5.22 respectively,

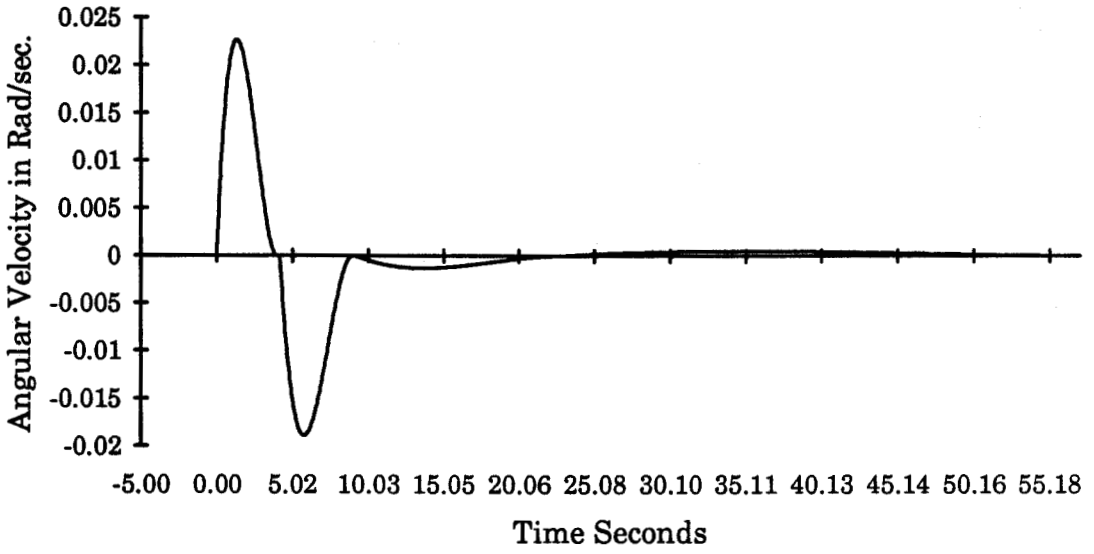

Figure 5.21: Angular Velocity of Inverted Pendulum.

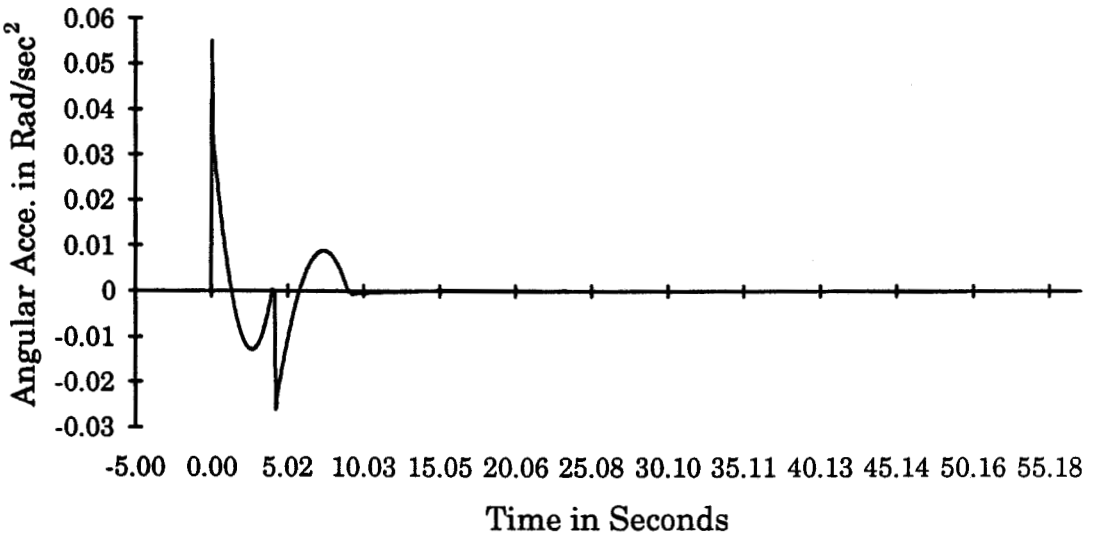

Figure 5.22: Angular acceleration of Inverted Pendulum.

As expressed in Eq. 4.9, the dynamic equation of the lower pendulum, the resultant offset β of the pendulum, in this motion plan, from the vertical position is shown in Fig. 5.23,

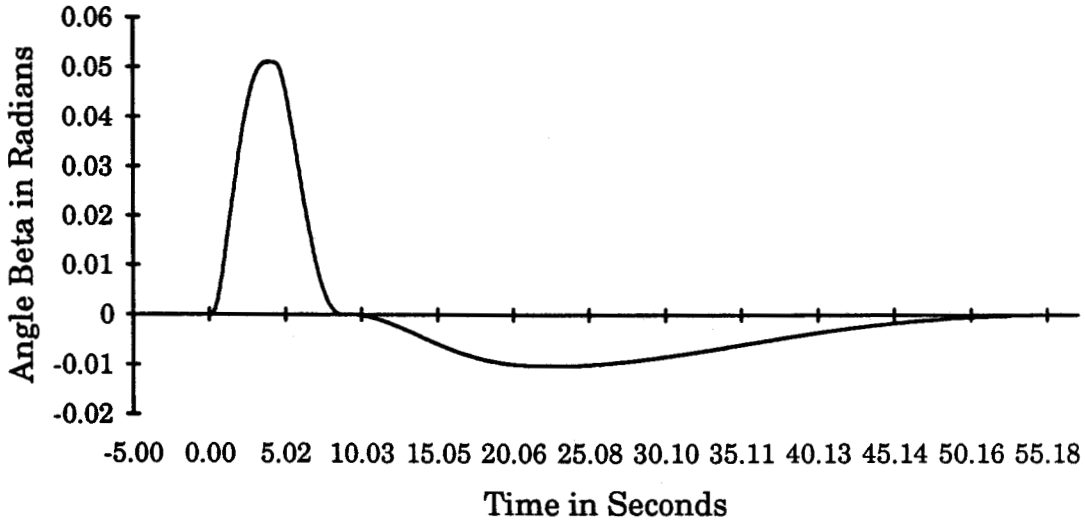

Figure 5.23: Offset of Simple Pendulum from vertical during the motion.

The error angle between calculated and estimated β in this planning is as shown in Fig. 5. 24,

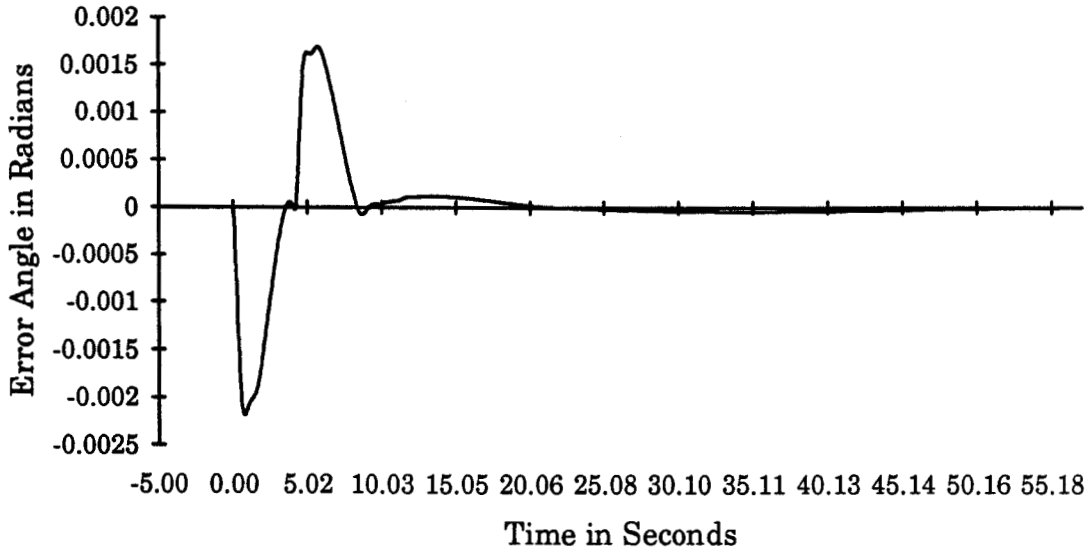

Figure 5.24: Error angle between calculated and estimated β.

From the above two simulations a comparison between continuous and piece wise planning can be done. The continuous motion planning shows some advantages over piece wise planning. The continuous planning gives greater stability to the system and a lower error in the β estimation is obtained.

5.4 MOTION PLANNING

Fig 5.17 shows a continuous motion plan to be employed to obtain the desired trajectory in the motion of the inverted pendulum system. This motion plan includes the acceleration function of the axle and the angular position of the inverted pendulum. The generated plan commands the servo control system, which produces the control torque to make the system move according to the plan.

As shown in the graphical representation of the motion plan, Fig. 5.17 different types of velocity function for a time, t, have been used. The magnitude of the acceleration vector depends upon the required task, i.e., the required distance, x_d to be traveled in time t_d. This requires the generation of the acceleration functions for the different intervals. This task requires a considerable amount of time to find the necessary acceleration functions and interval time for each motion task.

The motion plan should be generated before the motion task starts so the control system could follow the plan to complete the motion in real time.

There are several algorithms that could be used to generate the motion plan. Among them, a Knowledge Base System is one of the preferable techniques. Generally, a Knowledge Base System consists of a knowledge data base, knowledge reasoning, a knowledge base planner, and a learning system. In this project, an overview of the knowledge based approach will be given as a possible solution to the problem of control implementation for the motion of the inverted pendulum system.

Fig. 5.25 shows a knowledge based motion planning system. The knowledge base consists of past experience plans called knowledge data base,

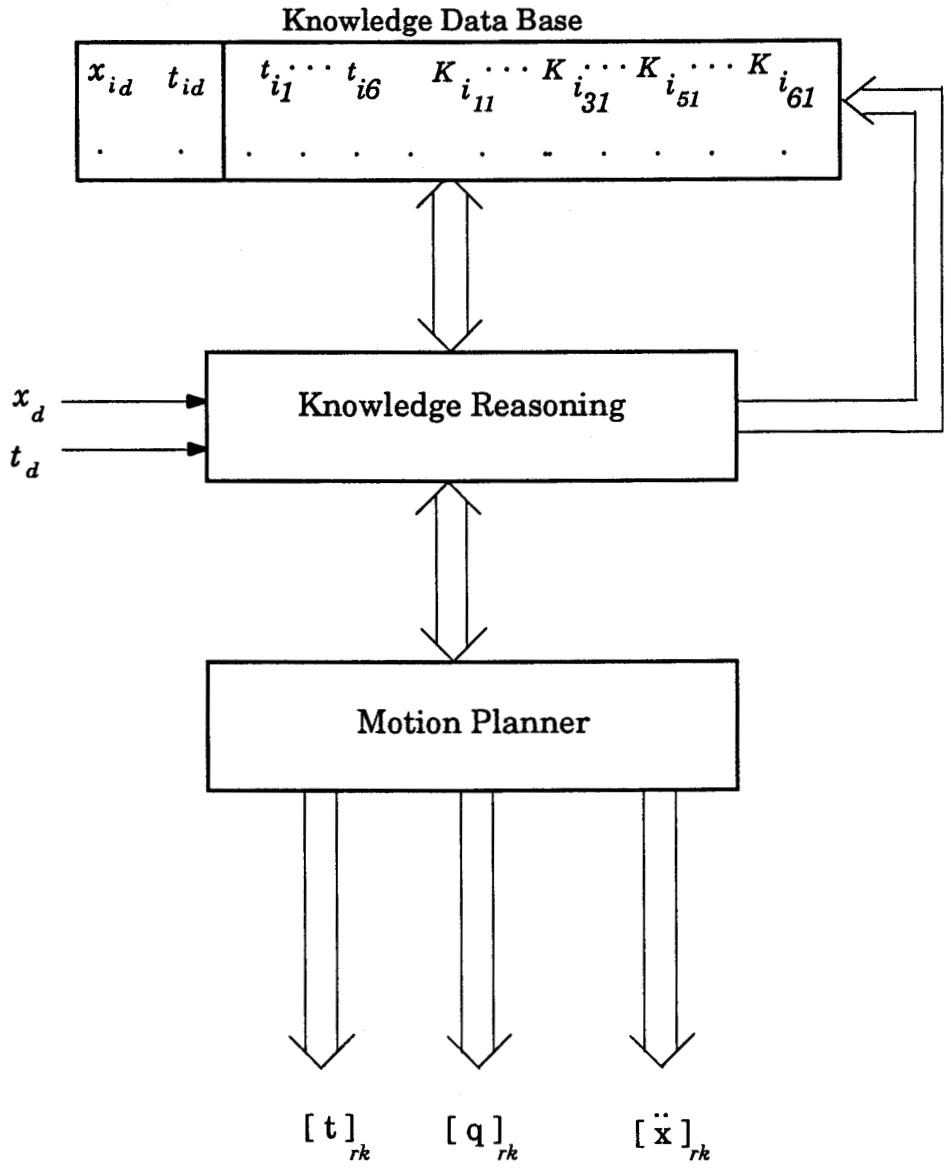

Figure 5.25: Knowledge Base Motion Planner.

Each element in the knowledge data base represents the coefficients of motion, Eq. 5.3, and the corresponding time interval. The values t_{i1}, t_{i2}, t_{i3}, t_{i4}, t_{i5}, t_{i6} represent the intervals of the different phases and K_{i11}, K_{i12}, K_{i13}, K_{i31}, K_{i32}, K_{i31}, K_{i51}, K_{i52}, K_{i53}, K_{i61}, K_{i62}, K_{i63} represent the coefficients for Eq. 5.3. The elements, x_{id} and t_{id} represent the corresponding required distance to be covered and the duration of time respectively. This stored knowledge could be obtained from the past experience of the planner. The most important layer of the knowledge base planning system is the knowledge reasoning. This

section is responsible for the determination of the parameters required for the current task, x_d in t_d. The reasoning takes place using the linear interpolation method for the estimation of required parameters from the stored knowledge. The motion planner develops the motion vectors, $[\ddot{x}]_{rk}$, $[q]_{rk}$, and $[t]_{rk}$. The new knowledge will be stored in the knowledge data base for future use by a feedback loop from the knowledge planner to the knowledge data base.

5.4.1 Knowledge Data Base

This is the computer data base where the knowledge acquired during past experience has been organized in two row vectors of R^n and R^m of dimensions n and m respectively. The row vector R^n is called Desired Vector, [DV], and R^m vector is the corresponding Knowledge Vector, [KV].

$$[\ DV\ ]_{R^n} \ ===> \ [\ KV\ ]_{R^m}$$

therefore,

$$[\ DV\ ] ====> \ [\ x_{id}\ \ t_{id}\ ], \text{ and}$$

$$[\ KV\ ]==> [\ t_{i1}\ \ t_{i2}\ \ t_{i3}, t_{i4}\ \ t_{i5}\ \ t_{i6}\ K_{i11}\ \ K_{i12}\ \ K_{i13}\ K_{i31}, K_{i32}, K_{i31}, K_{i51}, K_{i52},$$

$$K_{i53}, K_{i61}, K_{i62}, K_{i63}\ ]$$

$$i = 0,1,2,.....,N$$

N is the total number of knowledge vectors in the knowledge data base.

5.4.2 Data Base Structure

The knowledge data base is organized in hierarchical fashion in a top down method. This method makes it easier to search the knowledge in the data base during the reasoning period. The entries in the knowledge base have been structured as shown in Table 5.5,

Table 5.5: Knowledge Data Base

Cell *i= 1,2 ....., N*	Desired Vector	Knowledge Vector
1	$[\ DV\ ]_1$	$[\ KV\ ]_1$
2	$[\ DV\ ]_2$	$[\ KV\ ]_2$
.	. . . .	. . . .
.	. . . .	. . . .
N-1	$[\ DV\ ]_{(N-1)}$	$[\ KV\ ]_{(N-1)}$
N	$[\ DV\ ]_N$	$[\ KV\ ]_N$

Each data row vector is known as a data cell, i = 1,2,...,N. So, each data cell consists of [DV] and [KV] vectors R^2 and R^{18} respectively. The new set of data will be augmented in the knowledge data base. This way the knowledge data base becomes more and more experienced. This experienced data base can then produce more accurate motion planning.

5.4.3 Reasoning

The reasoning method is very important in the generation of a motion plan. The qualitative knowledge from the knowledge data base is very important. The first and most important task of the reasoning algorithm is to get all the knowledge and the desired vector, for corresponding t_d from the knowledge data base. After getting all required vectors, the linear interpolation in x_{id}'s will be applied. In this way, the approximated knowledge vector for the corresponding desired vector [x_d t_d] will be developed. The reasoning algorithm is as shown in Fig. 5.26 and Fig. 5.27,

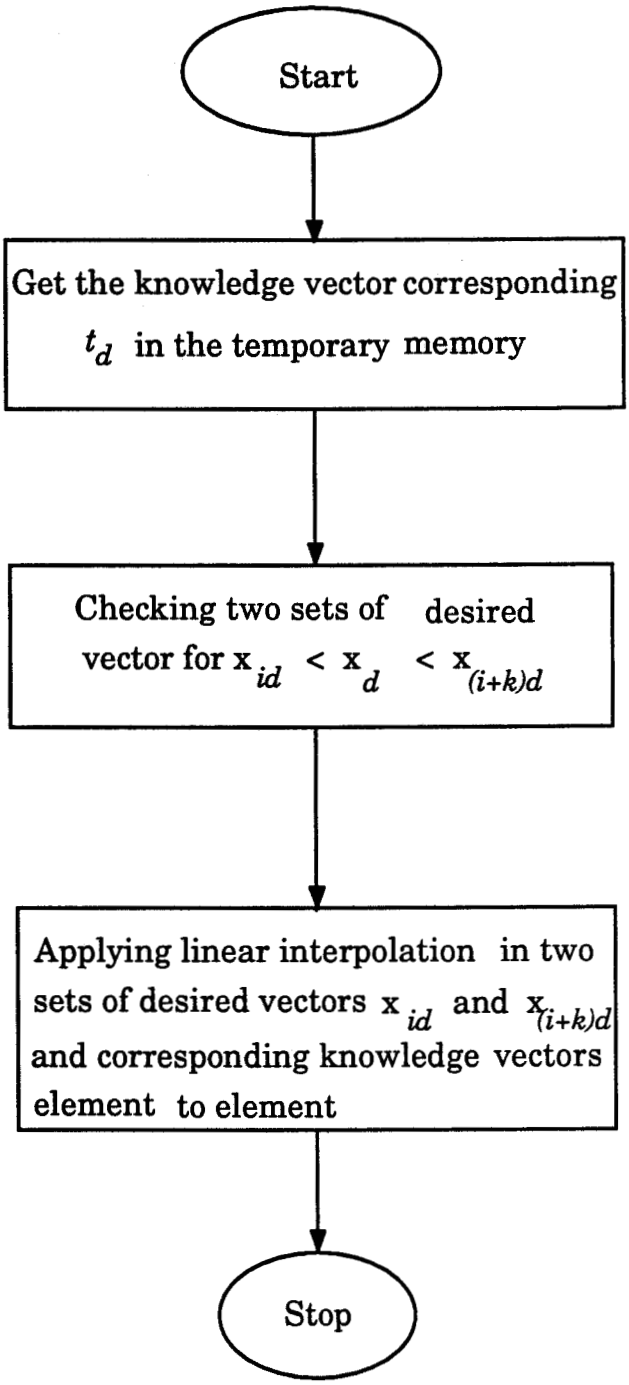

Figure 5.26: Reasoning algorithm, flow diagram.

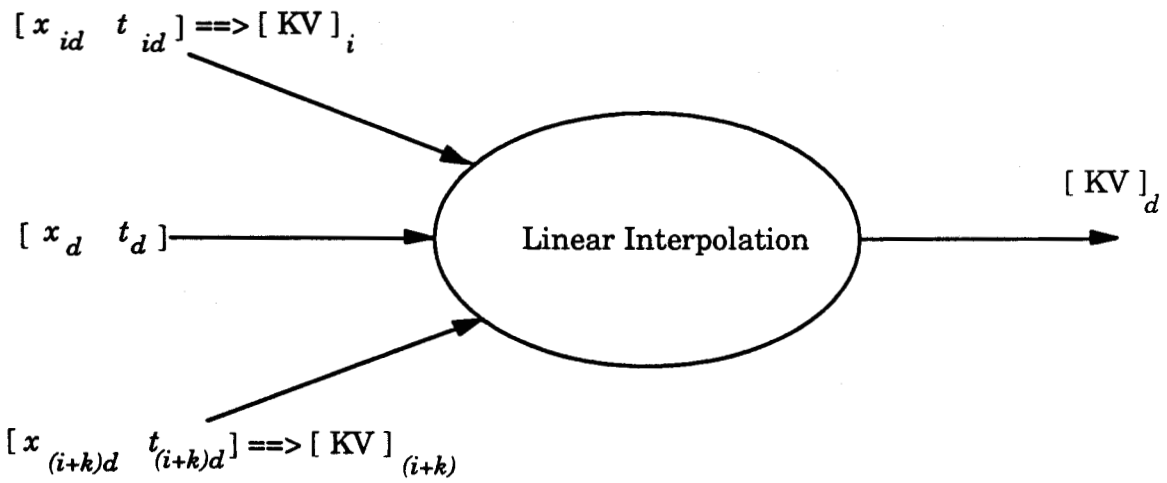

$$x_{id} < x_d < x_{(i+k)d} \quad \text{and,} \quad t_{id} = t_{(i+k)d}$$

Figure 5.27: Reasoning algorithm, star diagram.

5.4.4 Motion Planner

This section generates the final motion plan, i.e., the linear acceleration function, $[\ddot{x}]_{rk}$, the angular position vector, $[\ q\ ]_{rk}$ and the time interval vector, $[\ t\ ]_{rk}$. These vectors are generated on the basis of knowledge generated from the knowledge reasoning with the equation Eq 5.3.

5.5 CONTROL

This section will describe a preliminary control strategy that could allow the inverted pendulum system to move autonomously over variable terrain. The overall control of the inverted pendulum system, Fig. 4.1, could be divided into the motion phase and stabilization phase.

5.5.1 Motion Phase

This controls the motion of the inverted pendulum system, Fig. 4.1, according to the plan developed by the knowledge base motion planning system. The controller controls the linear acceleration of the axle and the angular position of the inverted pendulum, determined by the equation, Eq. 5.3. This constrained motion requires a control torque that is to be applied

between the inverted pendulum and the axle of the wheel. The required linear acceleration and the angular position need to be regulated according to the motion plan. Thus a control system is required to regulate both these variables.

Fig 5.28 shows the basic block diagram of a feedback control system,

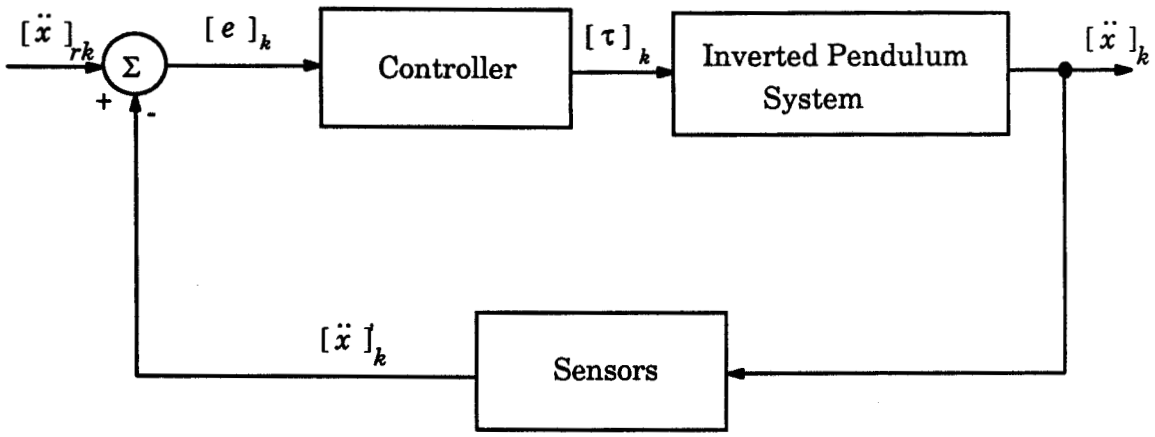

Figure 5.28: Basic Feedback Control system for motion phase.

where,

$[\ddot{x}]_{rk}$ is the required acceleration of the cart (from motion plan),

$[\ddot{x}]_k$ is the actual acceleration of the cart at time k (measured),

and $[\ddot{x}]_k$ is the feedback acceleration of the cart at time k.

5.5.2 Stabilization Phase

This phase is responsible for balancing the inverted pendulum in the vertical position. This phase starts at time t_6 in the motion plan. In this phase the importance of linear velocity of the axle will no longer be valid and only the angular position and velocity of the inverted pendulum becomes important. At the balanced position, both θ and $\dot{\theta}$ should be zero so that the inverted pendulum remains in the absolute vertical position. The angular deviation of the inverted pendulum from the vertical position must be adjusted to keep the inverted pendulum in a balanced position. Thus, an active controller is required to control the balance of the inverted pendulum. This controller remains active until the new motion cycle starts.

Fig. 5.29 shows a block diagram of a feedback controller for stabilization of the inverted pendulum in a balanced vertical position,

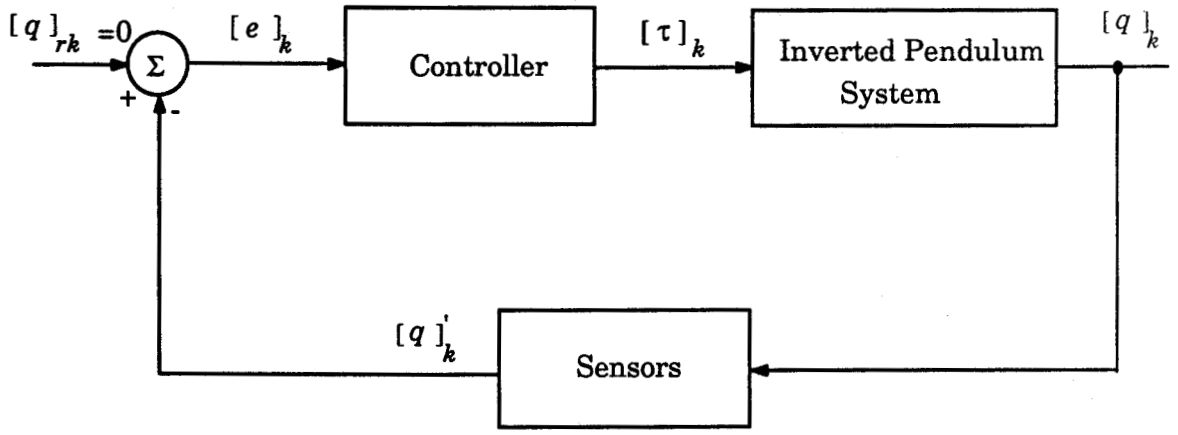

Figure 5.29: Feed Back Control for stabilization of the inverted pendulum.

where,

$[q]_{rk}$ is the desired vector $\left[\theta \quad \dot{\theta}\right]_{rk}^{T}$,

$[q]_k$ is the output vector $\left[\theta \quad \dot{\theta}\right]_{k}^{T}$,

and $[q]'_k$ is the feedback vector $\left[\theta \quad \dot{\theta}\right]_{k}^{'T}$.

Fig. 5.28 and Fig. 5.29 show the basic block diagram of a conventional feedback control system. The controller generates a control torque vector depending upon the task. The motion control torque is developed during the motion of the system and the stabilizing torque during the stabilization phase.

5.6 CONTROLLER DESIGN

The overall control system consists of two different control algorithms, motion and stabilizing. These control systems must be coordinated to control the inverted pendulum system dynamically during the motion and at rest. Thus, the above two control systems, Fig. 5.28 and 5.29 can be combined into a single unit with a switching system that changes the mode of the controller, as shown in Fig. 5.30,

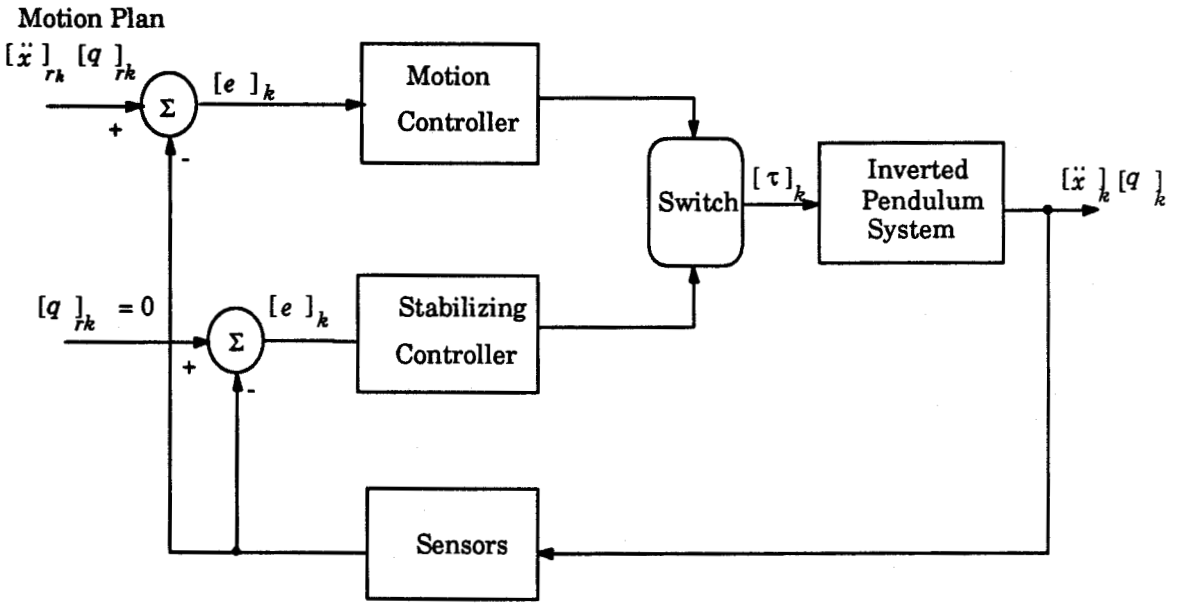

Figure 5.30: Integrated feedback control.

The coordinator or switch changes the controller mode at the beginning of motion cycle and at the end of the motion cycle, i.e., t_6. The switch action can be represented by the timing diagram, as shown in Fig. 5.31.

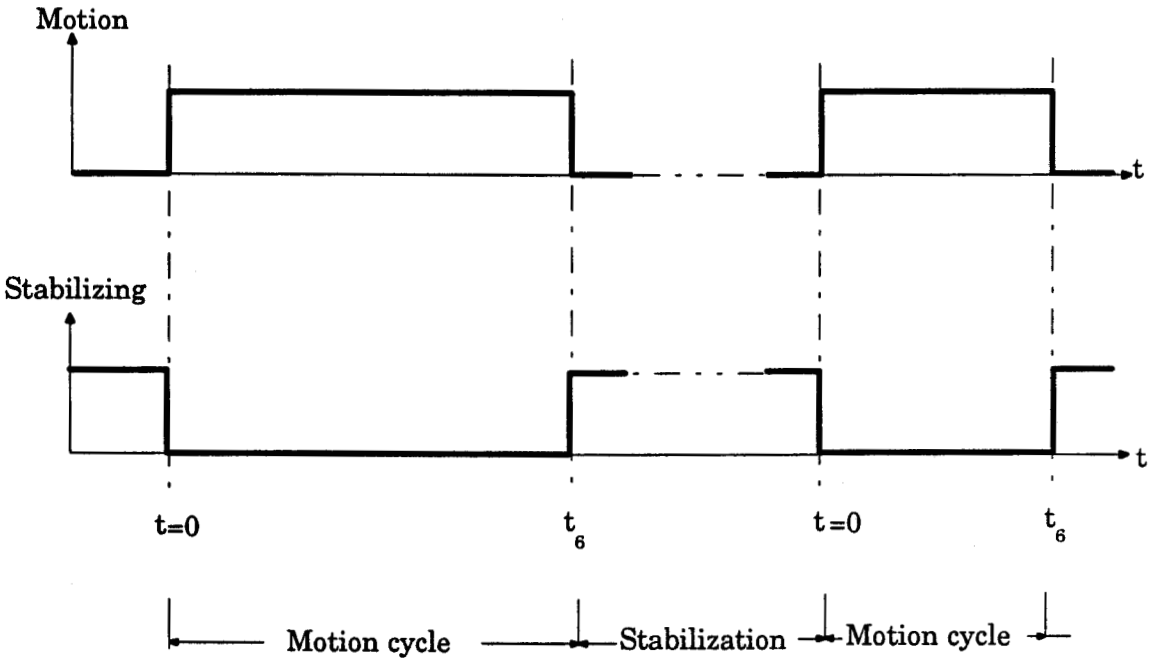

Figure 5.31: Timing diagram of switching.

The torque required on a flat terrain depends only upon the magnitude and derivatives of θ and the linear acceleration of the axle, $\ddot{x}$. As the wheel rolls on a slope, the required torque also depends upon the slope gradient in addition to the torque in the horizontal plane; the required torque is non-linear. A servo control system is needed to cope with the non-linearity appearing in the system to reduce the stability problem. The conventional PID controller has been widely used in servo systems. The PID servo system is fairly good if the speed and the accuracy are not critical. The algorithm of the PID control system is mainly based on the system mathematical model. Thus the performance of the PID controller is heavily dependent upon the exactness of the mathematical model of the corresponding physical system. However, the mathematical model of any physical system depends upon the availability of the information and also the inclusion of the possible coefficients and dynamics at the time of system modeling. The exact modeling of a physical system is very difficult when the system undergoes changes.

The Model Reference Adaptive Control (MRAC) technique could be employed to cope with the environmental uncertainties. Its algorithm is to develop an error signal by comparing the reference input with the process output and adjusting the parameters of the controller through a suitable adaptation algorithm based on a parameter estimation method. This technique has a disadvantage in that it requires the transfer function of the system. The transfer function of the system is very difficult to model if the system is operating under uncertainties. So the one disadvantage of this technique is the transfer function of the uncertainties that can not be modeled and another disadvantage is storing and processing the large amount of data needed to adapt the controller. Thus this system is also not very suitable if the degree of uncertainties and the non-linearity is high.

Incorporating human intelligence into an automatic control system could be a more efficient solution in the control of non-linear system in uncertainty environments. Car-driving in foggy day is an example of control of a non-linear system with uncertainty. The driver uses his intelligence to navigate the car rather than the solution of differential equations of the road and fog in that particular time. Humans use symbolic or qualitative descriptions of control rather than mathematical solutions. Motion control is

an another example of non-linear control by humans using qualitative knowledge.

5.6.1 Servo Control System

In order to control the balance of the inverted pendulum during motion and at rest a control torque is needed. This control torque is applied in the inverted pendulum with respect to the axle. Thus, only one torque is applied in the system. The open loop configuration of the system with the driving system, DC motor, can be expressed in a block diagram, as shown in Fig. 5. 32,

Figure 5. 32: Open Loop Model.

The characteristics of driving system, DC Motor, is given in Appendix D and also a preliminary design method of a closed-loop controller for Fig. 5.32 is given in Appendix E.

5.7 CONCLUDING REMARKS

This chapter has been devoted to the development of a motion planning algorithms for the inverted pendulum system. Two types of motion planning algorithms were discussed followed by the simulations of the system mathematical model for a prescribed planning. Some advantages of continuous motion planning over piece-wise motion planning were highlighted. An overview of Knowledge Based motion planning algorithm was also studied.

A preliminary examination of a controller that controls the system in motion and stabilizes the system at rest was also discussed.

6. SUMMARY, CONCLUSIONS AND FUTURE DIRECTIONS

6.1. SUMMARY

This thesis has described the simulation of an inverted pendulum system that could stably traverse both flat and changing terrain. The required task, that of balancing the center of mass of the proposed model (inverted pendulum) into the line of gravity that passes through the axle and the center of mass, has been carried out by applying a control torque on the inverted pendulum with respect to the wheel axle. The imbalance of the inverted pendulum from the vertical position has been measured with respect to the reference direction of gravity.

The maintenance of a stable posture is important to all unstable mobile systems. For humans it is challenging because of our physical structure. A human's center of body mass lies 2/3 of the body height over two spindly structures, the legs. This mass is required to be balanced along the line of gravity that passes through the pivot point. This line of gravity is the reference line for balancing the body posture. The balancing of a human body into an upright position requires the sensing of the direction of gravity.

To establish the dynamic balance of an inverted pendulum in different terrains, during motion and at rest, a method of sensing the direction of gravity has been developed and tested. An inertial element, a rigid simple pendulum, has been used as a sensor to do this task. Several simulations were carried out to estimate the direction of gravity in horizontal and changing terrains.

A mathematical expression has been formulated to find the direction of gravity in various terrains when the pivot point of the simple pendulum is in

motion. The offset of the pendulum's center of mass from an absolute equilibrium, assumed to be the line of gravity that passes through the center of mass and the pivot point at zero motion, has been measured in terms of possible available information from the sensory system. This offset, the angle of a simple pendulum with the vertical during motion, then was used to measure the imbalance of the inverted pendulum from the vertical position.

An algorithm for task oriented motion planning of the proposed model has been developed and tested in simulation. The continuous motion planning used by humans has better stability than piece-wise motion planning; the same logical ideas have been considered to plan the motion of the unstable mechanical system. A learning program was executed, in near real time, to simulate the control torque that is required for the desired motion, and the balance of the inverted pendulum model, studied in this project. This simulation was carried out in flat and changing terrains with sufficient static friction provided by the surface of the terrain to avoid wheel slip.

The importance of dynamic balance for an unstable mobile system in unstructured terrain has been outlined in Chapter 2. This includes the importance and uses of an inertial sensing system to detect the direction of gravity in changing terrain which is needed to accomplish the dynamic balance.

Modeling of a physical system is important in order to represent the system in an equivalent mathematical model for analysis of dynamic behavior. Several techniques exist to find the system dynamics. One popular technique, Lagrangian dynamics, was used to model the proposed dynamic system in this project. The dynamic behavior of the simple pendulum, which has a dynamic pivot point, in different conditions was studied in Chapter 3. Some important simulation results were also included.

The design of an inverted pendulum system has been described in Chapter 4. The design considerations and the required sensory system for balance have been examined. Several simulation results for different initial conditions of the system were also shown. A mathematical expression was

formulated to estimate the direction of gravity during the motion of the inverted pendulum in different terrains. Some simulation results of the estimation of the direction of gravity, in flat and changing terrains were also shown and discussed.

Planning the motion of an unstable mobile system while keeping its body within a balanced position is a task oriented problem. By incorporating the inertial information, an algorithm for motion planning was developed to move the inverted pendulum system to accomplish the desired motion in various terrains. The idea used in the development of such an algorithm was similar to the assumed motion plan used by a human. The algorithm of this motion planning was discussed in Chapter 5. The entire control of the system was divided into two phases: motion and stabilization. An overview of a control system that could be used to control the motion of an inverted pendulum, coordinated with the task oriented motion plan, has been discussed.

6.2. CONCLUSIONS

The objectives of this project have been to develop and test a simulation of a sensory system that can determine the direction of gravity in a changing terrain, and to develop and test an algorithm and a model for motion planning of an inverted pendulum system in unknown terrains. Both of these objectives were attained in the project.

The work reported in this thesis describes a technique to find the direction of gravity in a changing terrain. The detected inertial information, the direction of gravity, has been used to find the imbalance of an inverted pendulum from the unstable equilibrium position, the vertical. This imbalance has been successfully used to plan the motion of the inverted pendulum system, in a way similar to human motion. The developed algorithm, for a task oriented motion plan, has been successfully employed in simulation to move the inverted pendulum system with balanced posture.

6.3. FUTURE DIRECTIONS

From the various simulation results, the gravity sensing system for locating the direction of gravity is highly affected by the motion of the point where the sensor is pivoted. The error in the estimation of the direction of gravity is significant at the transition in the motion which cannot be neglected. This error is small in the continuous motion. Further improvement in the gravity sensing technique, based on the inertial element could be done to avoid the error at the transition. Furthermore, a continuous motion plan could be developed to make the system stable during the motion.

Future work envisaged in the area of dynamic balance includes the integration of this technique with a control system to build a truly unstable autonomous mobile robot, that could be used more efficiently than existing stable robots in unstructured terrain.

REFERENCES

1. Donner, M. D., "Real-Time Control of Walking", *Birkhäuser* Boston, 1987.

2. Raibert, M. H., and Sutherland, I. E., " Machines That Walk", *Scientific American*, 248 (2) 1983, pp. 44-53.

3. McGhee, R. B., "Some Finite state Aspects of Legged Locomotion", Mathematical Biosciences, Vol. 2, 1968, pp. 67-84.

4. McGhee, R. B., " Control of Legged Locomotion Systems", *Proc. Joint Automatic Control Conference*, San Francisco, 1977, pp. 205-215.

5. McGhee, R. B., and Pai, A. L., " An approach to Computer Control for Legged Vehicles", *Journal of Terramechanics*, Vol. 11, No. 1, 1974, pp. 9-27.

6. Frank, A. A., and McGhee, R. B., " Some Considerations Relating to the Design of auto pilots for Legged Vehicles", *Journal of Terramechanics*, Vol. 1, No. 1, 1969, pp. 23-25.

7. Pfeiffer, F., Weidemann, H. J., and Danowski, P., "Dynamic of Walking Stick Insect", *IEEE Control System*, Feb. 1991, pp. 9-13.

8. Takehara, K., "Japan's ARTRA robot moves forward", *Nuclear Engineering International*, Jan. 1992, pp. 39-41.

9. Kessis, J. J., Rambant, J. P., Penn'e, J., Wood, R., and Matter, N., "Hexapod Walking Robots with artificial Intelligence Capabilities", *Theory and Practice of Robotics and Manipulators*, Edited by Morecki, G. B., and Kedzior, K. Kogan Page, London: pp. 395-402.

10. Waldron, K. J., and McGhee, R. B., " The Adaptive Suspension Vehicles", *IEEE Control System Magazine*, Dec. 1986, pp. 7-12.

11. Mosher, R. S., "Test and Evaluation of a Versatile Walking Truck", *Proceedings on Symposium on Off-Road Mobility Research*, 1968, pp. 359-379.

12. Raibert, M. H., 1985, *Legged Robots that Balance,* MIT Press. Cambridge, Massachusetts.

13. Miura, H. and Shimoyama, I., "Dynamic walk of a biped", *International Journal of Robotics Research*, Vol. 3, 1984, pp. 60-74.

14. Winter, D. A., Patla, A. E. and Frank, J. S., "Assessment of Balance control in humans", *Medical Progress through Technology*, Vol. 16, 1990, pp. 31-51.

15. Kuritsky, M. K., and Goldstein, M. S., "Inertial Navigation", *Autonomous Robot Vehicles*, edited by Cox, I. J. and Wilfong, G. T., 1990, pp. 96-116.

16. Nashner, L. M., "Balance Adjustments of Humans Perturbed while walking", *Journal of Neurophysiology*, Vol. 44, 1980, pp. 650-664.

17. Nashner, L. M., "A Model Describing Vestibular Detection of Body Sway Motion", *Acta Otolarng*, Vol. 72, 1971, pp. 429-436.

18. Koozekanani, S. H., and Duerk, J., "Determination of body Segment parameters and their effect in the calculation of the position of center of pressure during postural sway", *IEEE Trans. on Biomedical Engg.*, Vol. BME-32, No. 1, January 1985, pp. 67-69.

19. Shimba, T., "An Estimation of center of Gravity from Force Platform Data", *Journal of Biomechanics*, Vol. 17, No. 1, 1984, pp. 53-64.

20. Soames, R. W., and Atha, J.," The validity of physique-based inverted pendulum models of postural sway behavior", *Annels of Human Biology*, Vol. 7, No. 2, 1980, pp. 145-153.

21. McGhee, R. B., and Kuhner, M. B., "*On the Dynamic Stability of Legged Locomotion Systems. In Advances in External Control of Human Extermities*", Gavrilovic, M. M., and Wilson, A. B. Jr. (eds).

Jugosav Committee for Electronics and Automation, Belgrade, 1969, pp. 431-442.

22. Passerello, C. E., and Huston, R. L., "Human Attitude Control", *J. Biomechanics*, Vol. 4, 1971, pp. 95-102.

23. Luttgens and Wells, "Scientific Basis of Human Motion", Kineslogy, 7th ed. 1982, *CBS college Publishing*.

24. Rosenbaum, D. A.,"Human Motor Control", *Academic Press, Inc.* San Diego, California 92101, 1991.

25. Winter, D. A., "Sagittal Plan Balance and posture in Human Walking", *IEEE Engineering in Medicine and Biology Magazine*, Sept. 1987, pp. 8-11.

26. Hemami, H., and Jaswa, V. J., "On a Three-Link Model of the Dynamics of Standing Up and Sitting Down", *IEEE Tans. on Systems, Man, and Cybernetics* , Vol. SMC-8, No. 2, Feb. 1978, pp. 115-120.

27. Furuta, K., Ochiai, T., and Ono, N., "Attitude control of a triple Inverted pendulum", *International Journal of Control*, Vol. 39, No. 6, 1984, pp. 1351-1365.

28. Anderson, C. W., "Learning to Control an Inverted pendulum using Neural Networks", *IEEE Control System Magazine*, April 1989, pp. 31-36.

29. Lin, C. E., and Sheu, Y., "A hybrid-control Approach for Pendulum-Car Control", *IEEE Trans. on Industrial Electronics*, Vol. 39, No. 3, June 1992, pp. 208-214.

30. Furuta, K., Kajiwara, H., and Kosuge, K., "Digital control of a double inverted pendulum on an inclined rail", *International Journal of Control*, Vol. 32., No. 5, 1980, pp. 907-924.

31. Shannon, B., Personal Communication, 1985, ref. [12], page 11.

32. Connel, M.E., and Utgoff, P.E., " Learning to Control a Dynamic

Physical System", *Proc. American Association for Artificial Intelligence*, 1987, Vol.2, pp. 456-460.

33. Higdon, D. T., and Cannon, R. H., " On the Control of Unstable Multiple Output Mechanical System", *Proc. of Winter Annual Meeting, ASME Winter Annual Meeting*, Vol/Issue/Date: / 63-wa-148/1963, pp. 2-12.

34. Mori, S., Nishihara, H., and Furuta, K., "Control of Unstable Mechanical system Control of Pendulum", *International journal of Control*, Vol. 23, No. 5, 1976, pp. 673-692.

35. Sandler, Ben-Zion, " Designing the Mechanisms for Automated Machinary", *Robotics*, Prentice Hall, 1991.

36. Kumar, V. R., and Waldron, K. J., "A Review of Research on Walking Vehicles", *The Robotics Review 1*, edited by O. Khatib, J. J. Craig and T. L. Perez, The MIT press, 1989.

37. Mosher, R. S., " Exploring The Potential of a Quadruped", *SAE-PAPER 690191*, Jan. 1969, pp. 2-10.

38. Zheng, Y. F., "Acceleration Compensation for Biped Robots to Reject External Disturbances", *IEEE Trans. System Man and Cybernetics*, Vol. 19, No. 1, Jan. 1989, pp. 74-84.

39. Kato, T., Takanishi, A., Ishikawa, H., and Kato, I., "The realization of the Quasi Dynamic Walking by the Biped walking Machine", *4Th CISM-IFTOMM Symposium on theory and practice of Robots and Manipulators*, Zaborow, Poland, Sept. 1981, pp. 408-418.

40. Kajita, S., Yamaura, T., and Kobayashi, A., "Dynamic Walking Control of a Biped Robot Along a potential Energy Conserving Orbit", *IEEE Trans. on Robotics and Automation*, Vol. 8, No. 4, Aug. 1992, pp. 431-436.

41. Zheng, Y. F., and Shen, J., "Gait Synthesis for the SD-2 Biped Robot to Climb sloping Surface", *IEEE Trans. on Robotics and Automation*, Vol. 6, No. 1, Feb. 1990, pp. 86-96.

42. Vieville, T., and Faugers, O. D., "Computation of Inertial Information On a Robot", *Robotic Research*, 1990, pp. 57-65.

43. Graizer, B.M, "On Inertial Seismometry", *Izevestiya, Earth Physics*, Vol. 25, No.1, 1989, pp. 26-29.

44. Nashner, L. M., "Adaptive Reflexes Controlling the Human Posture", *Experimental Brain Research*, Vol. 26, 1976, pp. 59-72.

4.5. Radin, S. H., and Folk, R.T.,"Physics for Scientists and Engineers", *Prentice-Hall, Inc.* Englewood Cliffs, 1982.

46. Wells, D. A., "Theory and Problems of Lagrangian Dynamics", *Schuam Outline Series, McGraw-Hill Book Company*.

47. Williams, P. W., " *Numerical Computation*", *Thomas Nelson and Sons Ltd*, 1972, ISBN 0 17 771018 7.

48. James, M. L., Smith, G. M., and Wolford, J. C., "Applied Numerical Methods for Digital Computation", *IEP- A Dun Donnelley Publisher*, New York.

49. "DC Motors Speed Control Servo Systems", *An Engineering Handbook by Electro-Craft Corp.*, Minnesota 55343.

50. Nise, N. S., "Control Systems Engineering", *The Benjamin/Cummings Publishing Company Ltd.*, 1991.

APPENDIX A

LAGRANGIAN DYNAMICS

This appendix shows the Lagrangian method of writing the dynamic equations of an n degrees of freedom (DOF) system. Using Lagrangian method, it is easy to express the dynamic behavior of simple to complex dynamic systems. This method is based on the scalar quantities kinetic energy, potential energy, and dissipative energy. Each of these quantities can be expressed in any coordinate system. The Lagrangian method automatically takes full account of vector quantities force, velocity, acceleration, etc. This method consists of proper components, force, torque, and acceleration expressed in the selected coordinates regardless of system complexities [46].

Derivation of Lagrangian equations

The Newtonian equations of motion define the force acting on a particle of mass, m in terms of its resulting acceleration. Assuming a constant force, F, with three components in the inertial frame, the equations of motion can be expressed as,

$$F = iF_x + jF_y + kF_z,$$

and,

$$F_x = m\ddot{x}, \quad F_y = m\ddot{y}, \quad F_z = m\ddot{z}, \tag{A.1}$$

where m is the mass of the particle, $\ddot{x}$, $\ddot{y}$, and $\ddot{z}$ are the linear accelerations in x, y, and z coordinates.

These forces result in the displacement of the mass an amount ds, with components $\delta x, \delta y$, and δz. Thus the virtual work done on the mass, m is ,

$$\delta w = m(\ddot{x}\,\delta x + \ddot{y}\delta y + \ddot{z}\delta z) = F_x\,\delta x + F_y\delta y + F_z\delta z,$$

or,

$$m(\ddot{x}\,\delta x + \ddot{y}\delta y + \ddot{z}\delta z) = F_x\,\delta x + F_y\delta y + F_z\delta z. \qquad \text{(A.2)}$$

The right side of Eq. A.2 shows the work done by the applied force and left side shows the change in energy of the mass. This relation is known as D'Alembert's equation.

A great variety of coordinates may be required to represent the n DOF physical system and the corresponding dynamic equations. Hence, for convenience, a letter q has been used to represent the coordinates regardless of their nature. This letter q is referred to as a generalized coordinate.

When there are two degrees of freedom, the x, y, z coordinates of mass m can be written as the functions of two generalized coordinates q_1 and q_2,

therefore,

$$x = x(q_1, q_2), \quad y = y(q_1, q_2), \quad z = z(q_1, q_2). \qquad \text{(A.3)}$$

Eq. A.3 can be written in differential form,

$$\delta x = \frac{\partial x}{\partial q_1}\delta q_1 + \frac{\partial x}{\partial q_2}\delta q_2, \qquad \text{(A.4.1)}$$

$$\delta y = \frac{\partial y}{\partial q_1}\delta q_1 + \frac{\partial y}{\partial q_2}\delta q_2, \qquad \text{(A.4.2)}$$

$$\delta z = \frac{\partial z}{\partial q_1}\delta q_1 + \frac{\partial z}{\partial q_2}\delta q_2, \qquad \text{(A.4.3)}$$

substituting these equations in D'Alembert's equation Eq. A.2 gives:

$$\delta w = m(\ddot{x}\frac{\partial x}{\partial q_1} + \ddot{y}\frac{\partial y}{\partial q_1} + \ddot{z}\frac{\partial z}{\partial q_1})\delta q_1 + m(\ddot{x}\frac{\partial x}{\partial q_2} + \ddot{y}\frac{\partial y}{\partial q_2} + \ddot{z}\frac{\partial z}{\partial q_2})\delta q_2,$$

$$= (F_x \frac{\partial x}{\partial q_1} + F_y \frac{\partial y}{\partial q_1} + F_z \frac{\partial z}{\partial q_1})\delta q_1 + (F_x \frac{\partial x}{\partial q_2} + F_y \frac{\partial y}{\partial q_2} + F_z \frac{\partial z}{\partial q_2})\delta q_2. \qquad (A.5)$$

Considering the work done when only q_1 is allowed to vary, thus $q_2 = 0$, Eq. A.5 will reduces to,

$$\delta w_{q1} = m(\ddot{x} \frac{\partial x}{\partial q_1} + \ddot{y} \frac{\partial y}{\partial q_1} + \ddot{z} \frac{\partial z}{\partial q_1})\delta q_1 = m(F_x \frac{\partial x}{\partial q_1} + F_y \frac{\partial y}{\partial q_1} + F_z \frac{\partial z}{\partial q_1})\delta q_1. \qquad (A.6)$$

Now, since,

$$\ddot{x} \frac{\partial x}{\partial q_1} = \frac{d}{dt}\left(\frac{\partial (\dot{x}^2/2)}{\partial \dot{q}_1}\right) - \frac{\partial (\dot{x}^2/2)}{\partial q_1}, \qquad (A.7)$$

substituting Eq. A.7 with similar relations involving y and z in Eq. A.6 then Eq. A.6 can be written as,

$$\partial w_{q1} = \left[\frac{d}{dt}\left\{m \frac{\partial}{\partial \dot{q}_1}\left(\frac{\dot{x}^2 + \dot{y}^2 + \dot{z}^2}{2}\right)\right\} - m \frac{\partial}{\partial q_1}\left(\frac{\dot{x}^2 + \dot{y}^2 + \dot{z}^2}{2}\right)\right]\delta q_1,$$

$$= (F_x \frac{\partial x}{\partial q_1} + F_y \frac{\partial y}{\partial q_1} + F_z \frac{\partial z}{\partial q_1})\delta q_1, \qquad (A.8)$$

since, $\frac{1}{2}m(\dot{x}^2 + \dot{y}^2 + \dot{z}^2)$ is the kinetic energy T of the particle. Thus,

$$\frac{d}{dt}\left(\frac{\partial T}{\partial \dot{q}_1}\right) - \frac{\partial T}{\partial q_1} = F_x \frac{\partial x}{\partial q_1} + F_y \frac{\partial y}{\partial q_1} + F_z \frac{\partial z}{\partial q_1}, \qquad (A.9.1)$$

and

$$\frac{d}{dt}\left(\frac{\partial T}{\partial \dot{q}_2}\right) - \frac{\partial T}{\partial q_2} = F_x \frac{\partial x}{\partial q_2} + F_y \frac{\partial y}{\partial q_2} + F_z \frac{\partial z}{\partial q_2}, \qquad (A.9.2)$$

Eq. A.9.1 and A.9.1 can be written in general form as,

$$\frac{d}{dt}\left(\frac{\partial T}{\partial \dot{q}_r}\right)-\frac{\partial T}{\partial q_r}=F_q \ , \tag{A.10}$$

where,

$$F_q = F_x \frac{\partial x}{\partial q_r}+F_y \frac{\partial y}{\partial q_r}+F_z \frac{\partial z}{\partial q_r}. \tag{A.11}$$

F_q is called the generalized force. The generalized force may consist of conservative, non-conservative and dissipative forces in the coordinate of interest. Thus F_q can be written as,

F_q = conservative + dissipative + non-conservative,

$$=-\frac{\partial V}{\partial q_r}+\frac{\partial D}{\partial \dot{q}_r}+ F_{qr},$$

where V and D are potential and dissipative energy respectively,

thus the Lagrange generalized system equation is given as:

$$\frac{d}{dt}\left(\frac{\partial T}{\partial \dot{q}_r}\right)-\frac{\partial T}{\partial q_r}=-\frac{\partial V}{\partial q_r}+\frac{\partial D}{\partial \dot{q}_r}+F_{qr} \tag{A.12.1}$$

or $$\frac{d}{dt}\left(\frac{\partial T}{\partial \dot{q}_r}\right)-\frac{\partial T}{\partial q_r}-\frac{\partial D}{\partial \dot{q}_r}+\frac{\partial V}{\partial q_r}=F_{qr} \ , \tag{A.12.2}$$

where F_{qr} is the non-conservative (applied force or torque in the coordinate of interest, q_r).

Inverted Pendulum (standing)

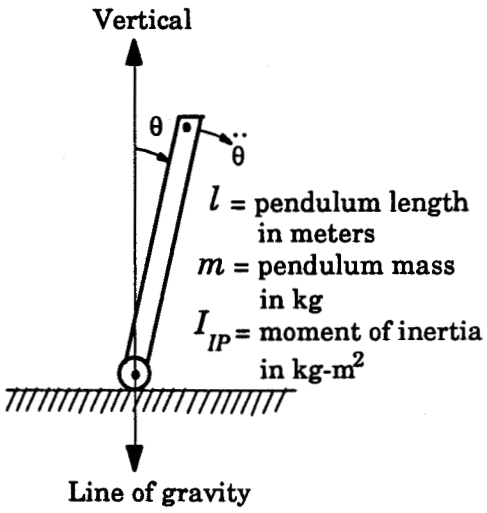

Figure A.1: Inverted pendulum, standing.

In this case, there is only one generalized coordinate, the angle of rotation of the inverted pendulum about the pivot point, θ.

Total kinetic energy of the system, T, for rotation about pivot point,

$$T = \frac{1}{2}(ml^2 + I_{IP})\dot{\theta}^{\,2}, \tag{A.13}$$

so $$\frac{\partial T}{\partial \dot{\theta}} = (ml^2 + I_{IP})\dot{\theta},$$

and,

$$\frac{\partial T}{\partial \theta} = 0,$$

thus, the equation of motion for rotation has a term,

$$\frac{d}{dt}\left(\frac{\partial T}{\partial \dot{\theta}}\right) - \frac{\partial T}{\partial \theta} = (ml^2 + I_{IP})\ddot{\theta} = F_\theta. \tag{A.14}$$

The potential energy, V,

$$V = mgl\cos(\theta), \tag{A.15}$$

so $$\frac{\partial V}{\partial \theta} = -mgl\sin(\theta\ ).$$

In the absence of friction,

$$F_\theta = mgl\sin(\theta\ ) - \tau, \tag{A.16}$$

So, the dynamic equation of the inverted pendulum Eq. 3.1 is,

$$mgl\sin(\theta) - (ml^2 + I_{IP})\ddot{\theta} = \tau\ , \tag{A.17}$$

where g is the acceleration of gravity and t is the external torque about the point of support to counter the acceleration of the inverted pendulum towards the ground.

Inverted Pendulum with Linear motion in flat terrain

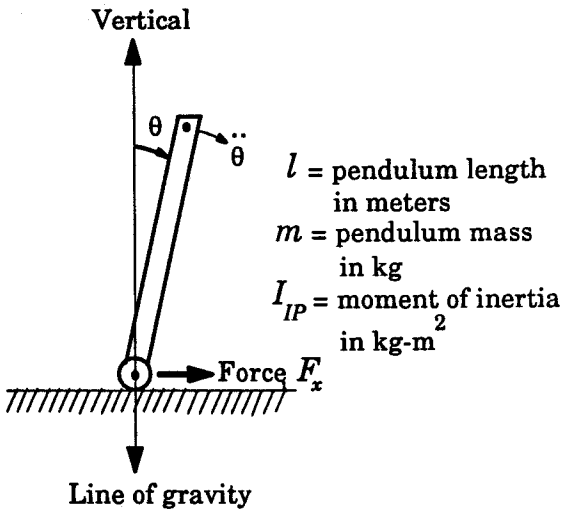

Figure A.2: Inverted pendulum with motion.

In this case, there are two generalized coordinates, θ and x. Total kinetic energy of the system is, T,

$$T = \frac{1}{2}m\dot{x}^2 + ml\cos(\theta\ )\dot{x}\dot{\theta} + \frac{1}{2}(ml^2 + I_{IP})\dot{\theta}^{\,2}, \tag{A.18}$$

$$\frac{\partial T}{\partial \dot{x}} = m\dot{x} + ml\cos(\theta\ )\dot{\theta},$$

$$\frac{d}{dt}\left(\frac{\partial T}{\partial \dot{x}}\right) = m\ddot{x} + ml\cos(\theta)\ddot{\theta} - ml\sin(\theta)\dot{\theta}^2,$$

and,

$$\frac{\partial T}{\partial x} = 0.$$

The potential energy, V,

$$V = mgl\cos(\theta), \tag{A.19}$$

$$\frac{\partial V}{\partial x} = 0,$$

$$F_{qr} = -\frac{\partial V}{\partial x} + F_x = F_x,$$

$$\frac{d}{dt}\left(\frac{\partial T}{\partial \dot{x}}\right) - \frac{\partial T}{\partial x} = F_{qr},$$

so the dynamic equation of the inverted pendulum in the x direction is,

$$m\ddot{x} + ml\cos(\theta)\ddot{\theta} - ml\sin(\theta)\dot{\theta}^2 = F_x. \tag{A.20-a}$$

Now, finding the equation of rotation of inverted pendulum about the point of support,

$$\frac{\partial T}{\partial \dot{\theta}} = ml\cos(\theta)\dot{x} + (ml^2 + I_{lP})\dot{\theta},$$

$$\frac{d}{dt}\left(\frac{\partial T}{\partial \dot{\theta}}\right) = ml\cos(\theta)\ddot{x} - ml\sin(\theta)\dot{x}\dot{\theta} + (ml^2 + I)\ddot{\theta},$$

$$\frac{\partial T}{\partial \theta} = -ml\sin(\theta)\dot{x}\dot{\theta},$$

$$\frac{\partial V}{\partial \theta} = -ml\,g\sin(\theta\ ),$$

$$F_{qr} = -\frac{\partial V}{\partial \theta} = ml\,g\sin(\theta\ ),$$

$$\frac{d}{dt}\left(\frac{\partial T}{\partial \dot{\theta}}\right) - \frac{\partial T}{\partial \theta} = F_{qr},$$

$$ml\cos(\theta\ )\ddot{x} + (ml^2 + I)\ddot{\theta}\ - ml\,g\sin(\theta\ ) = 0. \qquad \text{(A.20-b)}$$

Thus we have two degrees of freedom system, x and θ, and have two dynamic equations, Eq. A.20(a) and Eq. A.20(b).

Inverted Pendulum with Linear motion in changing terrain

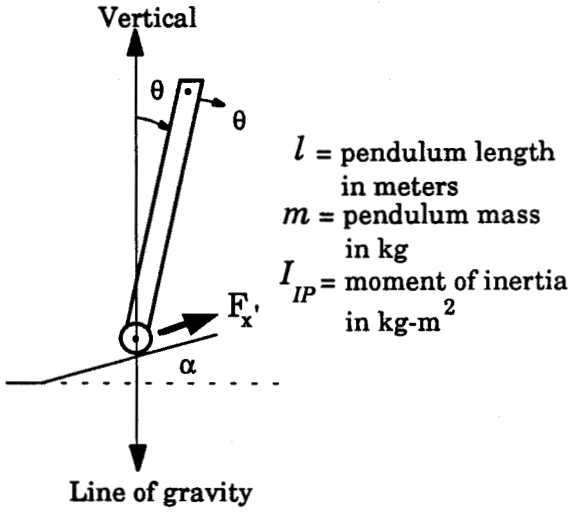

Figure A.3: Inverted Pendulum on a slope.

Kinetic energy of the system, T:

$$T = \frac{1}{2}m\dot{x}' + \frac{1}{2}mx'^2\dot{\alpha}^2 + ml\cos(\theta+\alpha)\dot{x}'\dot{\theta} - mlx'\sin(\theta+\alpha)\dot{\alpha}\dot{\theta} + \frac{1}{2}(ml^2 + I_{IP})\dot{\theta}^2, \qquad \text{(A.21)}$$

where x' is the distance traveled in the slope,

$$\frac{\partial T}{\partial \dot{x}'} = m\dot{x}' + ml\cos(\theta)\dot{\theta},$$

$$\frac{d}{dt}\left(\frac{\partial T}{\partial \dot{x}'}\right) = m\ddot{x}' - ml\sin(\theta+\alpha)(\dot{\theta}+\dot{\alpha}) + ml\cos(\theta+\alpha)\ddot{\theta},$$

$$\frac{\partial T}{\partial x'} = mx'\dot{\alpha}^2 - ml\sin(\theta+\alpha)\dot{\alpha}\,\dot{\theta},$$

the potential energy of the system,

$$V = mgx'\sin(\alpha) + ml\,g\cos(\theta), \tag{A.22}$$

$$\frac{\partial V}{\partial x'} = mg\sin(\alpha),$$

$$\frac{d}{dt}\left(\frac{\partial T}{\partial \dot{x}'}\right) - \frac{\partial T}{\partial x'}$$

$$= m\ddot{x}' + ml\cos(\theta+\alpha)\ddot{\theta} - ml\sin(\theta+\alpha)\dot{\theta}^2 - mx'\dot{\alpha}^2.$$

$$= F_{x'} + mg\sin\alpha$$

The equation of linear motion of point of support is,

$$m\ddot{x}' + ml\cos(\theta+\alpha)\ddot{\theta} - ml\sin(\theta+\alpha)\dot{\theta}^2 - mx'\dot{\alpha}^2 = F_{x'} + mg\sin\alpha, \tag{A.23}$$

In a similar way we can write the equation for angular motion,

$$ml\cos(\theta+\alpha)\ddot{x}' - 2\,ml\sin(\theta+\alpha)\dot{x}'\dot{\alpha} -$$

$$mlx'\cos(\theta+\alpha)\dot{\alpha}^2 - mlx'\sin(\theta+\alpha)\ddot{\alpha} + (ml^2 + I_{IP}). \tag{A.24}$$

$$= ml\,g\sin(\theta)$$

Simple pendulum with moving pivoting support

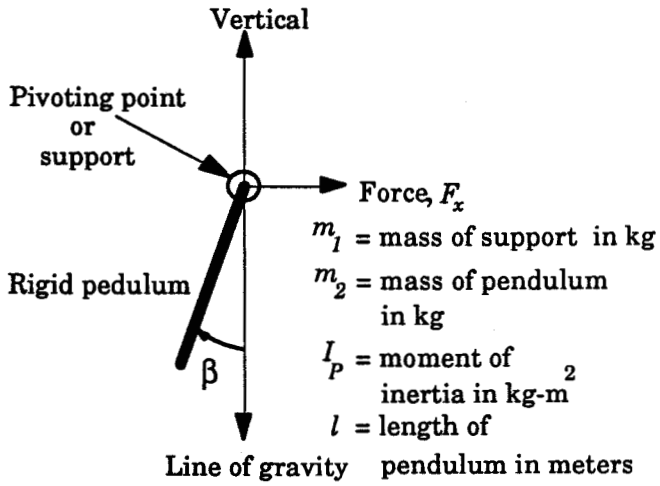

Figure A. 4: Simple pendulum with moving support

Kinetic energy of the system, T:

$$T = \frac{1}{2}m\dot{x}^2 - ml\cos(\beta)\dot{\beta}\,\dot{x} + \frac{1}{2}(ml^2 + I_p)\dot{\beta}^2, \tag{A.25}$$

$$\frac{\partial T}{\partial \dot{\beta}} = (ml^2 + I_p)\dot{\beta} - ml\cos(\beta),$$

$$\frac{d}{dt}\left(\frac{\partial T}{\partial \dot{\beta}}\right) - \frac{\partial T}{\partial \beta} = F_{qr},$$

$$\frac{d}{dt}\left(\frac{\partial T}{\partial \dot{\beta}}\right) = (ml^2 + I_p)\ddot{\beta} - ml\cos(\beta)\ddot{x} + ml\sin(\beta)\dot{x}\,\dot{\beta},$$

$$\frac{\partial T}{\partial \beta} = ml\sin(\beta)\dot{x}\,\dot{\theta},$$

potential energy of the system, V,

$$V = -ml\,g\cos(\beta), \tag{A.26}$$

$$F_{qr} = -\frac{\partial V}{\partial \beta} = -ml\,g\sin(\beta),$$

therefore,

$$ml\cos(\beta)\ddot{x} - (ml^2 + I_p)\ddot{\beta} - mlG\sin(\beta) = 0. \tag{A.27}$$

In the same way, the dynamic equation of the pivoting point can be written as,

$$m\ddot{x} - ml\cos(\beta)\ddot{\beta} + m\,l\sin(\beta)\dot{\beta}^{\,2} = F_x. \tag{A.28}$$

APPENDIX B

NUMERICAL INTEGRATION

The rate of change of a variable frequently occurs in physical systems. The mathematical equations, associated with physical systems, are often expressed in terms of n^{th} order differential equations. The nature of the equations depends upon the complexities of the physical system that is being modeled. A robotics system is expressed in terms of highly non-linear dynamic differential equations. The analytical solutions of such a set of equations are often not possible. Approximate methods of solution are the only available approach.

This appendix describes the Euler-Trapezoidal method of numerical integration or solution of differential equations. This method was used in the work of the project.

The Euler-Trapezoidal method is a predictor-corrector numerical method in which an initial prediction (initial value of integration) is corrected by an iterative process to find the new starting point in the solution. The number of iterations in the process depends upon the required accuracy in the solution.

The expression $y^n = f(x, y, y', y'', ..., y^{n-1})$ is a general form of an n^{th} order non-linear differential equation. The analytical solution of this equation is very difficult. Generally, the numerical solution involves finding the gradient in the solution curve. The gradient is calculated after an increment in the time, h. The new calculated point will be a function of the initial point. The Trapezoidal method uses the average gradient method to find the new starting point for the next calculation [47]. The

Euler-Trapezoidal method of numerical integration can be written in the following steps,

1) find $y_1^{(0)} = y_0 + h\, f(x_0, y_0)$,

2) calculate the derivative at the points $(x_0 + h, y_1^{(0)})$,

3) use the average of the derivatives at the ends of the intervals, $y_1^{(0)}$ and y_0 to a new approximation $y_1^{(1)}$,

$$y_1^{(1)} = y_0 + \frac{h}{2}\left(f(x_0, y_0) + f(x_0 + h, y_1^{(0)})\right),$$

4) further corrections can be made until the error reduces to a sufficiently low value,

$$y_1^{(r+1)} = y_0 + \frac{h}{2}\left(f(x_0, y_0) + f(x_0 + h, y_1^{(r)})\right),$$

where $r = 1,2,\ldots\ldots$ is the iteration to correct the error,

5) after a sufficient number of corrections the new value, y_1 can be taken as the starting point of the next interval and the process is continued until the end of the interval is reached.

APPENDIX C

BACKWARD DIFFERENCE METHOD

An analytical method of differentiation is possible only if there exists a analytical function which can be differentiated. Finding first, second and n^{th} derivative of a function which is defined only by tabulated data or experimentally determined curves, a numerical method of differentiation could be used. Three types of numerical differentiation are possible depending upon the available data points: forward, backward and central. Forward differentiation only possible if the future data points are available in advance. This type of differentiation is only possible in off-line calculation where the data are available previously. Backward differentiation uses the gradient of the curve by taking the differentiation of past and present data [48]. This type of differentiation is useful in on-line calculation. The past data must be stored in memory. Central differentiation is more accurate than both forward and backward, however it uses both past and future data so this type of method is useful for off-line calculation. This appendix shows the calculation of first and second derivatives from stored data using the backward difference method.

(a) backward- difference expression with error of order h,

$$y_i' = \frac{y_i - y_{i-1}}{h},$$

$$y_i'' = \frac{y_i - 2y_{i-1} + y_{i-2}}{h^2},$$

(b) backward difference expression with error of order h^2,

$$y_i' = \frac{3y_i - 4y_{i-1} + y_{i-2}}{2h},$$

$$y_i'' = \frac{2y_i - 5y_{i-1} + 4y_{i-2} - y_{i-3}}{h^2},$$

where h is the time interval between two data points.

APPENDIX D

DC MOTOR CHARACTERISTICS

The torque needed to drive the wheel could be obtained from a d-c motor. The speed and torque of a DC motor can be varied by controlling the motor input voltage. The DC motor converts electrical energy into mechanical energy. The amount of mechanical energy depends upon the motor characteristics and the supplied electrical energy.

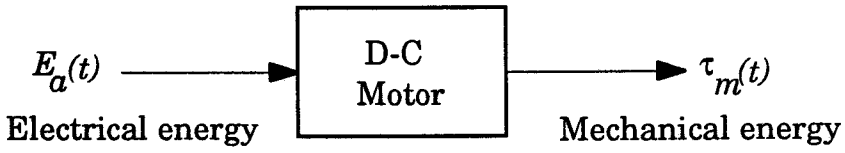

Figure D1: Relation between electrical and mechanical energy

Electrical Equivalent Model

An electrical equivalent model of a DC motor is shown in Fig. D.2,

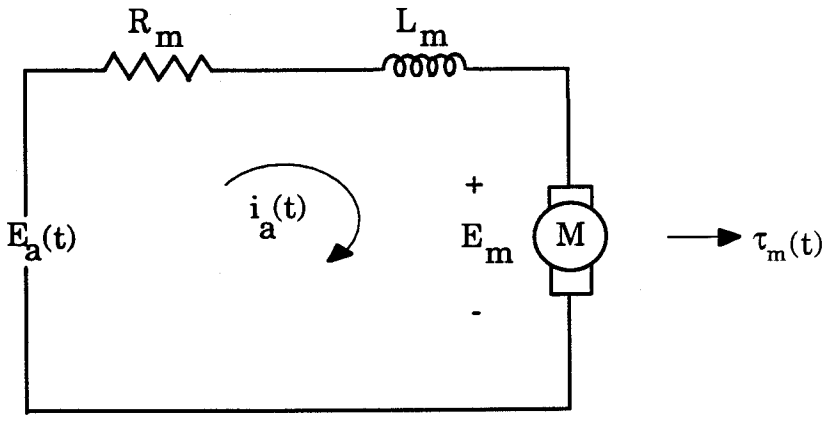

Figure D.2: Electrical model of a DC motor.

The electrical equation can be written as,

$$E_a(t) = R_m i_a(t) + L_m \frac{di_a(t)}{dt} + E_m(t) \qquad \text{(D1)}$$

where, $E_a(t)$ is the armature input voltage at time t. R_m, L_m and $i_a(t)$ are the armature resistance, inductance and current respectively. $\tau_m(t)$ is the torque developed by motor. The mechanical energy developed from the motor in the response of applied electrical energy is given as torque, $\tau_m(t)$. The $E_m(t)$ is the armature back emf and is expressed as,

$$E_m(t) = K_E \omega_s = K_E \frac{d\phi_m}{dt} \qquad \text{(D2)}$$

where, K_E is the motor voltage constant in v/rpm, ω_s is the angular velocity and ϕ_m is the angle of the shaft in rad/sec and radian respectively.

The torque developed by the motor is proportional to the magnitude of the armature current, $i_a(t)$,

$$\tau_m(t) = K_T i_a(t), \qquad \text{(D3)}$$

where, K_T is the motor torque constant in torque/amp.

The wheel and motor are coupled by a gear which is defined as coupling ratio,

$$K_{CR} = \frac{\phi_w}{\phi_m}, \qquad \text{(D4)}$$

where, ϕ_W is the angular position of the wheel.

The relation between the distance traveled in the x direction and the angular position of the wheel is given by,

$$x(t) = (\pi d).(\frac{1}{2\pi}).\phi_w$$
$$= (2\pi r).(\frac{1}{2\pi}).\phi_w \qquad \text{(D5)}$$

therefore,

$$x(t) = r\phi_w$$

provided the ground kinetic friction is enough avoid slippage of the wheel.

Eq. D1 can be combined with Eqs. D2,D3,D4, and D5,

$$E_a(t) = \frac{R_m}{K_T}\tau_m(t) + \frac{L_m}{K_T}\frac{d}{dt}(\tau_m(t)) + \frac{K_E}{rK_{CR}}\frac{d}{dt}(x(t)). \qquad \text{(D1)'}$$

Dynamic Equation

The dynamic equations of the motor can be written as,

$$\tau_m(t) = (J_m + J_L)\frac{d}{dt}(\omega_m) + D\omega_m + T_f + T_L,$$

with $\omega_m = K_{CR}\omega_w$ then,

$$\tau_m(t) = (J_m + J_L)K_{CR}\frac{d}{dt}(\omega_w) + K_{CR}D\omega_w + T_f + T_L, \qquad \text{(D6)}$$

where, τ_L, τ_f and D are the load opposing torque, friction torque and velocity dependent friction torque respectively. J_m and J_L are the motor and load moment of inertia respectively [49].

Transfer Function Between Motor Speed to Voltage

Eqs. D1 and D5 describe the electrical and dynamic models of the motor. The relation between the voltage and the speed is necessary for

designing a servo controller that provides control on the speed of the motor. Thus the transfer function of the motor is required to be evaluated.

The transfer function of the motor, the ratio between motor speed to armature applied voltage, can be written as,

$$G_m(s) = \frac{\omega_m(s)}{E_a(s)},$$

with τ_L=0, τ_f =0 then, and J=J_m+J_L,

$$G_m(s) = \frac{K_T}{(sL_m + R_m)(sJ + D) + K_E K_T},$$

The transfer function has two poles [55], and Eq. D6 can be written as,

$$G_m(s) = \frac{K_T}{JL_m} \frac{1}{(s - p_1)(s - p_2)}. \qquad \text{(D7)}$$

The poles p_1 and p_2 are the solution of characteristic equation,

$$L_m J s^2 + (L_m D + R J)s + (R_m D + K_E K_T) = 0. \qquad \text{(D8)}$$

With the inductance L_m is much smaller than the term $\frac{R_m{}^2 J}{K_E K_T}$, the approximate solution of Eq. D8 can be found with:

$$p_1 = -\frac{K_E K_T}{R_m J}, \text{ and}$$

$$p_2 = -\frac{R_m}{L_m}$$

therefore,

$$G_m(s) = \frac{\frac{K_T}{L_m J}}{\left(s + \frac{K_E K_T}{R_m J}\right)\left(s + \frac{R_m}{L_m}\right)}. \qquad \text{(D9)}$$

APPENDIX E

STABILITY ANALYSIS

The motion and the balance control for the inverted pendulum system, studied in this project required a controller that generates necessary control torque. This control torque is applied between the inverted pendulum and the axle. This single torque is responsible for the motion control, control of angular motion of inverted pendulum during the motion, and the stabilization of inverted pendulum after the motion period.

In order to select a controller that performed the required task, the physical characteristics of the system must first be analyzed. This appendix shows the analysis of the system in S-domain. The open-loop stability of the system and necessary requirements for closed loop stability will be shown with the aid of Root-Locus method.

Recalling, Eq. 4.8,

$$m_{IP}\ l_{IP}\ \cos(\theta)\ddot{x} + \left(m_{IP}\ l^2{}_{IP} + J_{IP}\right)\ddot{\theta} - m_{IP}\ l_{IP}\ g\sin(\theta) + c_1\dot{\theta} = -\tau, \tag{4.8}$$

and Eq. D1',

$$E_a(t) = \frac{R_m}{K_T}\tau_m(t) + \frac{L_m}{K_T}\frac{d}{dt}(\tau_m(t)) + \frac{K_E}{rK_{CR}}\frac{d}{dt}(x(t)). \tag{D1}'$$

with $\theta \leq 5$ degrees, $c_1 = 0$, Eq. 4.8 can be linearized,

$$m_{IP}\ l_{IP}\ r\dot{\omega}_w + \left(m_{IP}\ l^2{}_{IP} + J_{IP}\right)\ddot{\theta} - m_{IP}\ l_{IP}\ g\theta = -\tau,$$

and with Eq. D4, and $L_m \approx 0$, the Eq. (D1)' can be written as,

$$E_a(t) = \frac{R_m}{K_T}\tau_m(t) + \frac{K_E}{K_{CR}}\omega_w(t)$$

Converting above two equations into *s*-domain for analysis,

$$m_{IP}\ l_{IP}\ rs\omega_w(s) + \left(m_{IP}\ l^2{}_{IP} + J_{IP}\right)s^2\theta(s) - m_{IP}\ l_{IP}\ g\theta(s) = -\tau(s),$$

or,

$$m_{IP}\ l_{IP}\ rs\ \omega_w(s) + \left[\left(m_{IP}\ l^2{}_{IP} + J_{IP}\right)s^2 - m_{IP}\ l_{IP}\ g\right]\theta(s) = -\tau(s), \qquad \text{(E.1)}$$

and

$$E_a(s) = \frac{R_m}{K_T}\tau_m(s) + \frac{K_E}{K_{CR}}\omega_w(s),$$

or,

$$\tau_m(s) = E_a(s)\frac{K_T}{R_m} + -\frac{K_T}{R_m}\frac{K_E}{K_{CR}}\omega_w(s). \qquad \text{(E.2)}$$

Combining Eqs. E.1 and E.2 then,

$$\frac{R_m}{K_T}\left(m_{IP}\ l_{IP}\ r\ s - \frac{K_T}{R_m}\frac{K_E}{K_{CR}}\right)\omega_w(s) + \frac{R_m}{K_T}\left[\left(m_{IP}\ l^2{}_{IP} + J_{IP}\right)s^2 - m_{IP}\ l_{IP}\ g\right]\theta(s) = -E_a(s). \qquad \text{(E.3)}$$

Eq. E.3 has been approximated as a second order system with one input, $E_a(s)$, and two outputs, $\omega_w(s)$ and $\theta(s)$. There are two controlled variables ω_w and θ. A separate controller could be designed for each of these variables.

Analysis for Angular Position Controller Design

The open loop transfer function for angular position to input voltage can be derived by neglecting the horizontal component of Eq. E.3. Thus,

$$\frac{\theta(s)}{E_a(s)} = \frac{\frac{R_m}{K_T}}{\left[m_{lP}\ l_{lP}\ g - \left(m_{lP}\ l^2{}_{lP} + J_{lP}\right)s^2\right]} \qquad \text{(E.4)}$$

this transfer function has two real poles at $\pm\sqrt{\left(\frac{m_{lP}l_{lP}g}{\left(m_{lP}l^2{}_{lP} + J_{lP}\right)}\right)}$. These poles are located both in left and right hand sides in the s-plane, as shown in Fig. E.1,

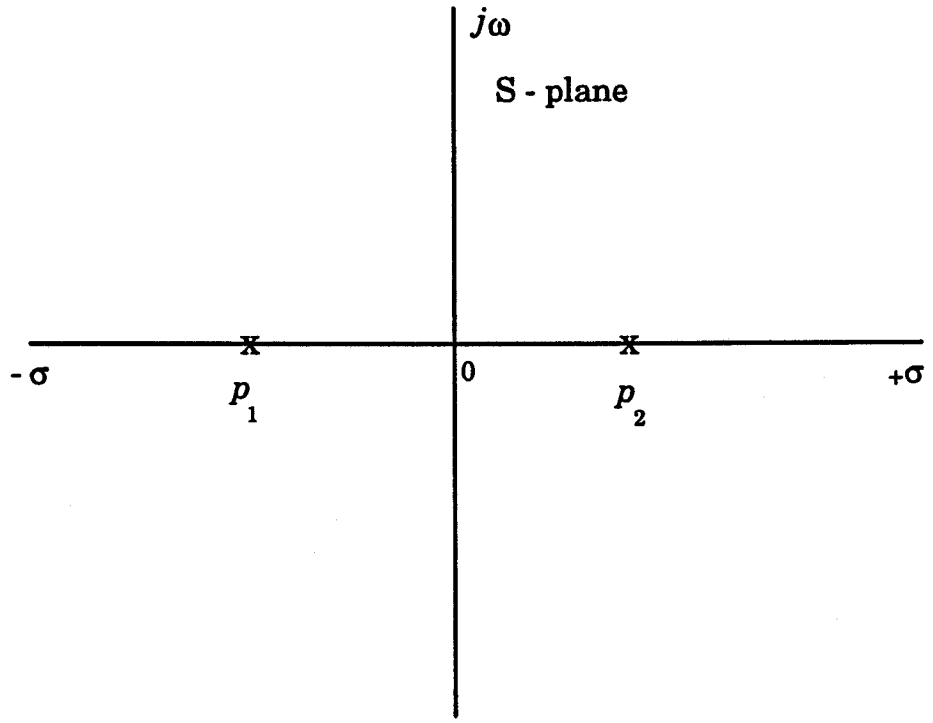

Figure E.1: Poles in S - plane.

From the location of the open loop poles, it is apparent that the system is unstable. The system could be made stable by adding an open loop zero, z, left to the open loop pole p_1,

$$\frac{\theta(s)}{E_a(s)} = \frac{\frac{R_m}{K_T}(s+z)}{\left[m_{IP}\ l_{IP}\ g - \left(m_{IP}\ l^2{}_{IP} + J_{IP}\right)s^2\right]}. \qquad \text{(E.5)}$$

The root-locus of open loop transfer function with added zero is shown in Fig. E.2,

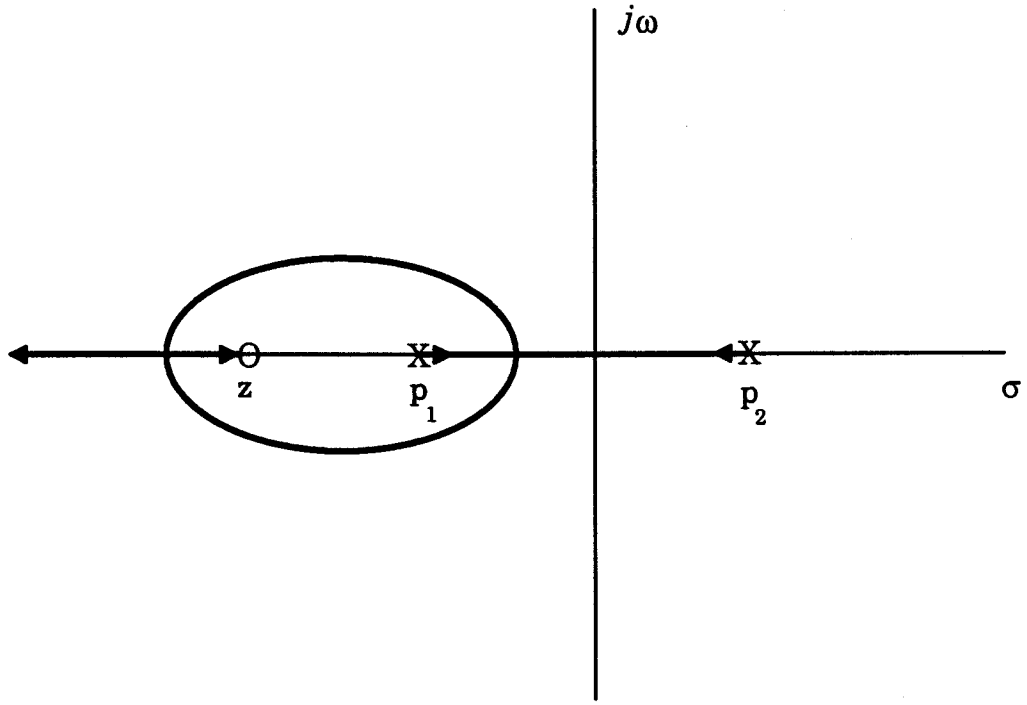

Figure E.2: Root-Locus diagram of open loop transfer function with added zero.

The system can be made stable by choosing a closed loop pole left to the imaginary axis. The closed loop pole should intersect on the root-locus, Fig. E.2.

Analysis for Linear Velocity Controller Design

The open loop transfer function for linear velocity to input voltage can be derived by neglecting the angular component of Eq. E. 3.6. Thus,

$$\frac{\omega_w(s)}{E_a(s)} = \frac{\frac{K_T}{R_m}}{\left(\frac{K_T}{R_m}\frac{K_E}{K_{CR}} - m_{IP}\ l_{IP}\ r\ s\right)}. \qquad \text{(E.6)}$$

This transfer function has a pole at $\frac{K_T}{R_m}\frac{K_E}{K_{CR} m_{IP}\ l_{IP}\ r}$ as shown in Fig. E.3,

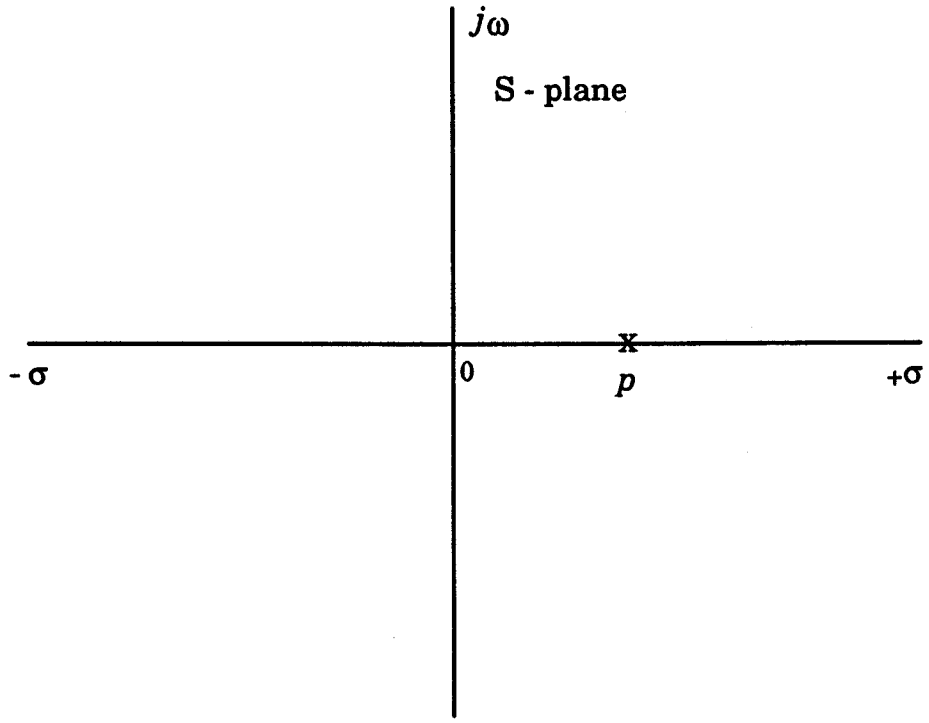

Figure E. 3: Poles in S - plane.

From the location of the open loop pole, it is apparent that the system is unstable. The system could be made stable by adding an open loop zero, *z*, left to the imaginary axis and an open loop pole at the origin in original transfer function, Eq. E.6,

$$\frac{\omega_w(s)}{E_a(s)} = \frac{\frac{K_T}{R_m}(s+z)}{s\left(\frac{K_T}{R_m}\frac{K_E}{K_{CR}} - m_{IP}\ l_{IP}\ r\ s\right)} \qquad \text{(E.7)}$$

The root-locus of open loop transfer function with added zero and pole is shown in Fig. E.4,

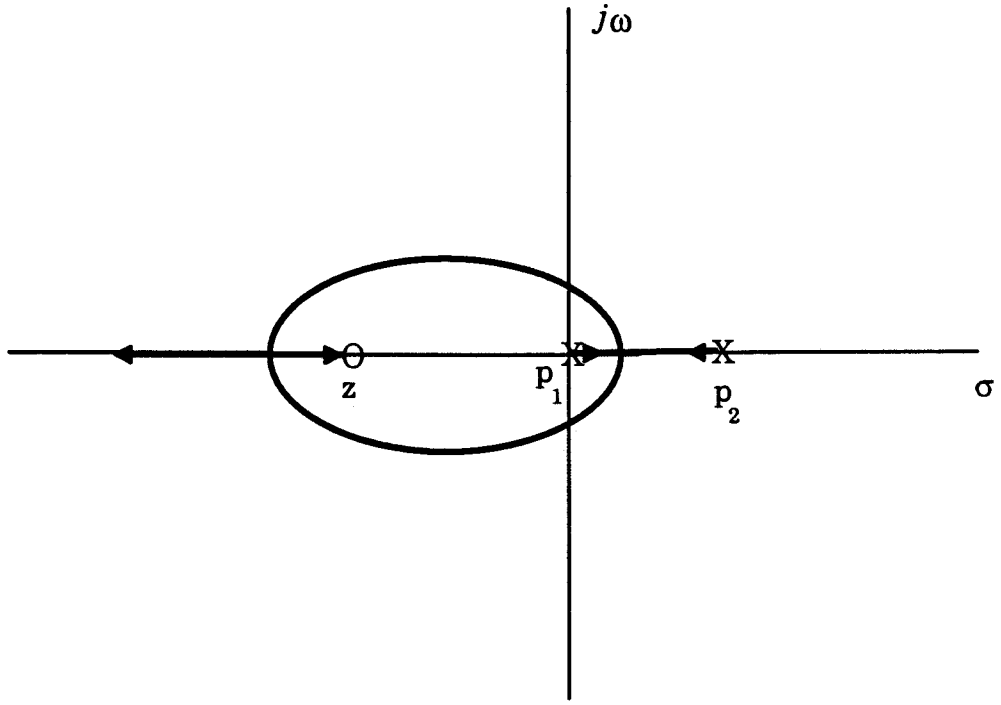

Figure E.4: Root-Locus diagram of open loop transfer function with added zero and pole.

The system can be made stable by choosing a closed loop pole left to the imaginary axis. The closed loop pole should intersect on the root-locus, Fig. E.4.